Optimization of aircraft trajectories over the North Atlantic Airspace

Imen Dhief

THÈSE

En vue de l'obtention du

DOCTORAT DE L'UNIVERSITÉ DE TOULOUSE

Délivré par : *l'Université Toulouse 3 Paul Sabatier (UT3 Paul Sabatier)*
Cotutelle internationale *ENSI*

Présentée et soutenue le *Date de defense (21/09/2018)* **par :**

IMEN DHIEF

Optimization of aircraft trajectories over the North Atlantic Airspace

---

JURY

M. SAMEER ALAM	NTU Singapour	Rapporteur
M. JACCO HOEKSTRA	TU Delft	Rapporteur
M. MANUEL SOLER	Université Carlos Madrid	Examinateur
M. VOJIN TOSIC	Faculty of Transport Serbie	Examinateur
M. PIERRE MARECHAL	UPS Toulouse	Examinateur
MME. NOUR ELHOUDA DOUGUI	EPFL Lausanne	Examinatrice
M. DANIEL DELAHAYE	ENAC	Directeur de thèse

École doctorale et spécialité :
EDAA : Ecole Doctorale Aéronautique et Astronautique
Unité de Recherche :
OPTIM-ENAC
Directeur(s) de Thèse :
Daniel DELAHAYE, *Nour Elhouda DOUGUI* et *Noureddine HAMDI*
Rapporteurs :
Sameer ALAM et *Jacco HOEKSTRA*

Dedication

To my Mom and Dad, to my two sisters and brother, to my family and friends

Résumé

L'objectif de cette thèse est de proposer de nouvelles approches plus efficaces pour améliorer la situation du trafic aérien dans l'Atlantique Nord (NAT). NAT est considéré comme l'espace aérien océanique le plus utilisé dans le monde. Le contrôle du trafic aérien dans cet espace confronte plusieurs difficultés dues aux différences de fuseaux horaires, aux demandes des passagers et aux vents forts induits par les jet-streams. De plus, la prédiction et le contrôle des trajectoire de vol sont très limités à cause de l'abscence de couverture radar. Par conséquent, une structure de routes, appelée Organized Track System (OTS), est établie dans le NAT et des normes de séparation très rigide sont imposés. Tous ces facteurs obligent les vols à suivre des trajectoires non optimales, ce qui influence négativement la consommation de carburant et le coût total du vol.

Dans le cadre des projet lancé pour moderniser le systéme de gestion du trafic aérien, de nouvelles technologie de communication, de navigation et de surveillance ont été développés, l'un des plus prometteurs étant l'ADS-B. L'utilisation de l'ADS-B permet d'exploiter de nouvelles et différentes méthodes d'organiser le trafic, alternative à l'OTS, ce qui constitue l'axe principal de notre travail.

Tout d'abord, nous étudions la possibilité d'introduire le Free Flight Concept (FFC) dans le NAT. En effet, nous proposons une nouvelle approche pour organiser le trafic aérien NAT en se basant sur un comportement d'essaim. En effet, le trafic est considéré comme un système Multi-Agent où tous les vols coopèrent, grâce à l'ADS-B, afin de construire leurs trajectoires, tout en détectant et en résolvant les conflits entre eux. Les trajectoires résultantes sont efficaces en terme de temps de croisière. Cependant, ils ne sont pas robustes contre les changements du vents.

Ensuite, nous proposons une nouvelle structure de route qui bénéficie du jet stream. Cette structure de route est appelée Wind-Optimal Track Network (WOTN), et est construite en considérant les normes de séparation réduites. WOTN couvre un plus grand espace aérien que l'OTS, afin de gérer un trafic plus dense. En gros, WOTN est construit de telle sorte que des pistes parallèles proches sont mis-en place pour suivre le jet-stream et les transitions entre les pistes n'est autorisé que dans les sections d'entrée et de sortie de la structure. Les résultats révèlent l'importance de mettre en place une structure de route afin de garantir des trajectoires robustes face aux vents forts.

Enfin, nous proposons une approche permettant aux aéronefs de sortir en toute sécurité de la structure de la route en cas d'urgence.

Abstract

The objective of the present thesis is to propose new more efficient trends to improve the air traffic situation over the North Atlantic (NAT) airspace. In fact, the NAT is considered to be the most congested oceanic airspace in the world. For many years, air traffic control in this airspace has experienced many difficulties caused by the time zone differences, passenger demands and strong winds induced by the jet streams. This leads to high congestion in the airspace especially at peak hours. Furthermore, flight trajectory prediction and control are very limited due to the lack of radar coverage in oceanic airspace. To support conflict-free flight progress, a structure of routes, called Organized Track System (OTS), is established in the NAT and very restrictive separation standards are applied. These rigid rules oblige flights to follow non-optimal trajectories, which negatively influences the fuel consumption and the total flight cost.

In order to guarantee efficient traffic separation in the context of ever increasing traffic density, alternative means of communication, navigation and surveillance were developed and progressively be implemented, one of the most promising being the Automatic Dependent Surveillance-Broadcast (ADS-B). The widespread use of ADS-B makes it possible to organize traffic in new ways, as an alternative to the OTS, which is the main focus of the current work.

First of all, we investigate the possibility of introducing the *Free Flight Concept* (FFC) in NAT. Indeed, we present an approach to construct and organize NAT traffic based on a swarm behavior. Here, the traffic is considered as a *Multi-Agent* system where all flights cooperate, thanks to ADS-B equipage, in order to construct their trajectories, while detecting and resolving conflicts between each other. The resulting trajectories are efficient in term of cruise time. However, they are not robust regarding changing winds.

Next, we propose a new route structure for eastbound NAT traffic that benefit from the jet stream. This route structure is called Wind-Optimal Track Network (WOTN), and is constructed based on the reduced separation norms. WOTN covers larger airspace than the OTS, in order to handle the growing traffic. Roughly, WOTN is constructed in such a way that nearby parallel tracks are made to follow the jet streams and re-routing between tracks is only allowed in the input and output sections of the structure. Results reveal the importance of implementing a route structure in order to guaranty robust trajectories in the face of strong winds.

Finally, we propose an approach to allow aircraft to safely exit the route structure in case of an emergency.

The overall methodologies are implemented and tested with eastbound flight data over the NAT. We thereby produce conflict-free and robust trajectory planning for eastbound NAT flights, while benefiting from the reduced separation norms and the jet stream thus proving the efficiency of our approaches.

Acknowledgments

I would like to seize this chance to express my deepest thanks to people without whom it would not be possible to accomplish this important step in my life and to succeed my PhD. Because of your assistance and support, I evolved a lot not only at the professional level but also at the personal one.

First of all, I am proudly grateful to my supervisor Daniel Delahaye for his vital support and assistance. Your encouragement did not only make my research successful but also gave me an immense support morally and emotionally. Many thanks to you for your invaluable advises, for providing me with inspired ideas whenever I was lost in my researches and for always believing in my capabilities. Having the chance to work with you is the real investment in my thesis and I hope that we can continue to collaborate in the future.

I wish equally to thank my co-supervisor Nour Elhouda Dougui for believing in me and giving me the chance to be part of ENAC Optim Team, for assisting me especially during my internship and during the first year of my thesis and for helping to integrate with my research field.

I would like to pay my regards to my second supervisor Noureddine Hamdi for accepting belonging to my thesis committee and taking time to talk with me and encourage me on many occasions.

In addition, I would like to thank my thesis referee. First, I would like to thank M. Pierre Marichal for accepting being the president of my defense jury. Second, I would like to pay special thankfulness to my two reporters M. Jacco Hoekstra and M. Sameer Alam for carefully reviewing my thesis, for giving me very constructive and valuable comments and also for their encouraging and supportive reports. Besides, I would like to thank M. Vojin Tosic and M. Manuel Soler for raising their concerns by reading my thesis, for giving me part of their insightful comments, for their attentive listening and for their worthwhile discussion. Overall, I would extremely thank all my defense jury members for their favorable note and particularly their favorable comments that allow me to get my doctoral degree and also encourage me to continue my researches.

I further extend my personal gratitude to Olga Radionova which contributes a lot in my researches. Thank you for providing me with data, for helping me with my integration to this special ATM area and for elaborating with me a joint journal which was very beneficial for my research.

Many thanks to Mohamed Sbihi, to Andrija Vidosavljevic and to Catherine Mancel for providing me very interesting comments after my rehearsal for my thesis defence which helped a lot to improve my presentation.

Thanks to Supatcha for encouraging me, for the interesting discussions and for sharing her culture and bringing me very delicious Thai foods. Thanks to Serge Roux for his limitless helps and for being so patient to fix any computer problem.
Thanks to Georges Mykoniatis for paying his interest to my researches and for providing me with interesting references related to my researches.
Thanks to Marcel Mongeau for always spreading positive vibes.
Thanks to Gilles Baroin for generating nice video to illustrate my results.

Furthermore, I would like to thank all my fellow labmates in ENAC Optim Team: Romaric, Florian, Vincent, Isabelle, Ruixin, Jun, Tambet, Emmanuel, Paolo, Ning, Almoctar, Gabriel, Jeremie, Alice, Souleyman, Ahmed, Akinori and others, from each one I keep very good memories particularly when sharing lunches, sharing coffee-breaks, organizing picnics and playing cards. In particular, I would heartfeltly thank Ying, Ma Ji, Sana I., Sana R. and Man for all the fun we have had together in my last year, for stimulating discussions, for their support and for sharing very delicious foods. I would like also to pay special thanks to my friend Bilal who shares with me the experience of teaching.

I would like to give strong thanks, gratitude and appreciation to my closest friends Chekra, Dhouha, Ghada, Hend, Ibtissem, Ikbel, Imen, Ines, Insaf, Israa, Jihed, Maroua, Nadiya, Narjes and Wiem, each one of you has giving me special powerful things, has encouraged me in its way, and with each one of you I keep very particular, funny and unforgettable memories. I would like also to thank my friends Imed, Khaled, Mejdi, Raouf and Slim. Thank you all my friends for helping me at several occasions, for supporting me, for carefully listening to me whenever I have any problem, for bearing me at times of distress. It is whole-heartedly expressed that your support, your invaluable help and your presence in my life are primordial towards the success of my research.

Moreover, I express my very profound gratitude to my family. First, I would like to pay special thanks to my uncles Riadh and Mohamed for their unfailing support and their coutinous encouragement. Second, I would like to thank my cousin Amna for being always present to listen carefully to my concerns.

Last but not the least, I would like to keep the deepest thanks to my Mom and Dad, my two sisters Rihab and Rima and my brother Ahmed. Thank you for assisting me financially, for providing me with spiritual and emotional support, for always encouraging me. With your assistance, your benediction and your love through my whole life, I was able to accomplish this important step in my professional life and to become a Doctor.

Contents

List of Figures

List of Tables

List of Abbreviations

ADS-A	**A**utomatic **D**ependent **S**urveillance-**A**ddressed
ADS-B	**A**utomatic **D**ependent **S**urveillance-**B**roadcast
ADS-C	**A**utomatic **D**ependent **S**urveillance-**C**ontract
AFSS	**A**utomated **F**light **S**ervice **S**tation
APP	**A**irline **P**lanning **P**rocess
AT	**A**ircraft **T**rajectory
ARTCC	**A**ir **R**oute **T**raffic **C**ontrol **C**enter
ATA	**A**ctual **T**ime of **A**rrival
ATC	**A**ir **T**raffic **C**ontrol
ATCT	**A**ir **T**raffic **C**ontrol **T**ower
ATFM	**A**ir **T**raffic **F**low **M**anagement
ATM	**A**ir **T**raffic **M**anagement
ATS	**A**ir **T**raffic **S**ervices
ASAS	**A**irborne **S**eparation **A**ssurance **S**ystem
ASM	**A**ir**s**pace **M**anagement
CDM	**C**ollaborative **D**ecision **M**aking
CD&R	**C**onflict **D**etection and **R**esolution
CEP	**C**entral **E**ast **P**acific
CI	**C**ost **I**ndex
CPDLC	**C**ontroller-**P**ilot **D**ata-**L**ink **C**ommunication
CPV	**C**ylindrical **P**rotection **V**olume
ETA	**E**stimated **T**ime of **A**rrival
FAA	**F**ederal **A**viation **A**dministration
FFC	**F**ree **F**light **C**oncept
FIR	**F**light **I**nformation **R**egion
FL	**F**light **L**evel
FPL	**F**light **PL**an
GA	**G**enetic **A**lgorithm
GNSS	**G**lobal **N**avigation **S**atellite **S**ystems
GPS	**G**lobal **P**ositioning **S**ystem
GS	**G**round **S**peed
HF	**H**igh **F**requency
IAS	**I**ndicated **A**ir**S**peed
IATA	**I**nternational **A**ir **T**ransport **A**ssociation
ICAO	**I**nternational **C**ivil **A**viation **O**rganization

IFR	**I**nstrument **F**light **R**ules
MAS	**M**ulti-**A**gent **S**ystem
MLAT	**M**ulti-**LAT**eration
MNT	**M**ach **N**umber **T**echnique
NASA	**N**ational **A**eronautics and **S**pace **A**dministration
NAT	**N**orth **A**tlantic
NAT DLM	**NAT D**ata **L**ink **M**andate
NAT HLA	**NAT H**igh **L**evel **A**irspace
NextGen	**Next Gen**eration air transportation system
NM	**N**autical **M**ile
NMOC	**N**etwork **M**anager **O**perations **C**entre
OALT	**O**perationally **A**cceptable **L**evel of **T**raffic
OTS	**O**rganized **T**rack **S**ystem
OACC	**O**ceanic **A**rea **C**ontrol **C**enter
OCAs	**O**ceanic **C**ontrol **A**reas
OEP	**O**ceanic **E**ntry **P**oint
PRM	**P**referred **R**oute **M**essage
RLatSM	**R**educed **Lat**eral **S**eparation **M**inima
RLonSM	**R**educed **Lon**gitudinal **S**eparation **M**inima
RNP	**R**equired **N**avigation **P**erformance
RVSM	**R**educed **V**ertical **S**eparation **M**inimum
SA	**S**imulated **A**nnealing
SASP	**S**tate **A**viation **S**ystem **P**lan
SC	**S**tep **C**limb
SESAR	**S**ingle **E**uropean **S**ky **A**TM **R**esearch
SW	**S**liding **W**indow
TAS	**T**rue **A**ir**S**peed
TBO	**T**rajectory **B**ased **O**peration
TMA	**T**erminal **C**ontrol **A**rea
TRACON	**T**erminal **R**adar **A**pproach **Con**trol
UIR	**U**pper **I**nformation **R**egion
URET	**U**ser **R**equest **E**valuation **T**ool
UTC	**C**oordinated **U**niversal **T**ime
VFR	**V**isual **F**light **R**ules
VHF	**V**ery **H**igh **F**requency
WOTN	**W**ind-**O**ptimal **T**rack **N**etwork
WP	**W**ay-**P**oint

Introduction

Throughout several years, air transportation took a key role in enabling out both social and economical progress all over the world. It is very beneficial especially for traveling long distances and saving time since it is the fastest means of transport.

From a social point of view, air transportation broadens people's leisure and cultural experiences by promoting traveling across the globe. This is particularly important in understanding different cultures and nationalities, which in turn facilitates international integration and supports the development of multicultural societies. It has also an important role in improving living standards and alleviates poverty by enhancing the growth of tourism. It also improves people's well-being by making a wider range of holiday destinations, by providing seasonal fruits and vegetables, etc. In addition to this, air transport provides access to remote areas where other transport modes are limited. Therefore, several vital services are becoming available, such as food deliveries, hospitals, education, etc.

From an economic point of view, air transportation provides the only worldwide network which promotes and encourages the global business and tourism. According to IATA's latest financial forecast [47], the high profitability of airline companies is expected to continue in 2018. The overall revenue is expected to rise to 824 billion, from 2017 revenues of 754 billion. In addition, in 2018, about 4.3 billion passengers worldwide are expected to travel by air, which represent a growth of 4.9% compared to the previous year.

Despite the important development of this sector, air transportation system has always been forward-looking and is continuously changing in order to handle more traffic with greater safety, at a lower cost, and with reduced environmental impact. Currently, two major projects aim to modernize *Air Traffic Management* (ATM): the *Federal Aviation Administration* (FAA) *Next Generation Air Transportation System* (NextGen) project in USA and the *Single European Sky ATM Research* (SESAR) project in Europe. Both are complex and long-term processes aiming to improve ATM by implementing innovative technologies, capabilities and procedures. Therefore, with more powerful communication systems, more accurate surveillance, and more reliable automated support tools, the future technologies will improve safety, reduce delay as well as maximize airspace capacity. In the scope of these new achievements, the current work introduces innovative approaches to handle oceanic air traffic over the North Atlantic airspace in order to release the traditional oceanic traffic methods and apply more efficient ones while taking advantage from the new technologies.

Motivations and contributions

The North Atlantic airspace (NAT) (see Figure 1) connects two densly populated areas namely North America and Europe. It is considered to be the most congested oceanic airspace in the world.

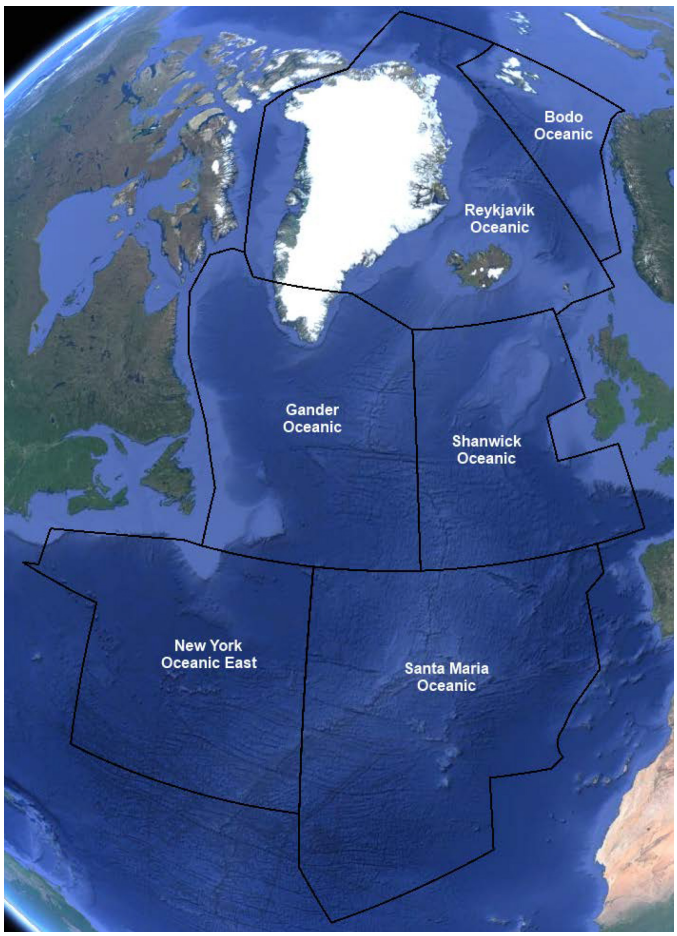

FIGURE 1 – North Atlantic Airspace (NAT) [49]

The traffic density of this airspace is increasing each year. Figure 2 illustrates the traffic growth over the last five years and estimations of the traffic growth for the following years. Indeed, Trans-Atlantic operations are expected to grow 5.3% annually from 2016 to 2021 [50]. Furthermore, the International Civil Aviation Organization (ICAO) forecasts an annual total NAT traffic increase up to more than $16,000$ flight per week in 2022 compared to about $13,500$ flight per week in 2017 (see Figure 2).

For many years, air traffic control in this airspace has experienced difficulties due to the limited radar coverage. To support conflict-free flight progress, a structure of routes, called Organized Track System (OTS) (see Figure 3), is established in the NAT airspace and very restrictive separation standards are applied.

Re-routing of aircraft from one track to another is rarely authorized because of these large separation standards. Therefore, aircraft are required to follow tracks that are not optimal given their departure and destination points. This leads to an increase in aircraft

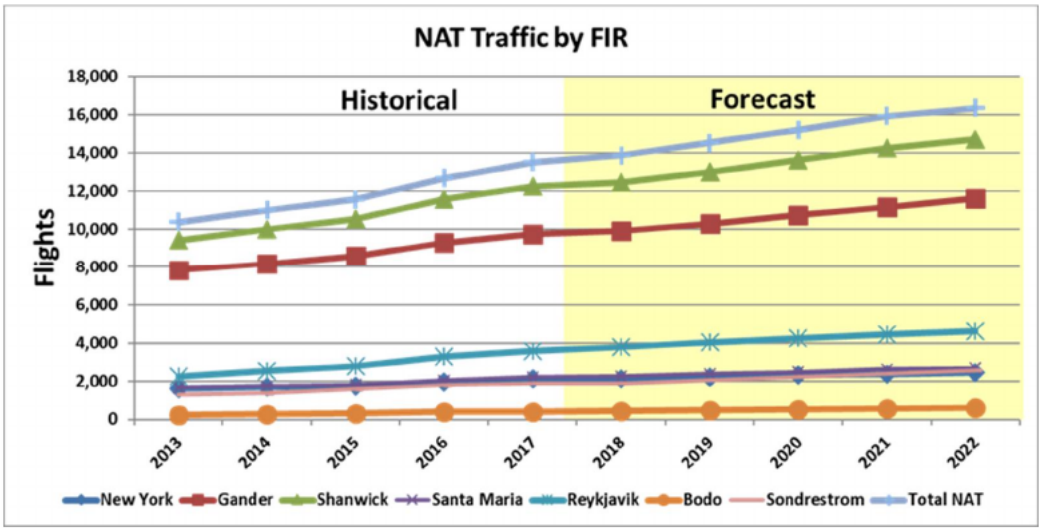

FIGURE 2 – Statistics and forecasts of the NAT traffic increase [50]

cruising time and congestion level in continental airspace at the input and output of the OTS.

In addition to this, aircraft operating in the NAT are subject to very strong winds induced by the jet stream. These streams are fast air currents forming a tube in the upper atmosphere, typically between 20,000 and 50,000 feet and running mainly in east direction, with a speed around 100kts and up to 200kts (see Figure 4). Therefore, eastbound traffic prefers to exploit the wind direction and fly on tailwind, contrary to westbound traffic which prefers to avoid headwind. The OTS structures, one for eastbound traffic and one for westbound traffic, are created daily to take into account the weather pattern. Nevertheless, as the jet stream width is very narrow, not all eastbound OTS tracks are wind optimal, which leads to a concentration of the eastbound NAT traffic on the tracks involving preferable wind. A study presented in [91] proves that flights using eastbound OTS tracks prefer to follow middle tracks, those that benefit more from the tail winds in the jet stream.

The development of the Automated Dependent Surveillance-Broadcast (ADS-B) systems provides an opportunity to improve the flight planning operations over the oceans by reducing separation norms. This reduction on the separation norms makes it possible to exploit new ways of organizing traffic, alternative to the OTS, which is the main objective of the present work.

In the current work, we propose to take advantage of the reliable aircraft-aircraft and aircraft-controllers communications made possible by ADS-B in order to propose more efficient routes to NAT flights. In this context, our first contribution introduces an innovative approach for planning NAT flight trajectories under the framework of *Free Flight Concept* (FFC). Indeed, eastbound NAT flights share several features, such as flying on the same direction and want to benefit from tailwind, for a long distance above the ocean. As a result, we consider the eastbound traffic as a set of birds flying in the same

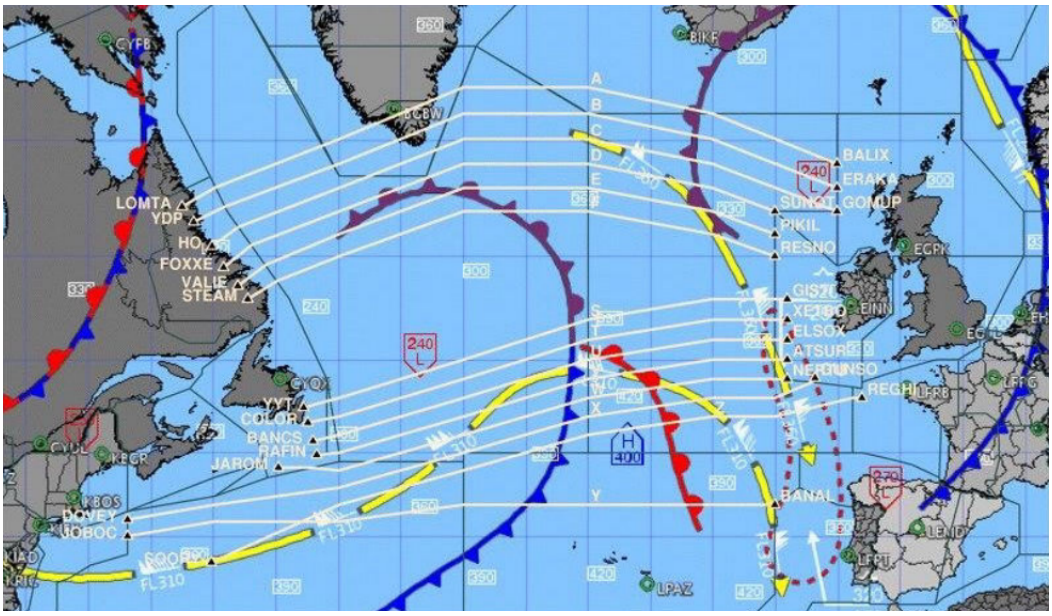

FIGURE 3 – Eastbound and westbound OTS tracks [91]

direction, forming a swarm behavior, and searching for the optimal paths to reach their destinations, while maintaining a separation distance between each other. This approach allows flights to follow free trajectories rather than flying on a route structure. This makes it possible for each individual flight to choose its own trajectory based on its preferences while ensuring a swarm behavior with its neighbors. However, the major drawback of this approach is that it generates trajectories that are not robust in terms of wind variations. This is a major problem since NAT airspace is exposed to strong wind variations caused by the jet stream. For this reason, in our second contribution, we propose a new wind-optimal route structure referred to as Wind-Optimal Track Network (WOTN). The main benefit behind WOTN is that it allow flights to follow both robust and wind-optimal trajectories. However, a problem raises in regards to the need for NAT flights to exit the route structure in case of an emergency. As a result, in our third contribution, we introduce an approach to organize the traffic inside our proposed route structure WOTN in a manner to enable each aircraft to safely exit WOTN at any given time.

Manuscript outline

This thesis is organized as follows. In chapter 1, first an overview of the current Air Traffic Management (ATM) system, including its definition and its basic components, is introduced. Then, ATM modernization plans, procedures and technologies are presented. Next, the North Atlantic Airspace (NAT), which represents the main subject of our study, is introduced. Afterwards, a short overview of optimization methods is presented, and a focus on the SA used in our approaches is given. This chapter is concluded by outlining the limitations faced by NAT flights, which represent the main challenge of the present thesis on which we concentrate our research effort.

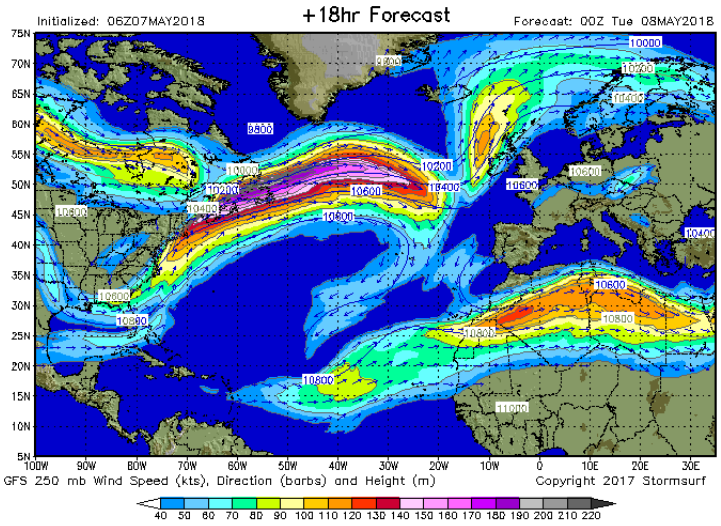

FIGURE 4 – Jet stream position and velocity on 08/05/2018 [107]

In chapter 2, we investigate the possibility of implementing FFC into NAT flights. To this end, we propose a decentralized cooperative method to simulate the flight progress within the NAT. The chapter starts by presenting several previous related works aimed at introducing the FFC into the framework of air traffic conflict detection and resolution problems, quantifying the benefit coming from applying FFC, and applying multi-agent systems to address certain ATM issues. Afterwards, we present and discuss our proposed approach.

The main challenge of the strategic planning under FFC is dealing with high levels of uncertainty, resulting, in particular, from the wind prediction errors. Thus, robustness of the flight trajectories is crucial: we want to ensure that the required separation is maintained for the proposed flight schedules regardless of the changing wind conditions.

In chapter 3, we propose a new route structure as an improvement of the current OTS to accomplish the following goals:

— allow eastbound flights to follow the jet stream direction which is beneficial for the en-route fuel consumption,

— reduce separation norms, assuming that all aircraft implement the ADS-B system,

— enable re-routing inside the route structure in a safe manner in order to alleviate congestion in the continental airspace,

— propose robust flight trajectories under changing wind conditions.

The chapter starts with a literature review of previous works aimed at improving the NAT situation, and investigating the benefit coming from applying wind-optimal flight trajectories. Then, the proposed new route structure is presented and discussed further.

In chapter 4, an improvement of the proposed route structure is presented in order to take into account some operational features of the NAT traffic. Indeed, during flight, some unexpected emergencies can occur and force the aircraft to change its trajectory. Therefore, contingency procedures are established in order to allow an aircraft to deviate from its planned track. Chapter 4 discusses the compatibility of the actual contingency

procedures with the proposed route structure. In addition to this, a solution to some inconsistencies is proposed.

Chapter 1

Background and problem context

In this chapter, we first describe the current Air Traffic Management (ATM) system, including its definition and its basic components. Further, we introduce some procedures and technologies in the framework of ATM modernization aimed at improving safety and increasing efficiency in air traffic operations. In section 1.2, we restrict the general ATM properties being defined to the case of the North Atlantic Airspace (NAT). Thus, the specific features of NAT, including separation norms and flight progress, are highlighted. In section 1.3, a short overview of optimization methods is presented, and a focus on the SA used in our approaches is then given. This chapter is concluded by outlining the limitations faced by NAT flights, which represent the main challenges of the present thesis and where we concentrate our research effort.

1.1 Air Traffic Management

In this section, an overview of the current ATM situation, including its main components, concepts, systems and future trends, is presented.

1.1.1 Air Traffic Management components

Air traffic management (ATM) is a system that covers all the activities involved in ensuring the safety and the efficiency of air traffic. It represents procedures, technologies and human resources which make sure that aircraft are guided safely in the sky and on the ground. Airspace is well managed in order to accommodate with the traffic over time. Air traffic is managed through the three following components systems:

— Airspace Management (ASM) is the process by which airspace options are selected and applied to meet the needs of the ATM community. The primary purpose of ASM is to ensure efficient utilization of available airspace as one continuum, taking into account real short-term needs of its various civil and military users (e.g. airlines, military forces, companies performing aerial work etc.) in order to prevent interference from all users and to facilitate the continuous sharing of

information by all partners participating in a rolling CDM (collaborative decision-making) [1] process.

— Air Traffic Flow Management (ATFM) is a system that manages the air traffic flow in order to prevent congestion in the air and to ensure that the available capacity is used effectively. It is performed to forecast traffic up to one year in advance before real-time operations in order to anticipate the impact of severe weather and to propose delay and reroute solutions. Its main objective is to balance on the one hand operational, economic and environmental considerations, and on the other hand the capacity and demand to maximize resource utilization.

— Air Traffic Control (ATC) is a process performed by ground-based air traffic controllers who assist aircraft on the ground and through controlled airspace, and also provide advisory services to aircraft in non-controlled airspace. The ultimate objective of ATC worldwide is to prevent collisions, organize and maintain the order of air traffic flow, while satisfying as much as possible the pilot's requests.

Thus, ATC controls the air traffic in real time, while ATFM is in charge of the strategic phase. Further in this section, the features of ATC and ATFM are presented in more details.

The ATFM plans operations up to one year in advance in order to consolidate the air traffic forecasts issued by the airlines and the capacity plans issued by the ATC centers and airports. For instance, in Europe, this system is managed by the Network Manager Operations Centre (NMOC, previously called CFMU) of Eurocontrol. NMOC acts essentially as a coordination center for European flight planning. It collects flight plans from every flight performed under Instrument Flight Rules (IFR) [2] in Europe. Then, it analyzes the compatibility of the requests to ensure that at any given moment there is sufficient ATC capacity available to handle demand. If the request is not compatible with the airspace structure or the capacity limit, NMOC suggests alternative routes or delays. Then, it distributes the approved flight plan to all local ATC centers overflown by the considered flight in Europe. Once flight plans are established, it is the role of ATC to take over and to maintain flights safely separated in the sky, and at the airports where they land and take off.

Two kind of airspace can be distinguished:

— *Controlled airspace* refers to a predefined portion airspace within which air traffic control service is provided to IFR and to Visual Flight Rules (VFR) [3] flights [4] accordingly with the airspace classification.

1. CDM is the process focusing on how to decide on a course of action articulated between two or more community members. It aims at improving the performance of the ATM system while balancing the needs of individual ATM community members

2. Instrument Flight Rules (IFR) are a set of regulations that enable aircraft to operate under low visibility caused by weather or darkness and when the pilot is unable to navigate using visual references.

3. Visual Flight Rules (VFR) are a set of regulations that enable aircraft to operate in weather conditions with visual reference to the ground, and by visually avoiding obstructions and other aircraft.

4. IFR flight and VFR flight refers to a flight conducted in accordance with IFR and VFR rules, respectively

— *Uncontrolled airspace* refers to the airspace in which air traffic control does not exert any executive authority, although it may act in an advisory manner.

The International Civil Aviation Organization (ICAO) has divided the world airspace into Flight Information Regions (FIRs). The classification of the airspace within FIRs determines which country controls a particular airspace, stipulates the rules and procedures to be applied, and provides the basic level of Air Traffic Services (ATS) [5]. A controlling authority is responsible for the management of each FIR and for ensuring that air traffic services are provided to the aircraft flying within it. Each FIR is usually divided into pieces that vary in function, size and classification. Classifications determine the procedures of flying within a piece of airspace and whether it is *controlled* or *uncontrolled*. In some cases, the FIR is divided vertically, in which case the lower portion remains named FIR, whereas the airspace above is named Upper Information Region (UIR).

ATC responsibilities and functions are mainly divided into the three following offices:

— Office of En Route and Oceanic Service which is performed by the Air Route Traffic Control Centers (ARTCCs). ARTCCs are established to provide air traffic service to aircraft operating on IFR flight plans within controlled airspace, and during their en route phases.

— Office of Terminal Service which is performed by two components, namely Terminal Radar Approach Control (TRACONs) and Control Towers (ATCTs). TRACONs and ATCTs have been established in order to provide safe, order and harmonized traffic flow within the vicinity of an airport.

— Office of Flight Services which is performed by Automated Flight Service Stations (AFSSs). AFSSs are air traffic facilities aiming to provide pilots with a variety of services, such as processing flight plans, pilot briefings and in-flight services. However, they are not involved in the control and separation of flights.

Each FIR is divided into several ARTTCs depending on its size and complexity. Then, each ARTTCs is partitioned into different *sectors* each of which is assigned to a group of controllers monitoring the air traffic. Thus, from the moment passengers enter an aircraft to take a flight until they leave it, there are numerous systems, procedures and people who ensure that the whole operation is carried out safely.

Typically, each flight profile is divided into different sections called *flight phases* which are presented in figure 1.1 and listed below:

— Preflight takes place at least 30 minutes before the flight take off. During this phase, the flight plan and the weather along the intended route are reviewed. Once the flight plan is approved, the aircraft is cleared to take off.

— Takeoff is the phase of flight in which an aircraft goes through a transition from moving along the ground to flying in the air, by speeding down the runway.

— Departure phase consists of lifting off the ground and climbing to a cruising altitude.

5. ATS is a generic term that includes flight information service, alerting service, air traffic advisory service and air traffic control service. It provides information to safely conduct flights, and alerts the relevant authorities if an aircraft is in distress

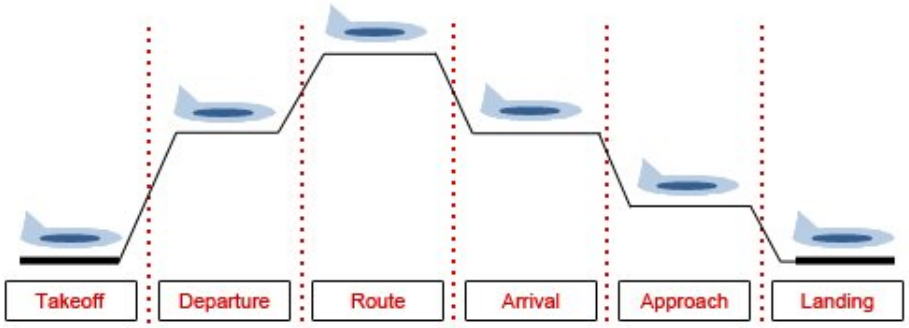

FIGURE 1.1 – Flight Phases

— En Route phase represent the majority of the flight. In this phase, the aircraft travels through one or more ARTTC at an established level, with practically constant configuration and speed.
— Arrival consists on decreasing the altitude when approaching to the destination airport. Clearance to descend is required from Terminal Control Area (TMA) [6].
— Approach is the phase in which the pilot aligns the aircraft with the designated landing runway.
— Landing is the phase when the aircraft lands on the designated runway, taxis to the destination gate and parks at the terminal.

In general, the main purpose of ATC consists on accomplishing safe, efficient, and cost-effective operations by offering the following services:

— *Separation:* ATC tracks each aircraft in flight, with surveillance radars on the ground and airborne transponders, in order to make sure that adequate separation is maintained and to detect and resolve conflicts as they arise.
— *Weather and flight information:* this service consists on giving information about expected weather conditions along the intended route in order to plan safer and more efficient flights.
— *Landing:* which consists on offering services that facilitate the movement of air traffic in the vicinity of airports and runways.

These services together comprise an integrated program, no part of which can be fully effective without the others. For instance, flight plans must take into account weather and traffic, then traffic must be routed safely to destination so that it arrives on time and can be handled at the airport with a minimal delay.

Real time control and terminal control are out of the scope for the present thesis. Here we are focusing on establishing an efficient flight plan at the strategic level taking into consideration both weather and traffic. The next section describes the flight planning procedures.

6. Terminal control area, known as TMA, is a controlled airspace set up at the confluence of airways surrounding a major airport to protect traffic climbing out from and descending into the airport.

1.1.2 Flight planning

The planning process encompasses all aspects of preflight assessments. This process starts from the longest-range involving aircraft acquisition to medium-range involving route planning and scheduling decisions. The planning activities start by an *Airline Planning Process* (APP) which is performed by the airlines. It consists on determining which type of aircraft should be assigned to each flight in order to match demand and capacity while considering the limitations imposed by the network structure. The main issue is to establish a trade-off between a number of tightly-constrained selection criteria, including aircraft economics, technical, operational and environmental performance. Once the aircraft chosen by the airline and its different characteristics are known, the next step is the *Flight Planning* process which consists on determining the specific routes to be flown. The flight planning task involves selecting the adequate routing (in terms of time, fuel burn, etc) while considering the available information (such as aircraft type, forecast weather conditions, aircraft performance, etc) in order to generate a *flight plan* (FPL) that can be approved by ATM services and programmed directly on the aircraft automation. The flight plan has to detail different flight aspects, namely routing, alternate airport options, fuel requirements and takeoff performance, which are subject to last-minute changes.

For each intended flight, the related aircraft is required to provide air traffic service units with a fully filled FPL. Then, the set of collected FPLs are analyzed and computed by the competent ATS units in order to facilitate the flight tracking process within ATC, flight information service and alerting service.

The FPL includes all information relevant to the specific planned flight, such as aircraft identification, flight rules, aircraft equipment on board, departure and destination airports. Moreover, it provides the pilot with all passing way-points on the route from departure airport to destination one, altitude to fly, speed to fly, fuel to carry and other aircraft performance factors such as takeoff power and flap settings. The flight plan is also supported by a briefing package that includes local, en-route and destination weather information, navigational data along the flight route and appropriate airport data. Thus, a FPL has to encompass all the legal and safety requirements such as aircraft weight limitations, route and altitude requirements and required fuel. In addition to the safety aspect, the FPL can impact the economic aspects of the flight by selecting the most economical route and altitude considering weather and traffic constraints, controlling the flying time and controlling the departure time based on destination weather.

Therefore, FPL elaboration is a very complex process involving a trade-off between several parameters and conditions which are subject to significant uncertainties. In the sequel, we will only focus on the *Flight Path*, or *Aircraft Trajectory* (AT), to be followed by the aircraft based on the established FPL. An AT, defined in four dimensions (space and time), has three main components, namely altitude, speed and way-points (WPs).

Aircraft altitude: This represents the height reached by the aircraft above sea level. It is expressed in terms of *feet* for lower altitudes, and in terms of *Flight Levels*

(FLs) at higher altitudes. FLs consists of surfaces of constant atmosphere pressure and are spaced 1000 feet apart. The last two zeros of a FL are usually left out, so an altitude of 37,000 feet (11,280 meters) is known as FL370.

Aircraft speed: Commonly, there are four speeds a pilot is principally concerned with, which are *Indicated Airspeed* (IAS), *True Airspeed* (TAS), *Ground Speed* (GS) and *Mach number*.

- IAS is the speed displayed on the aircraft static airspeed indicator. It is measured in knots.
- TAS corresponds to the IAS corrected for altitude and non-standard temperature. Concretely, it represents the speed of the aircraft relative to the airmass in which it is flying. For slow speeds, it can be calculated by using a flight calculator, and the data required are static air temperature, pressure altitude and IAS. Above approximately 100 knots, the compressibility error rises significantly and TAS must be calculated using the *Mach number*.
- *Mach number* is a quantity representing the ratio of the speed of an aircraft to the speed of sound in the surrounding air. It defines how quickly an aircraft travels with respect to the speed of sound. At higher altitudes (generally beginning around FL280), most aircraft fly a particular Mach number instead of IAS. It is usually used in a special technique, referred to as Mach Number Technique (MNT). MNT is a technique whereby aircraft operating successively along suitable routes are cleared by ATC to maintain appropriate Mach Numbers for a relevant portion of the en route phase of their flight.
- GS is the speed of the aircraft relative to the ground. It is calculated by a ratio between TAS and the speed vector of tail/head wind at aircraft altitude. This speed is measured by radars.

Aircraft trajectory: An aircraft trajectory is a description of the path followed by the aircraft when flying between airports. It can be represented by a sequence of WPs to be followed. Each WP is designated by 3D coordinates in space (latitude, longitude and altitude). WPs are connected with straight segments called links. These links actually represent the great circle distance joining these WPs.

While flight plan calculations are necessary for safety and regulatory compliance, they also provide airlines with an opportunity for cost optimization by enabling them to determine the optimal route, altitudes and speeds which affects directly fuel costs. However, establishing an effective flight plan can be challenging because it involves a number of different constraints. An optimized flight plan must not only take into account aircraft performance and weather, but also route restrictions from ATC and all relevant regulatory restrictions. Furthermore, reducing the fuel burn impact of an aircraft is not limited to consuming the least fuel possible, but other cost metrics must also be considered. The Cost Index (CI) is a constant used by airlines to determine the operating cost of the flight. The CI includes several parameters such as the fuel price, the number of

crew members working during the flight, and the flight duration which influences directly the global cost of the flight. A CI close to zero indicates that the operation costs for the flight are low, and thus the flight duration would also be low.

Another important factor to consider when optimizing a trajectory is the aircraft weight. In fact, the heavier the aircraft is, the lower the optimal altitude is located. For the initial climb, a constant aircraft speed is selected to climb to a specific altitude. The optimal climb speed is selected in terms of CI. A slower climb speed will result in a shorter traveled distance, but to a longer time to reach the final destination. However, a higher speed will reduce the time, but will increase the fuel consumption. Thus, the CI determines a trade-off between deferent criteria in order to provide the appropriate choice of the profile to be used.

In the flight cruising phase, two types of climb can be made, either a Step Climb (SC) or a continuous climb. The continuous climb provides the minimum fuel consumption, as the optimal altitude will be reached quickly. However, the SC technique consists in ascending in steps of 1000ft, 2000ft or 4000ft depending on the flight level rules applied on the particular airspace being flown. In each step, a cruise phase is performed.

Furthermore, wind influence is an important factor to be considered too. Indeed, with a stronger tailwind, smaller flight times and fuel burns are obtained. In case of headwinds, reducing the flight time requires increasing the airspeed, thus increasing the fuel burn as well.

Therefore, once flight plans are gathered, a prediction of the traffic situation can be made. Then, mandatory change can be issued to the flight plan in order to avoid conflicts by ensuring aircraft separation.

1.1.3 Airspace congestion

Congestion in transportation occurs when demand exceeds infrastructure capacity, causing delays in travel time, especially during peak periods. In air transportation, congestion is subdivided into two groups according to the part of airspace involved:

— *Terminal congestion* which refers to the congestion that occurs on the airport surfaces and in surrounding terminal airspace and,

— *En-route congestion* which refers to the congestion involved in the en-route section of flights.

The main responsibility of ATM is to manage the flow of air traffic when congestion occurs. To resolve a congested situation, specific maneuvers can be performed. In practice, aircraft can be delayed briefly in holding patterns, they can be rerouted when airborne or held on the ground prior to departure. ATC must assure that no downstream sector or airport exceeds the Operationally Acceptable Level of Traffic (OALT). The OALT defines the maximum number of aircraft allowed in a specific sector or airport.

Air traffic regulations require that flights maintain a specific separation distance, in order to avoid conflicts and to ensure a sufficient margin of safety considering potential errors. The standard separation norm between aircraft in a terminal area is 3NM in the horizontal plane or 1000ft in the vertical plane. For en-route flight, controllers rely on

vertical, *lateral* and *longitudinal* separation norms in order to maintain the safe separation between aircraft.

— *Vertical separation* is achieved by requiring aircraft to operate at different altitudes or flight levels within controlled airspaces. For low altitudes (below FL290), the vertical separation minimum is 1000 feet. Above FL290, 1000 feet vertical separation are available for aircraft that meet the equipment requirements of Reduced Vertical Separation Minimums (RVSM) [7], otherwise 2000 feet vertical separations are required.

— *Lateral separation* is the distance that has to be kept between aircraft operating at the same flight level, usually expressed in terms of nautical miles. It is ensured by requiring operation on different routes or in different geographical locations.

— *Longitudinal separation* is the required spacing between aircraft following the same or diverging tracks at the same altitude, expressed in units of time or miles. Basically, longitudinal separation is achieved by applying a speed control, ensuring that the speed of the following aircraft does not exceed the speed of the leading one. In some cases, reduced separation can be applied if the leading aircraft is maintaining a higher speed than the following one.

Aircraft are considered to be in *conflict* when these separation norms are violated. Thus, we can conclude that at any given time, each aircraft reserves a bounded block of airspace that can be defined as a three-dimensional cylinder, referred to as *Cylindrical protection volume* (CPV). In order to avoid aircraft conflicts, ATC has to make sure that the CPV of one aircraft does not overlap any other CPV.

An efficient management of airspace capacity, potential conflicts, congestion and induced delays, is a primordial issue faced by ATM. In order to ensure an optimized use of different air traffic resources and to maintain safe and efficient flights, the ATM process is performed through three levels of management:

— *strategic level* is performed by ATM centers from several hours to several days before real time operations. It is dedicated to helping the Air Navigation Service Providers (ANSPs) to better predict the capacities of their control centers in order to balance capacity and demands. During this phase, the traffic of the day is predicted and scheduled. The strategic phase must deal with the inherent uncertainties caused essentially by wind variation in order to take better decisions.

— *pre-tactical level* takes place few hours before real time operations and aims to optimize the overall ATM network performance, while minimizing delays and costs. During this phase, the strategic plan is updated using more accurate information on expected traffic conditions and demands, available capacity and weather forecast.

— *tactical level* takes place during the real time operations. During this phase, the ATC is in charge of resolving conflicts between aircraft, being already en route, as well as preventing them from entering a restricted area.

7. designates a particular volume of airspace where a reduction of the vertical separation standards at high altitudes is applied. RVSM airspace is reserved for aircraft with specially certified altimeter and autopilot systems

Significant efforts are made to enable greater flexibility and adaptability in airspace and flight operations, along with ensuring improved traffic flow, capacity, efficiency, and safety. A key part is the implementation of adequate communication, navigation and surveillance tools. The next section explores different systems used in supervising air traffic.

1.1.4 Surveillance, communication and navigation systems

ATC systems are responsible for satisfying a set of fundamental functions such as traffic surveillance, communication, navigation and information gathering in order to conduct air traffic safely and efficiently. The main systems implemented by the ATC in order to organize and structure the airspace are given below. First, controllers observe continuously the traffic situation through a surveillance system. Then, they issue clearances to aircraft through a communication system. Finally, the aircraft follow the cleared route using a navigation system.

1.1.4.1 Surveillance systems:

Surveillance systems are used in order to monitor the air traffic situation and to prevent collisions. For several years, *radars* have been the fundamental mean of surveillance used for most domestic airspaces. Two types of radar can be distinguished:

— *Primary surveillance radar* sends out a pulse of radio energy that are reflected by aircraft. Thus, controllers get the range and bearing of each detected aircraft. The main advantage of the primary radar is that no action is required from the aircraft to provide a radar return. However, their disadvantages are that, firstly, the detected aircraft can not be identified and no altitude information is given. Secondly, it is prone to false targets such as rain, birds, etc.

— *Secondary surveillance radar* requires the target aircraft to be equipped with an operating transponder. The transponder relies on each interrogation signal by transmitting a pulse response containing the identification of the responding aircraft and other aircraft data.

Another more recent ground-based surveillance technique is the *multi-lateration* (MLAT). MLAT relies on a set of ground stations that are strategically located around an airport in order to detect each aircraft transponder signal. MLAT targets are updated once per second, compared with about four-to-twelve second intervals for the radar targets.

1.1.4.2 Communication systems:

Communication systems provide the contact between different ATC components. It ensures both air-to-ground and ground-to-ground communications. The current ATC system relies basically on voice radio communications between traffic controllers and pilots, using the very high frequency range (VHF) in addition to high frequency (HF) for oceanic airspaces. Because of the nature of voice radio communications, only one transmission can be conducted at a time which limits the number of aircraft that can be managed on

a single frequency. Regarding the continuous increase of air traffic, voice communications are approaching saturation, especially during peak traffic periods.

1.1.4.3 Navigation systems:

Navigation systems enable aircraft to fly exactly the planned route. There are several types of ground-based navigation systems such as NDB, VOR/DME and ILS. These systems allow the aircraft to navigate along fixed routes.

Despite the use of all the above-mentioned techniques and procedures in order to maintain air traffic safety and efficiency, the ATM system is still constrained by several limitations due to controller's workload and space saturation.

In fact, The International Air Transport Association (IATA) expects 7.2 billion passengers to travel in 2035, which corresponds to nearly the double of the 3.8 billion air travelers in 2016 [48]. As a direct consequence, the Airbus Global Market Forecast estimates a 4.4% global annual air traffic growth for the next 20 years [4].
From the other side, in a control sector, the higher the number of aircraft, the more the control workload increases (in a nonlinear manner). A limit exists beyond which the controllers in charge of a control sector are unable to accept additional aircraft, obliging these new aircraft to travel around the sector, moving through less charged neighboring sectors. In this case, the sector is said to be saturated. This critical state should be avoided, as it provokes a cumulative overloading phenomenon in preceding sectors which can back up as far as the departure airport.

Thus, challenges to accommodate the increasing traffic in an already saturated airspace, to increase controller's productivity and to improve the whole system efficiency, are continuously progressing. Some of the future trends to reach a more performant and efficient airspace are described in the next section.

1.1.5 Future trends in Air Traffic Management

Research aimed at improving the capacity, efficiency and performance of ATM system has attracted considerable attention in recent years, particularly in the United States and in Europe. Currently, NASA, MIT and Georgia Tech are involved in work on the subject within the framework of the Next Generation air transportation system (NextGen) project. In Europe, the DSNA, the DLR, the NATS, the NLR, etc are involved in similar activities linked to the Single European Sky ATM Research (SESAR). These projects share several concepts in order to reach modernization in both ATC procedures and technology used. The new ATM system will rely on several paradigms in order to make ATC more efficient and flexible; some of them are listed bellow.

***4D Aircraft Trajectories* (4D-ATs)** consists on designing aircraft trajectory in four dimensions: lateral (latitude and longitude), vertical (altitude) and time. With a 4D

trajectory capability, controllers will have a synchronized view of the intended trajectory, which will improve its accuracy and enable precise adjustments.

***Trajectory Based Operation* (TBO)** is a new concept that leverages improvements in navigation accuracy, communications, surveillance, and automation in order to decrease the uncertainty of a 4D-AT. ATM will manage aircraft trajectories in an adapted airspace design that will no longer be constrained by artificial boundaries such as sectors or national borders. Furthermore, controllers will no longer rely on clearance-based methods of control. Instead, a more flexible procedure will be applied.

***Free Flight Concept* (FFC)** is a concept being developed to replace the current ATC control procedures by a new paradigm based on a non-centralized control. FFC allows aircraft to select their optimal route, altitude and speed in real time. In fact, parts of airspace are dynamically and automatically reserved in a distributed way using computer communication to ensure the required separation between aircraft. Thus, performances in terms of cruising times and fuel consumption will be optimized.

The integration of these new concepts into the existing airspace systems remains one of the largest challenges faced by ATM community. Thus, new reliable technologies have to be developed and implemented in order to facilitate the integration of the aforementioned modernizations. Several enhancements for dealing with these issue are listed below.

In *communication* The ability to exchange data between the aircraft and the ground via Data-Link communications significantly improves aviation communication, particularly in oceanic airspaces. Data-Link communications enable not only the generation of automated messages and ground side reception, but also allow message routing and transmission to aircraft avionics. Therefore, due to more efficient and accurate interactions via Data-Link communications, the productivity of controllers may be improved leading to a higher airspace capacity. One of the most widely known Data-Link systems is the *Controller-Pilot Data-Link Communications* (CPDLC). CPDLC is a two-way Data-Link system by which aircraft and air traffic controllers can exchange messages such as requests, clearances, emergencies, weather information, etc.

In *surveillance* A new surveillance system is introduced in the light of the implementation of satellite technologies, known as the *Automated Dependent Surveillance*, typically for use in areas where radar coverage does not exist. It is Automatic since it does not require any pilot or controller input to function, and Dependent because it requires operating airborne equipment. Using ADS, the aircraft automatically transmits its position report and intent data from its on-board navigation systems. There are different types of ADS systems.

— ADS-A (Addressed) where the aircraft transmits position reports to the ground only when requested from ATC.

— ADS-C (Contract) where the aircraft transmits position reports periodically at defined intervals.
— ADS-B (Broadcast) is the most advanced ADS system. ADS-B broadcasts an aircraft's position, altitude, velocity and other aircraft data, and transmits the broadcast data at hight update rates (1 second). These data are received by other equipped aircraft in the surrounding space, as well as by ground stations and ATC.

The North Atlantic Region is planned to be the first place where satellite based ADS-B surveillance will be used. In fact, on 14 January 2017 Iridium Communications Inc. succeed in launching its first 10 Iridium NEXT satellites into Low Earth Orbit [52]. This achievement is the start of a series of Iridium NEXT launches scheduled over the next 18 months. The main goal is to expand air traffic surveillance by installing ADS-B receivers on a constellation of about 70 Low Earth Orbit satellites in order to support real-time ADS-B operations within oceanic regions [31]. Furthermore, it is estimated that using ADS-B, air traffic surveillance will cover about 4 million square kilometers of airspace. This extension of surveillance coverage will save airline customers an estimated of $374 million in fuel costs by 2020 due to enabling more fuel-efficient routings, especially in oceanic airspaces [17].

In *navigation* A more precise and accurate navigation aid has been implemented, known as the Global Navigation Satellite Systems (GNSS). GNSS is a network of orbiting satellites, which provide together a global coverage. So far, two GNSS have been installed and started to be used, namely the United States' Global Positioning System (GPS) and the Russian system GLONASS. China and Europe are also developing systems, BeiDou and Galileo respectively, which are expected to be operational by 2020.

Finally, one can conclude that the future of ATM systems will mainly rely on distributed structures based on sharing the separation and management tasks between controllers and flight crews.

In this work, we aim at improving the air traffic situation particularly in the North Atlantic airspace (NAT). Therefore, several new approaches, in the framework of ATM modernization, are proposed to address air traffic improvement in NAT. In the next section, a detailed focus on NAT features is presented in order to outline its specificities and constraints.

1.2 Air Traffic Control in North Atlantic oceanic airspace

After describing the global ATM system via its components and procedures, we restrict the scope to the air traffic situation in the North Atlantic Airspace (NAT) which is the main focus of the present study.

1.2.1 NAT airspace

The North Atlantic airspace (NAT) is considered to be the most congested oceanic airspace since it connects two densely-populated areas i.e. Europe and North America. In

order to control this vast airspace, it was divided into five Oceanic Control Areas (OCAs), namely Reyjavik, Shanwick, Gander, Santa Maria Oceanic and New York Oceanic. Each OCA is supervised by an independent Oceanic Area Control Center (OACC). Since February 04^{th}, 2016 the Bodo Oceanic Control Area has been included to the NAT airspace [31] (Figure 1.2).

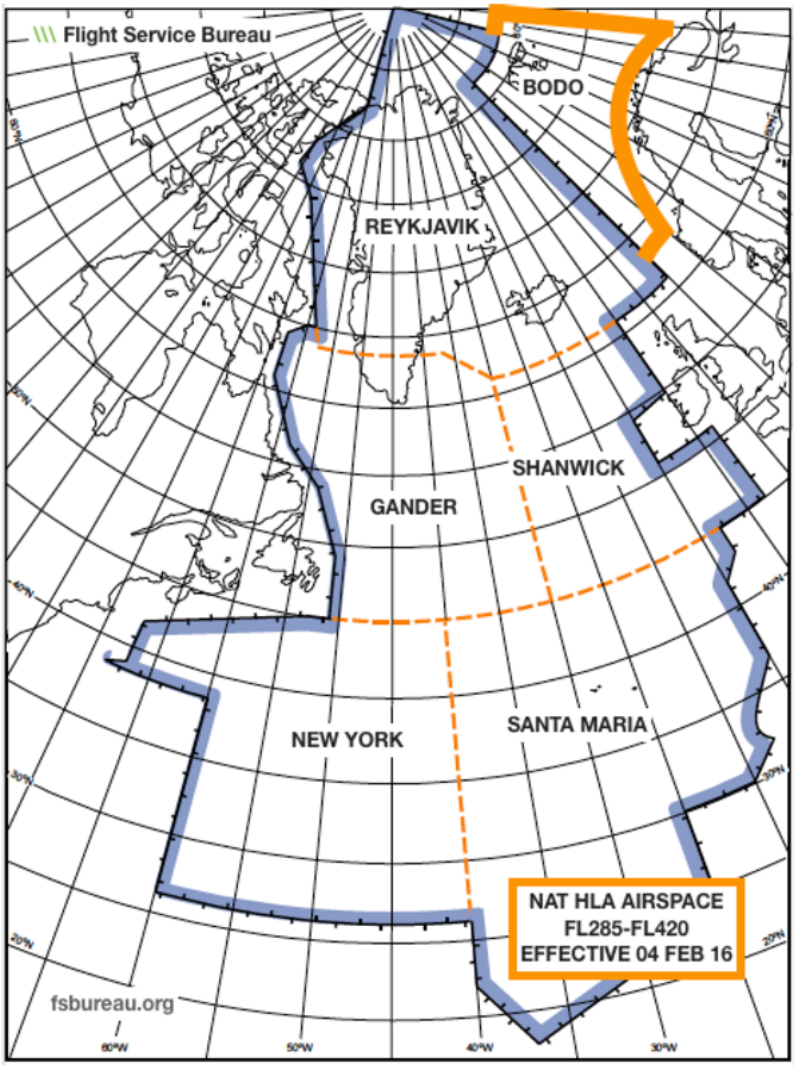

FIGURE 1.2 – NAT airspace boundaries [31]

The OACCs have to deal with several particularities of this specific oceanic airspace. First, air traffic density crossing the NAT is steadily increasing. According to [8], there are currently about 1400 flights that cross the NAT daily and the traffic density is steadily increasing.

In addition to this, aircraft operating in the NAT are subject to very strong winds induced by the jet streams. Jet streams are fast air currents forming a tube in the upper atmosphere, typically between $20,000$ and $50,000$ feet and running mainly in east direction, with an average speed around 100kts, and up to 200kts. Ideally, eastbound flights would prefer to exploit the jet stream strong tailwind, while westbound flights

would rather avoid the jet stream headwind. As a result, the traffic demand becomes highly concentrated within the two flows.

Finally, most parts of the NAT airspace suffer from the lack of surveillance means as flights cannot be tracked by the traditional radars. It is therefore crucial to establish safe, robust and optimal procedures in order to organize this huge traffic volume.

A set of high standards of navigation performance and accuracy, referred as Minimum Navigation Performance Specifications (MNPS), is established in a part of the NAT, between FL285 and FL420, referred to as NAT MNPS airspace. In February 2016, this portion of airspace is re-designed as NAT High Level Airspace (NAT HLA) [31]. Basically, all flights operating within the NAT HLA airspace are required to achieve the highest standards of horizontal and vertical navigation performance and accuracy.

1.2.2 Organized Track System

Due to the passenger demand and time zone differences, air traffic in the NAT is concentrated within two major opposite-directional flows: the westbound flow departs from Europe in the morning and has the peak traffic crossing the $30W$ longitude between 11:30 Coordinated Universal Time (UTC) and 19:00 UTC; the eastbound flow departs from North America in the evening and has the peak traffic crossing the $30W$ longitude between 01:00 UTC and 08:00 UTC.

In order to provide NAT air traffic with the best services, a system of pre-defined tracks referred as the Organized Track System (OTS) is introduced in 1965 [1]. The OTS is created daily and independently for eastbound and westbound traffic, taking into account the position of the jet streams, as to accommodate as many flights as possible close to their minimum time tracks and altitude profiles (Figure 1.3). The night-time OTS is produced by the Gander OACC center while the day-time is performed by the Shanwick OACC center.

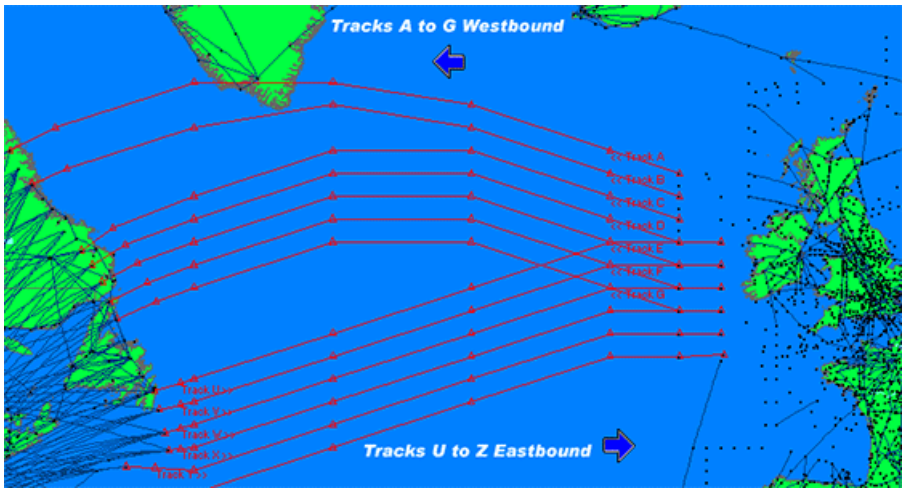

FIGURE 1.3 – Eastbound and westbound OTS tracks [115]

Each OTS includes 5 to 7 nearly parallel tracks spread within flight levels from FL310 to FL390 [31]. About 10 way-points are fixed for each track. The appropriate OACC is in charge of OTS construction once that basic minimum time tracks have been determined. To do so, the position of the OTS track takes into account airline preferred routes and airspace restrictions such as danger areas and military airspace.

The OTS track construction relies on a set of Collaborative Decision Making (CDM) procedures. CDM process starts with a former-applied system in the NAT region, referred to as Preferred Route Message (PRM). All NAT operators are asked to submit information about their optimum tracks, PRMs, of all their flights intending to operate during the upcoming peak traffic period, in order to enable oceanic planners to take into consideration operators preferred routes in the OTS construction. This information should be provided as far in advance as possible, in a predefined format. Then, the corresponding agency (Gander OACC for eastbound tracks and Shanwick OACC for westbound tracks) publish the proposed tracks on an Internet site so that the interested parties can view and discuss. OACC planners also cooperate with adjacent OACCs and domestic ATC agencies to make sure the proposed system is pertinent. The publishing agency does consider any comments and performs any agreed changes in the final track design [31].

It is important to notice that use of OTS tracks is not mandatory. Currently, about half of NAT flights operate on the OTS [31]. Nevertheless, aircraft may fly on random routes which remain clear of the OTS or plan a route which crosses the OTS. However, in the latter case, operators must be aware that significant changes in their flight routes are very likely to be required during most of the OTS traffic periods.

Flights intending to use the OTS have to be planned to enter a predefined OTS track at a predefined flight level and follow it at a constant speed to the NAT HLA exit unless a change to the flight plan is requested and approved by the NAT controllers. However, such requests, especially those including changing OTS track, often get rejected from a safety perspective because of the large separation norms.

The OTS is the most significant route structure within the NAT HLA. Furthermore, other route systems exist within and adjacent to NAT HLA. Due to their low traffic frequency, these structure will not be addressed in the present study.

1.2.3 Separation standards in NAT

Separation norms refer to the minimum distance that must be kept between aircraft operating in controlled airspace and are typically defined for vertical, lateral and, in some cases, longitudinal separation. As in a non-radar environment aircraft position prediction is less precise, separation norms in oceanic airspaces are much higher than in the continental ones: lateral separation is extended to 60 NM (111.11 km), compared to 5 NM in continental airspace, and vertical separation is 1000 feet (304.8 m) if below $FL410$ and 2000 feet if above $FL410$ [100].

The OTS is constructed to comply with these separation norms: OTS tracks maintain the lateral separation (60 NM) and OTS flight levels are separated by 1000 feet (tracks are below $FL410$) [31]. In addition to this, once aircraft enter the OTS, controllers have to

ensure longitudinal separation which represents the hold time between two aircraft in the same track. The longitudinal separation is 10 minutes between two aircraft maintaining the same speed and following the same track, and becomes 15 minutes if an aircraft changes its track [101]. The three aforementioned separation standards are presented in Figure 1.4.

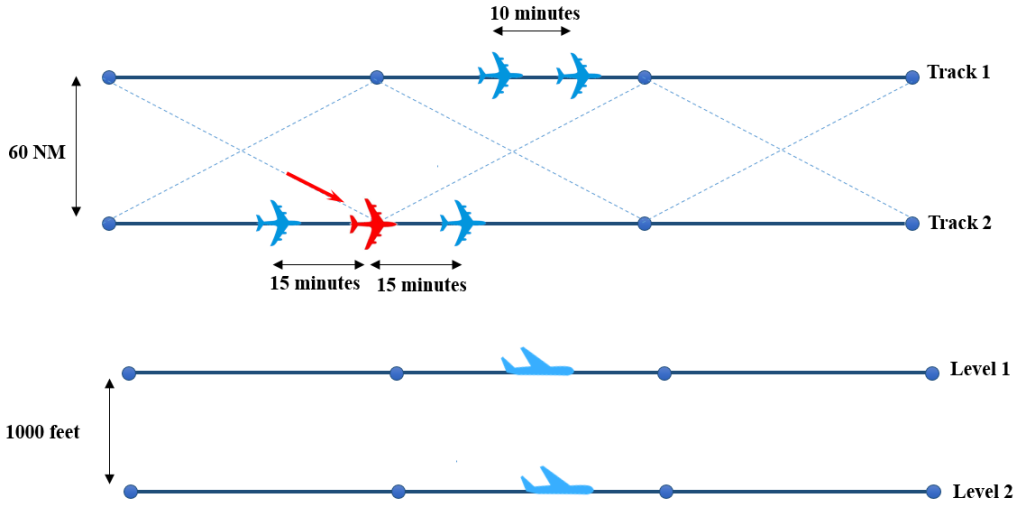

FIGURE 1.4 – Separation standards in oceanic airspace

This separation standard is adjusted to be applied with aircraft maintaining different speed assignments. In fact, the longitudinal separation between two aircraft following the same or diverging tracks, is assessed in terms of the differences between their ATAs (Actual Times of Arrival) or ETAs (Estimated Times of Arrival) at common way-points [31]. Basically, this separation is ensured by applying the Mach number technique (Section 1.1.2). Based on a practical experience, it has been proven that when two successive aircraft along the same track are maintaining the same Mach Number, they are more likely to maintain a constant time interval between each other than when using other techniques [31]. Thus, when the Mach number technique is applied, the minimum longitudinal separation is the following [51]:

— 10 minutes, or
— between 9 and 5 minutes inclusive, provided that the preceding aircraft is maintaining a true Mach number greater than the following aircraft in accordance with the following:
  — 9 minutes, if the preceding aircraft is 0.02 Mach faster than the following one;
  — 8 minutes, if the preceding aircraft is 0.03 Mach faster;
  — 7 minutes, if the preceding aircraft is 0.04 Mach faster;
  — 6 minutes, if the preceding aircraft is 0.05 Mach faster;
  — 5 minutes, if the preceding aircraft is 0.06 Mach faster.

In the frame of ATM technology modernization (Section 1.1.5), a continuous program of monitoring the safety and efficiency of flight operations throughout the NAT region is

undertaken. Thus, new plans, referred to as North Atlantic Data Link Mandate (NAT DLM) plans, are discussed to ensure the maintenance and further enhancement of both safety and traffic capacity of the airspace. The main goal of these plans is that the equipment rate of ADS-B on NAT airspace will be 83% in 2018, 95% in 2019, and will reach 100% by January 1, 2020 [109]. Based on these goals, current plans are in progress and have started to be effective. The first stage was established in 5 February 2015 where ADS-C and CPDLC equipage or equivalent (ADS-B) become mandatory for all aircraft operating between FL350 and FL390 on all NAT OTS tracks [31]. Then, on Dec 15, 2017 the mandate incorporates FL350 to FL390 throughout the NAT region [30]. The last stage is planned for Jan 30, 2020 where the mandate will incorporate FL290 and above throughout the NAT region [31].

Basically, such new requirements will improve the air traffic surveillance performances, as well as controller monitoring and intervention capabilities. Thus, a reduction on lateral and longitudinal separation minima, refereed to as RLatSM and RLongSM respectively, can be performed, and was part of the current and future plans of ICAO NAT region.

The first phase has been effective since Dec 2015, and the lateral separation has been reduced to 25 NM in NAT region. Practically, this reduced lateral separation minima (RLatSM) is accomplished by establishing one-half-degree spacing between OTS center tracks, instead of one degree, within the NAT OTS between FL350 and FL390 (Figure 1.5).

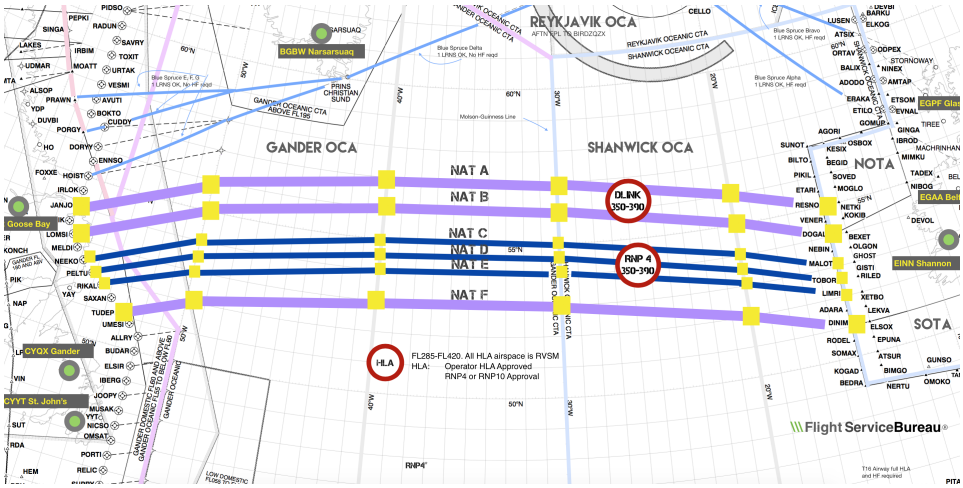

FIGURE 1.5 – NAT tracks with RLatSM [114]

Obviously, only aircraft with required navigation performance approval are eligible to operate on these one-half-degree spaced tracks. Furthermore, RLatSM is established between all OTS tracks between FL350 and FL390 from February 2018 [16].

Furthermore, thanks to ADS-B accuracy and performance, ATC is able to supervise and separate aircraft with improved precision and timing. For this reason, a significant reduction in the longitudinal separation standards (RLongSM) can be achieved. In NAT, in particular, we assume that the longitudinal separation of consecutive aircraft following the same track can be reduced from 10 minutes to 2 minutes, and from 15 minutes

to 3 minutes if an aircraft changes its track (Figure 1.6). This assumption is made with analogy with the reducing of the lateral separation to 25 NM. In fact, 2 minutes and 3 minutes represents almost the required times for the fastest commercial aircraft ($v_{max} \approx 600kts = 10NM/min$) to over fly 20 NM and 30 NM, respectively. Moreover, reducing 25 NM to 20 NM is conceivable since we are considering consecutive flights in the same track.

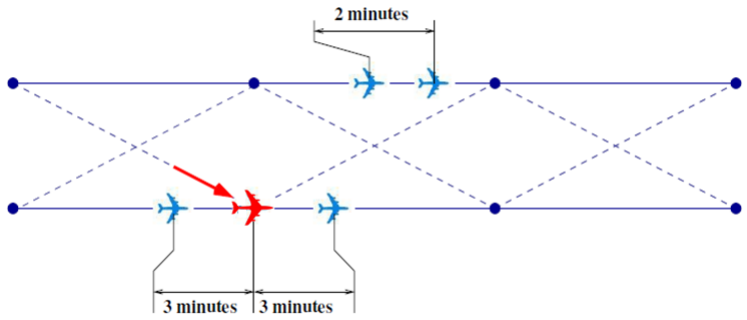

FIGURE 1.6 – Reduced longitudinal separation in NAT

To sum up, the application of reduced separation standards reveals several benefits that are considered and examined in the present work.

1.2.4 Current NAT operator procedures

All flights intending to cross the NAT are required to submit a flight plan to the corresponding OACC. Each flight plan has to contain all relevant information related to the flight as described in Section 1.1.2. Each flight route has to be very well described so that specified degrees of longitude (20W, 30W, 40W etc.) are crossed at whole degrees of latitude. Then, in real-time operations, each flight has to follow the successive declared way-points on a great circle route. However, when crossing areas where ADS-B surveillance and VHF voice coverage are available, airspace users are able to plan free routes through each relevant FIR between defined entry and exit points [31].

Currently, about half of the NAT traffic utilizes the OTS [31]. In the remaining of this section, we only consider flights that plan to operate on OTS tracks. Such flights have to point out this information in the flight plan, and specify its desired track, desired step climbs and Mach changes. In addition, it is required to estimate its entry time on the desired track as well as the entry time in the Oceanic FIR boundaries. Furthermore, operators are required to indicate their aircraft and crew capabilities such as ADS-B or NAT HLA Approval in the flight plan. Such information enable ATC to apply appropriate separation criteria to the flight, and thereby ensure that the full benefits of current capacity and safety improvement in the NAT are available for all appropriately equipped flights.

In real-time operations, all OTS flights should operate on great circle trajectories joining OTS track way-points at predefined FLs and at constant predefined Mach. The

planned Mach and FL for the OTS track should be notified to the concerned OACC at the last domestic reporting point prior to NAT entry. Then, the assigned FL and Mach must be delivered while the aircraft is within radar coverage, namely prior to entering NAT.

Oceanic clearances for many NAT flights are of a strategic nature, and basically a single flight level and Mach are strategically assigned for the entire crossing. Nevertheless, tactical surveillance and procedural control are sometimes exercised in the NAT HLA especially for performing step-climbs as fuel burn-off makes higher levels more optimal. Thus, pilots are required to request ATC approval for any en-route FL or Mach modification, even when such modifications are specified beforehand in the flights plan. Such modifications can be approved by ATC or denied depending on potential traffic conflicts. Furthermore, FL and Mach changes are only allowed at way-points. When so approved, pilots should initiate the climb without delay and report to ATC immediately upon leaving the old and once reaching the new cruising levels, unless ADS-B communication is used. It can be noticed that within the NAT, aircraft are only allowed to climb, and descent is denied in order to satisfy the optimal en-route fuel consumption flight profile. Practically, 2-FL climbs are rarely performed. Besides, speed difference between two successive way-points do not normally exceed 0.02 Mach [31].

In some case, pilots request a re-routing inside the OTS tracks in order to exit the OTS closer to their destination or to join another track involving more preferable wind. Such requests often get rejected by the ATC because of the traffic density, and from the safety perspective because of the large separation norms that must be imposed to re-routing aircraft.

Flights within the NAT controlled airspace are required to request oceanic clearances from the responsible OACC unit. It is recommended that oceanic clearances be requested at least 40 minutes prior to the Oceanic Entry Point (OEP), and the clearance should be given 20 minutes before the estimated time of reaching the OEP [31]. The clearance contains agreed flight information such as route, flight level and Mach number, that have to be respected by the pilot. The ATC usually tries to preserve the requested or planned profiles, which is not always possible in high-density traffic conditions. Thus, when requesting an oceanic clearance, the pilot should notify all the acceptable flight levels, alternative tracks and speeds. Furthermore, if the OEP on which the flight is cleared differs from that originally requested and/or the oceanic flight level differs from the current flight level, the pilot is responsible for requesting the necessary domestic re-clearance in order to be in compliance with its oceanic clearance when reaching the OEP. Once reaching an OEP, pilots have to deliver to ATC their position reports at all the designated points listed in the flight plan. ATC has to get positional information at approximately hourly intervals, in order to accommodate varying types of aircraft and varying traffic and meteorological conditions. Unless position reports are provided via ADS-B, if the estimated time for the next position such as reported to ATC, changes by more than three minutes, a revised report must be transmitted to the concerned ATC as soon as possible. In addition, pilots are required to report any change in cruise level as

soon as possible.

To sum up, ATC units are in charge of safely conducting air traffic across the NAT. However, they are exposed to several difficulties caused by the following particularities of the NAT:

— high traffic density and airspace congestion especially at peak hours.
— direct controller-pilot communications and radar-based surveillance are difficult to perform for the most part of the NAT.
— strong jet stream wind causing a perturbation on flight prediction.

These difficulties yield to very restrictive procedures imposed to aircraft intending to cross the NAT:

— an OTS structure with predefined track, FL and Mach assigned to aircraft, and any change is denied unless approved by ATC.
— requests for re-routing within OTS tracks often get rejected.
— very large separation norms.

For sure, these rigid rules negatively affect the airspace efficiency and are the direct cause of the following deficiencies:

— limit the number of flights authorized to cross the NAT.
— generate flight delays.
— cause flight deviations from the desired trajectories.
— result in additional congestion in the domestic airspace.

Thus, OACC planners and ATC units make every effort to optimize airspace efficiency in order to limit the aforementioned drawbacks.

In this work, we propose two new approaches in the framework of ATM modernization, to address air traffic improvement in the NAT. Each of these approaches is modeled as an optimization problem that we resolve using a meta-heuristic optimization method, called simulated annealing. The simulated annealing principle is described in the next section. This algorithm is adopted, afterwords, in order to address our particular NAT traffic organization problem.

1.3 Optimization approach used in the resolution algorithm

In this section, we will present the methodological principles involved in the optimization, before introducing the main principle of the Simulated Annealing (SA) algorithm which is applied in the present work.

1.3.1 Methodological principles in optimization

When faced with a real optimization problem, we must analyze the problem in a precise manner in order to choose the best method to use. Real optimization problems correspond to needs observed in industrial or operational contexts, and aim to improve the performances of an economic process connected with an operational company or management organization. In practice, these problems are identified by domain experts

who wish to develop an optimization principle in order to improve the performance of a system.

1.3.1.1 Modeling

The first stage in the optimization process consists of modeling the real problem using a mathematical abstraction which is as faithful as possible (see figure 1.7). Using this

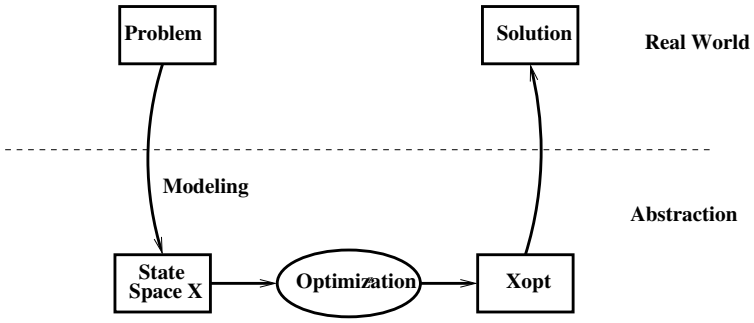

FIGURE 1.7 – Modeling process

abstraction, it becomes possible to develop solution algorithms which can be executed on a computer. This optimization process produces a set of solution points, which can then be implemented in the real world. In the past, because of the limitations of optimization algorithms, it was necessary to use models which were somewhat different from reality but for which solution methods existed. The solutions produced could therefore be rather different from the true solution in the real world. A classic example involves linear programming, for which we have efficient solution algorithms, but which requires linear modeling of the problem.

The modeling stage, then, consists of characterizing the state space and the objective space.

State space The state space represents the set of parameters of the system upon which we may act in order to optimize one (or more) objective(s). Examination of the properties of the state space then assists us in the choice of a suitable optimization method.

In most industrial optimization problems, the variables of the state space must remain within a sub-domain defined by a set of constraints. We obtain the following general model:

$$\begin{cases} \min y = f(\vec{x}) \\ \vec{x}_{opt} \in \mathcal{A} \subset \mathcal{X} \end{cases}$$

where $\mathcal{X}$ is the state space and $\mathcal{A}$ the feasible space delimited by the constraints. By studying the properties of $\mathcal{X}$ and $\mathcal{A}$, we can determine certain characteristics of the solution algorithm. Thus, the properties of connectivity and convexity of the admissible domain $\mathcal{A}$ are extremely important in guiding the choice of an optimization method. Within the group of convex state spaces, there is an extremely interesting sub-class for which the admissible domain is delimited by a set of hyperplanes making up a polytope. If,

moreover, the criterion is also linear, then we have a linear optimization problem for which we may use the Danzig simplex method, for example. In the same way, the properties of connectivity of the state space determine whether or not it will be necessary to allow the optimization method to violate constraints in order to transit from a component to another, to finally reach the optimum solution.

Based on the nature of state variables, we may group industrial optimization problems into three categories:

1. **continuous problem**
$$\mathcal{X} = \mathcal{U}_1 \times \mathcal{U}_2 \times ... \times \mathcal{U}_m$$
$$\mathcal{U}_i \subset \mathbb{R}\, i = 1, 2, .., m$$
We talk of optimization in a functional space when m is infinite (as in the case of trajectory optimization).
2. **discrete problem**
$$\mathcal{X} = \mathcal{I}_1 \times \mathcal{I}_2 \times ... \times \mathcal{I}_n$$
$$\mathcal{I}_i \subset \mathbb{Z}\, i = 1, 2, .., n$$
3. **mixed problem**
$$\mathcal{X} = \mathcal{U}_1 \times \mathcal{U}_2 \times ... \times \mathcal{U}_m \times \mathcal{I}_1 \times \mathcal{I}_2 \times ... \times \mathcal{I}_n$$

Mixed problems are the most difficult of the three classes to work with.

One very important point characterizing the state space is its dimension. Generally, the higher the dimension n of $\mathcal{X}$, the harder it will be to find the optimum.

Objective space The objective space represents the set of criteria which we wish to optimize. Based on the dimension of this space, we can identify two classes of problems:

— Mono-objective problems: this is the simplest case, insofar as a single criterion needs to be optimized and allows a total order relation between points of the space state in terms of the criterion. The objective function is thus a function of $\mathbb{R}^n$ in $\mathbb{R}$.

— Multi-objective problems: in this case, we need to optimize several criteria, associated with each point of the state space, simultaneously. The most critical aspect of such problems is linked to the loss of the total order relationship between the solutions. Effectively, the objective function is now a function of $\mathbb{R}^n$ in $\mathbb{R}^m$, where m represents the dimension of the objective space.

In the case of mono-objective problems, we may also characterize the objective space in relation to the optima of the criterion. We can then distinguish between two types of optima:

1. **Global optimum:** $\vec{x}^*$
$$f(\vec{x}^*) \leq f(\vec{x})\ \forall \vec{x} \in \mathcal{X}$$
$\mathcal{X}$ complete state space.

2. **Local optimum:** $\tilde{x}$

$$f(\tilde{\vec{x}}) \leq f(\vec{x}) \ \forall \vec{x} \in \mathcal{V}(\tilde{\vec{x}})$$

$\mathcal{V}(\tilde{\vec{x}})$ vicinity of $\tilde{\vec{x}}$.

Within the context of industrial optimization problems, we seek to determine global optima and to avoid being trapped on local optima.

All optimization methods require variations in the criterion across the state space in order to be directed towards the optima. This is the principle of locality in optimization.

Considering the separability of the objective function also allows us to simplify the resolution of an optimization problem. Let us take a function $f(\vec{x})$ to minimize for the space $\mathcal{X}$. If $f(\vec{x}) = f\{g(\vec{x}), h(\vec{x})\}$ and if

$$\left\{ \begin{array}{ll} min\ f(\vec{x}) \\ \vec{x} \in \mathcal{X} \end{array} \right. = f \left\{ \begin{array}{ll} min\ g(\vec{x}) \\ \vec{x} \in \mathcal{X} \end{array} \right. , \left. \begin{array}{ll} min\ h(\vec{x}) \\ \vec{x} \in \mathcal{X} \end{array} \right\}$$

then the function f is separable. This property allows us to independently optimize functions g and h, which may be simpler to process.

The principles of evaluation of the criterion also enable us to select more or less suitable resolution algorithms. We may distinguish between three different types of cases:

1. Criterion accessible in analytical form. This is the most "comfortable" case, but is unfortunately rare in the context of real problems. By canceling the associated gradient, it is sometimes possible to obtain an analytical form of the optimum (textbook case).
2. Criterion evaluated through numerical computations using real data. This is the most frequent of our three cases, in which we attempt to extract additional information to guide the algorithm (gradient, Hessian, etc.).
3. Criterion evaluated using a complex simulation process. In this case, where evaluation of the criterion is often costly in terms of resources, it is not possible to obtain additional information and we use methods which do not need a criterion value in order to converge.

1.3.1.2 Complexity

The complexity of resolution of an optimization problem is linked to the number of operations needed to determine the optimum. In the case of combinatory optimization problems, we consider an instance of a problem of size n for which a resolution algorithm has been proposed. This algorithm will execute a number K of operations to process the problem. This number K is generally dependent on n.

In the same way, we classify optimization problems based on the best algorithms for their treatment. Thus, we have a class of NP_Hard problems, which cannot be solved using a known polynomial algorithm. An examination of the complexity associated with an optimization problem allows us to select an optimization method.

1.3.1.3 Computation time

Given that each optimization method requires a minimum computation time, it is important to be aware of the time we have available to produce a solution. As an example, in the context of optimization of flight plans for a day, we have 24 hours. To solve conflicts between aircraft, we have 3 minutes; finally, for a problem concerning satellite frequency allocations, we must produce a solution in under 50 milliseconds. In cases where this constraint is critical, we need to look at parallel methods.

1.3.2 Optimization algorithm

Optimization methods may be divided into two categories: those which allow us to identify a local optimum, known as local methods, and those which are used to determine a global optimum, known as global optimization methods.

Then, depending on the mechanism used to move within the state space, we differentiate between deterministic and stochastic methods.

Several optimization algorithm are adopted and applied to resolve trajectory planning and air traffic management problems. Among deterministic methods, we find enumeration, Branch&Bound, the tunneling methods, etc. In stochastic methods, we find Taboo search, stochastic Branch&Bound, genetic algorithm, etc.

A wide variety of optimization algorithms exists, each suited to a certain category of problems. In this thesis, we apply another well-known stochastic method, that is the Simulated Annealing (SA), which is deeply described in this section.

In the early 1980s three IBM researchers, Kirkpatrick, Gelatt and Vecchi [59], introduced the concepts of annealing in combinatorial optimization. These concepts are based on a strong analogy with the physical annealing of materials. This process involves bringing a solid to a low energy state after raising its temperature. It can be summarized by the following two steps (see Figure 1.8):

— Bring the solid to a very high temperature until "melting" of the structure;
— Cool the solid according to a very particular temperature decreasing scheme in order to reach a solid state of minimum energy.

In the liquid phase, the particles are distributed randomly. It is shown that the minimum-energy state is reached provided that the initial temperature is sufficiently high and the cooling time is sufficiently long. If this is not the case, the solid will be found in a metastable state with non-minimal energy; this is referred to as *hardening*, which consists in the sudden cooling of a solid.

Simulated annealing is an extension of local search optimization and Metropolis algorithm. The two latter algorithms are introduced in Appendix A.

In the SA algorithm, the Metropolis algorithm is applied to generate a sequence of solutions in the state space S. To do this, an analogy is made between a multi-particle system and our optimization problem by using the following equivalences:

— The state-space points (solutions) represent the possible states of the solid;
— The function to be minimized represents the energy of the solid.

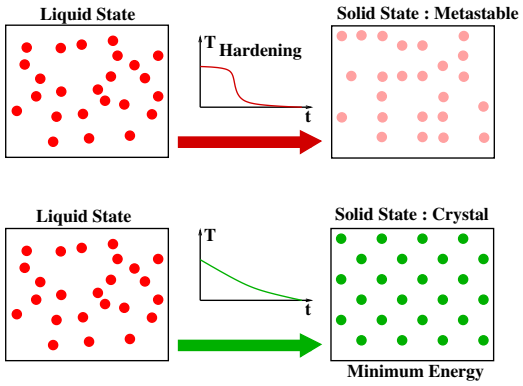

FIGURE 1.8 – When temperature is high, the material is in a liquid state (left). For a hardening process, the material reaches a solid state with non-minimal energy (metastable state; top right). In this case, the structure of the atoms has no symmetry. During a slow annealing process, the material reaches also a solid state but for which atoms are organized with symmetry (crystal; bottom right).

A control parameter c, acting as a temperature, is then introduced. This parameter is expressed with the same units than the objective that is optimized.

It is also assumed that the user provides for each point of the state space, a neighborhood and a mechanism for generating a solution in this neighborhood. We then define the acceptance principle:

Let (S, f) be an instantiation of a combinatorial minimization problem, and i, j two points of the state space. The *acceptance criterion* for accepting solution j from the current solution i is given by the following probability:

$$Pr\{\text{ accept } j\} = \begin{cases} 1 & \text{if } f(j) < f(i) \\ e^{\left(\frac{f(i)-f(j)}{c}\right)} & \text{else.} \end{cases}$$

By analogy, the principle of generation of a neighbor corresponds to the perturbation mechanism of the Metropolis algorithm, and the principle of acceptance represents the Metropolis criterion.

A *transition* represents the replacement of the current solution by a neighboring solution. This operation is carried out in two stages: generation and acceptance.

In the sequel, let c_k be the value of the temperature parameter, and L_k be the number of transitions generated at some iteration k. The principle of SA can be summarized as follows:

Simulated annealing

1. **Initialization** $i := i_{start}$, $k := 0$, $c_k = c_0$, $L_k := L_0$);
2. **Repeat**
3. **For** $l = 0$ **to** L_k **do**
   - **Generate a solution** j **from the neighborhood** S_i **of the current solution** i;
   - **If** $f(j) < f(i)$ **then** $i := j$ (j **becomes the current solution**);
   - **Else,** j **becomes the current solution with probability** $e^{\left(\frac{f(i)-f(j)}{c_k}\right)}$;
4. $k := k + 1$;
5. **Compute**(L_k, c_k);
6. **Until** $c_k \simeq 0$

One of the main features of simulated annealing is its ability to accept transitions that degrade the objective function.

At the beginning of the process, the value of the temperature c_k is high, which makes it possible to accept transitions with high objective degradation, and thereby to explore the state space thoroughly. As c_k decreases, only the transitions improving the objective, or with a low objective deterioration, are accepted. Finally, when c_k tends to zero, no deterioration of the objective is accepted, and the SA algorithm behaves like a Monte Carlo algorithm.

1.3.3 Evaluation-based simulation

In many optimization applications, the objective function is evaluated thanks to a computer simulation process which requires a simulation environment. In such a case, the optimization algorithm controls the vector of decision variables, X, which are used by the simulation process in order to compute the performance (quality), y, of such decisions, as shown in Figure 1.9.

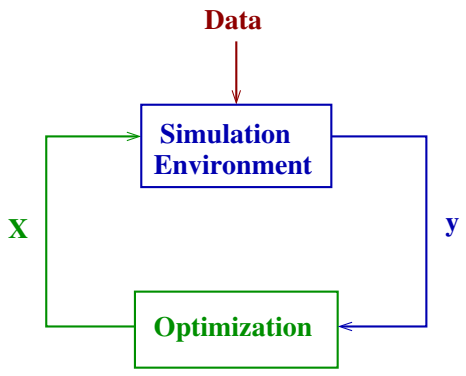

FIGURE 1.9 – Objective function evaluation based on a simulation process

In this situation, population-based algorithms may not be adapted to address such problems, mainly when the simulation environment requires huge amount of memory

space as is often the case in nowadays real-life complex systems. As a matter of fact, in the case of a population-based approach, the simulation environment has to be duplicated for each individual of the population of solutions, which may require an excessive amount of memory. In order to avoid this drawback, one may think about having only one simulation environment which could be used each time a point in the population has to be evaluated as follows. In order to evaluate one population, one first consider the first individual. Then, the simulation environment is initiated and the simulation associated with the first individual is run. The associated performance is then transferred to the optimization algorithm. After that, the second individual is evaluated, but the simulation environment must be first cleared from the events of the first simulation. The simulation is then run for the second individual, and so on until the last individual of the population is evaluated. In this case the memory space is not an issue anymore, but the evaluation time may be excessive and the overall process too slow, due to the fact that the simulation environment is reset at each evaluation.

In the standard simulated annealing algorithm, a copy of a state space point is requested for each proposed transition. In fact, a point $\vec{X}_j$ is generated from the current point $\vec{X}_i$ through a copy in the memory of the computer. In the case of state spaces of large dimension, the simple process of implementing such a copy may be inefficient and may reduce drastically the performance of simulated annealing. In such a case, it is much more efficient to consider a *come back* operator, which cancels the effect of a generation. Let G be the generation operator which transforms a point from $\vec{X}_i$ to $\vec{X}_j$:

$$\begin{array}{ccc} & G & \\ \vec{X}_i & \rightarrow & \vec{X}_j \end{array}$$

the comeback operator is the inverse G_i^{-1} of the generation operator.

Usually, such a generation modifies only one component of the current solution. In this case, the vector $\vec{X}_i$ can be modified without being duplicated. Depending on the value obtained when evaluating this new point, two options may be considered:

1. the new solution is accepted and, in this case, only the current objective function value is updated.
2. else, the come back operator G^{-1} is applied to the new position in order to come back to the previous solution, again without any duplication in the memory.

This process is summarized in Figure 1.10.

The *come back* operator has to be used carefully because it can easily generate undesired distortions in the way the algorithm searches the state space. For example, if some secondary evaluation variables are used and modified for computing the overall evaluation, such variables must also recover their initial value, and the *come back* operator must therefore ensure the coherence of the state space.

Optimization techniques are widely used in order to solve real life applications particularly in air traffic management. In fact, in complex problems that impose dealing with several operational and environmental constraints, an appeal to optimization techniques

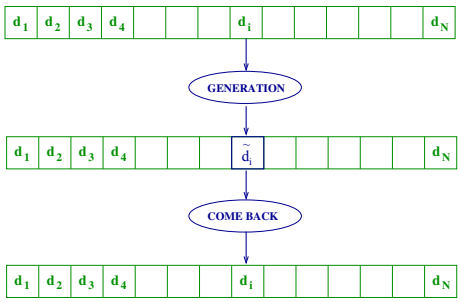

FIGURE 1.10 – Optimization of the generation process. In this figure, the state space is built with a decision vector for which the generation process consist of changing only one decision (d_i) in the current solution. If this modification is not accepted, this component of the solution recovers its former value. The only information to be stored is the integer i and the real number d_i.

is vital in order to converge to the appropriate solution. In the current work, we propose to apply optimization methods in order to establish new more efficient ways of organizing the NAT traffic. Therefore, we propose to leverage some specificity of the NAT, as well as reduced separation norms, in order to exploit different ways of traffic organization, alternative to the OTS. In the next section, we stress the point on the actual limitations faced by flights crossing the NAT, and then introduce our proposed solutions in the framework of the present study.

1.4 Problem statement in the present thesis framework

In this section, we start by presenting the limitations faced by the current NAT procedures, which motivate our study in the present thesis. Then, we describe our problem statement.

1.4.1 Current limitation of the NAT

In this chapter, we have discussed precisely the current ATM procedures and features applied to NAT. We summarize, here, the main difficulties for ATC to control NAT flights:

— high traffic density and airspace congestion due to traffic temporal and spatial concentration into two major flows,

— the lack of radar-based surveillance for the most part of the NAT,

— strong jet stream winds causing strong perturbations in flight prediction.

These difficulties leads to the following very firm rules and procedures, that are mandatory for NAT flights:

— an OTS route structure with predefined tracks attributed to aircraft,

— constant speed and flight levels until any desired change is approved by the ATC,

— very large separation norms,

— re-routing within OTS is very rarely approved by ATC, and leads to larger separation norms.

These rigid rules limit the efficiency of NAT airspace, and the efficiency of each single flight as well. In fact, the OTS structure reduces the number of flights authorized to cross the NAT at a given time. As a result, flights are penalized with huge delays and deviations from desired trajectories (horizontal and vertical). This situation induces additional congestion in the post and/or pre-oceanic continental airspace.

Furthermore, the current OTS structure is inefficient regarding increasing traffic volume. In fact, given that the width of the jet stream is 50 to 100 NM, only one or two OTS tracks can really benefit from the wind direction. This leads to a concentration of the traffic at links involving preferable winds, which becomes an issue regarding the NAT traffic growth. Thus, the question arises of whether the OTS will still be necessary to organize the NAT traffic in the future.

Reduction of the separation norms makes it possible to exploit different ways of organizing traffic, alternative to the OTS. Therefore, the present work aims at improving the traffic situation in the NAT by organizing the transatlantic traffic and scheduling flights at the strategic level of flight planning while ensuring that the required separation norms are maintained.

1.4.2 Benefits and operational acceptance of reduced separation norms

Several studies have discussed relaxation of separation standards with the availability of ADS-B in oceanic airspace [55, 56, 90, 105]. The main benefits coming from implementing ADS-B in oceanic airspace are outlined below:

— More efficient and predictable flight trajectories.
— Improved situational awareness, conflict detection and resolution.
— Better management of risk and application of safety management systems.
— Greater availability to operate at preferred altitudes.
— Ability to vary speed to access tail winds and avoid headwinds.
— Significant reduction in ATC and pilot workload.

Moreover, a brief computation of the efficiency of NAT tracks can prove the strong benefit behind reduced separation norms. In fact, the average distance across the NAT outside of surveillance is about $1,500$ NM. Thus, only 25 aircraft can fly at the same time within one OTS track implementing a longitudinal separation of 60 NM. If this longitudinal separation is reduced to 30 NM, the same track will accommodate 50 flight at the same time, and with 15 NM separation, it would be 100 aircraft. This means that the traffic density over OTS tracks will be able to increase up to 4 times more than the current traffic.

The communication and navigation performance required when separation norms decreases are presented in the report of The flight safety foundation [33]. In fact, lateral separation between aircraft on parallel or non-intersecting tracks is established in accordance with the following:

— For a minimum spacing between tracks of 50 NM a navigation performance of Required navigation performance (RNP) [8] 10, RNP 4 or RNP 2 is required.
— For a minimum spacing between tracks of 30 NM, a navigation performance of RNP 4 or RNP 2 is required.
— For a minimum spacing between tracks of 15 NM, a navigation performance of RNP 2 or GNSS equipage and direct controller-pilot VHF communication are required.

There are two important works that are progressing on assessing ADS-B systems with respect to reducing separation minima [33]:

— A joint working group made up of Nav Canada [9], UK NATS [10] and Air-services Australia representatives.
— State Aviation System Plan (SASP) work-group

This joint venture aim at financing, developing, deploying and operating solutions for tracking and monitoring aircraft anywhere in the world by using ADS-B. The resulting research and analysis anticipate lateral and longitudinal standard of 15 NM when using ADS-B combined with existing communications systems. The SASP advice suggests that the mathematical modeling and validation can confidently be completed by 2018 [18, 25, 33]. Nevertheless, this reduced lateral and longitudinal separation to 15 NM is not yet approved by the ICAO [2].

In [56], authors affirm that implementing a longitudinal and lateral separation of 10 NM in oceanic airspace is conceivable by increasing the data link performances in controller-pilot communication and surveillance. Authors reports also that new communication-surveillance systems introduced into aviation must take the eventual need for 10 NM separation in oceanic airspace.

To sum up, in order to produce a significant level of reduced separation minima, ADS-B need to be coupled with Future Air Navigation System (FANS), controller-pilot data link, Automatic Dependent Surveillance – Contract (ADS-C) and RNP-2 capabilities.

To be exact, in the current work we made the following assumptions:

— Longitudinal separation is decreased from 10 minutes to 2 minutes between consecutive aircraft on the same track, and from 15 minutes to 3 minutes when the aircraft changes its track.
— Lateral separation of 10 NM when aircraft are following parallel track and re-routing between these tracks is not allowed.

1.4.3 Problem statement

The strategic flight planning problem that we aim to solve in the present work considers a set of flight plans of a given day over the NAT. Our objective is to find alternative aircraft trajectories that resolve potential conflicts between aircraft and minimize the

8. RNP represents the level of performance required for an airspace. For instance, RNP 10 means that the navigation system must be able to calculate its position on each 10 NM of its trajectory.
9. NAV CANADA is a private, non-share capital corporation that owns and operates Canada's civil air navigation service (ANS).
10. NATS is the UK's leading provider of air traffic control services.

flight optimality criteria such as fuel consumption or trajectory length. There are generally different route optimality criteria such as total trajectory length, flight duration or fuel consumption. In this work, we choose to minimize the total cruising times since it is directly related to the fuel consumption. The given data include:

— Original flight schedules based on the submitted flight plans,
— Forecast wind fields,
— Separation norms,
— The maximum allowed departure delay time shift that can be allocated to each flight f_i, denoted d_{f_i}.

The flight data is obtained from the submitted flight plans for the transatlantic flights. Each flight plan includes the following data:

— Origin and destination airports;
— Desired departure time;
— Entry and exit points in the NAT airspace;
— Desired flight levels;
— Desired true airspeed.

The wind data is obtained from the GRIB files created by the meteorological centers (NOAA, Meteoblue, FNMOC) and available online [27].

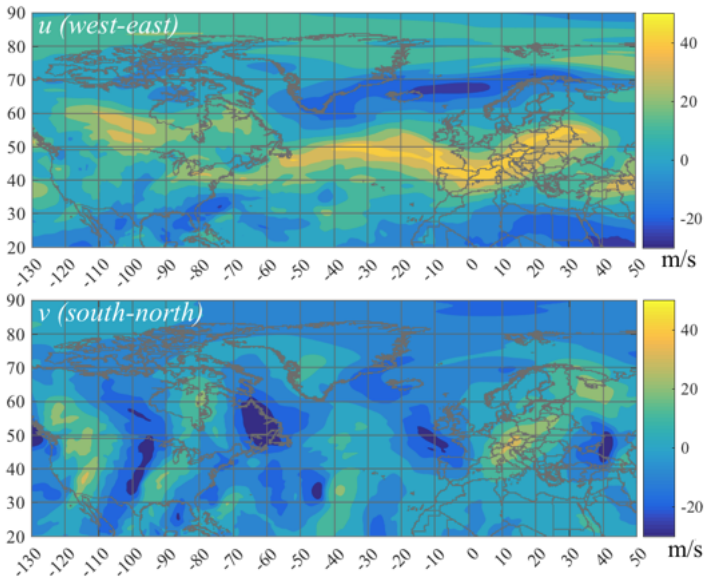

FIGURE 1.11 – Example of forecast wind field on July 15^{th} 2012 at 0000 UTC at FL370: W_u-component (top) and W_v-component (bottom), in m/s

This data is then converted into a 3-dimensional grid covering the world airspace, where each grid cell has the horizontal dimension of $(0.5° \times 0.5°)$ and vertical dimension of 1000 feet (one flight level), and contains W_u (west-east) and W_v (south-north) wind components. Each such grid corresponds to a particular hour of the day, with a 6-hour time step. Figure 1.11 shows an example of a wind field on July 15^{th} 2012 at 0000 UTC at FL370, extrapolated from the wind components at the grid cells (W_u-component on top, and W_v-component on bottom).

In addition to the nominal forecast wind field obtained from GRIB files, we want to consider uncertainty in wind prediction, in order to verify the robustness of the proposed solutions. Similarly to numerous related studies, for instance [37, 81, 88, 102], we introduce wind uncertainty via wind scenarios. Five wind scenarios are considered in this work, referred to as $s0$, $s1$, $s2$, $s3$ and $s4$, where $s0$ corresponds to the nominal forecast wind for the current day, and other scenarios are constructed as a combination of forecasts from the previous, current, and the next day (refer to [89] for more details). Figure 1.12 shows such scenarios for W_u-component (most meaningful for transatlantic flights) on July 15^{th} at 0000 UTC at $FL370$ within the NAT.

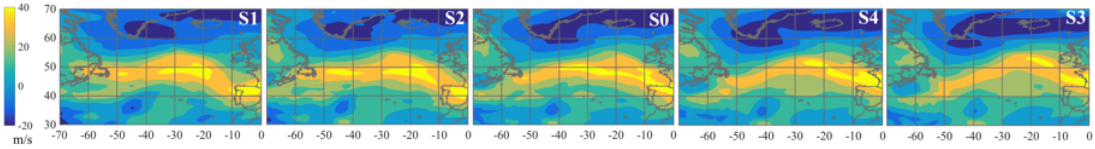

FIGURE 1.12 – Five forecast scenarios for W_u (east-west) wind component over NAT on July 15^{th}2012 at 0000 UTC at $FL370$

To simplify the simulations, we treat only eastbound traffic. As concluded in Section 1.2.2, the eastbound and westbound traffic flows are mainly separated in time due to passenger demands and time zone differences, and laterally due to the minimum-time flight routes. In addition to this, as from the current operational procedures, the eastbound flights occupy odd flight levels (ex. FL350, FL370), while the westbound flights are scheduled at even flight levels (ex. FL340, FL360). Thus, the flows are separated vertically as well. Taking these features into account, we can assume that flights within the opposite-directional flows never interact with each other and can be considered independently.

Furthermore, we consider reduced oceanic separation norms assuming that all aircraft are equipped with ADS-B. Such norms are given independently for each traffic organization methodology presented in the following chapters.

In addition to this, we concentrate our effort on conflict detection and resolution within the NAT only, as it is the main subject of the study. We omit the possible conflicts in the continental airspace which may be induced by our solution, considering that they are easier to resolve thanks to the relatively small continental separation norms. Thus, we end up with a conflict detection and resolution problem.

In the sequel of the present study, the computational experiments are compared to a set of 2D Wind-Optimal NAT trajectories that are generated using the optimization approach presented in [76]. These data are provided to us by the research team from NASA Ames Research Center (Mountain View, CA, USA), and contains 31 traffic days in July of 2012. More details on the construction and the conflict resolution procedure applied are presented in Appendix B.

In the next chapter, we investigate the FFC into NAT flights as the reduction in separation norms in NAT is been possible and has started to be implemented. Therefore, we propose a decentralized cooperative method to simulate the flight progress within the

NAT under FFC. The chapter starts with presenting several studies aimed at introducing the FFC under the framework of conflict detection and resolution problems, quantifying the benefit coming from applying FFC, and applying multi-agent systems to address part of ATM issues. Afterwards, we present and discuss our proposed approach.

Chapter 2

Flight planning based on Flocking Model

In this chapter, we present a new approach for planning a conflict-free flight trajectories over the NAT. This approach proposes that flights cooperate, as a multi-agent system, in the conflict detection and resolution process in order to find their best trajectories in a free-flight environment.

This chapter is organized as follows. First, we start with an introduction of the *Free Flight Concept* (FFC) and we illustrate this concept through several previous works. We also present several existing works proposing a multi-agent approach to resolve numerous ATM problems. After that, we formulate our problem as an optimization problem in order to resolve it using an optimization algorithm. Furthermore, we develop the mathematical model for the flight trajectory construction that we use in our simulations of flight progress. Finally, we present results of our simulations for real and artificial flight sets.

2.1 Background

ATC is responsible for maintaining a sufficient distance between aircraft to avoid dangerous situations and eventual collisions. Years ago, ATC was based on procedural separation which means that every aircraft reports its position and its clearance requests. Since World War II, radar has been used to monitor air traffic. In areas where there is no radar surveillance, such as oceanic airspaces, procedural separation is still used. The situational awareness of controllers is clearly lower in this situation compared to radar surveillance. Therefore, larger separation minima and predefined tracks (Section 1.2) are used.

In controlled airspaces, air traffic flows are structured into airways which are subroutes to fly from one sector to another (see Figure 2.1), and flight levels which are used as layers to separate aircraft. This organized traffic pattern enables one controller to monitor a complete sector by avoiding chaotic air traffic situations. In fact, separation problems are only limited to intersections between airways, altitude changes or overtaking conflicts. However, using airways has clear drawbacks:

— airways are generally not optimal routes: flight trajectories are not optimal from an aircraft point of view in terms of time and fuel consumption,
— sub-optimal use of airspace: traffic density is concentrated on airways, rather than using the full airspace.

A simulation study reported in [24] proves that self-separating aircraft flying almost direct routes yields a lower fuel consumption than aircraft following airways, even though aircraft using such airways do not have to recourse to a conflict avoidance maneuver. Naturally, aircraft prefer flying optimal routes with respect to fuel consumption and time while remaining within the safety margins. This could be considered via Free Flight Concept (FFC) (Section 1.1.5). In the FFC, the separation task is delegated to the pilot. The aircrew can ensure separation when they are aware of the surrounding traffic thanks to ADS-B availability. As mentioned in the previous chapter, such a system permits to broadcast not only identification and altitude but also the position, velocity and even a part of the intended route. Thus, every aircraft could use these data to ensure their self-separation. Assuming an aircraft is able to perform separation task, it will be able to fly optimal trajectories.

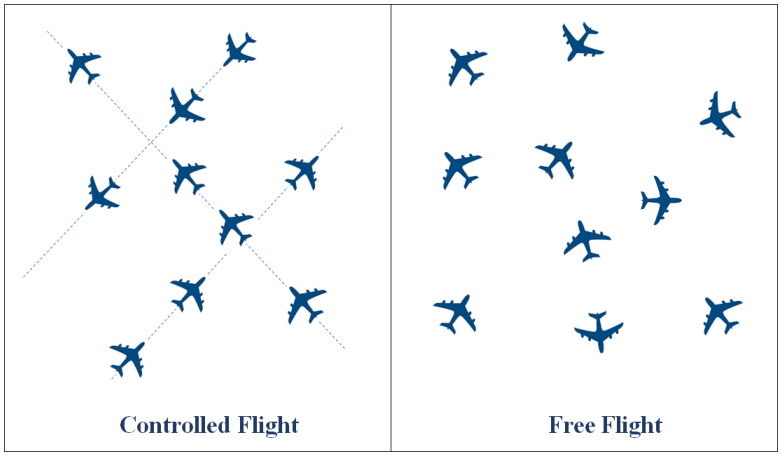

FIGURE 2.1 – Controlled flights vs Free Flights

The resulting ATM system will converge from a centrally controlled system to a distributed system with inter-connected elements (see Figure 2.1). We assume the complexity of such a system can be alleviated via applying Multi-Agent Systems (MASs). In the following sections, we present an overview of FFC and MASs.

2.1.1 Free Flight Concept (FFC)

FFC is proposed as a new concept in ATM. It is a decentralized control paradigm that enable aircraft to fly user-preferred routes by removing most of airspace restrictions and delegating part of the collision-avoidance responsibility from ATC controllers to pilots. Thus, pilots will not only be allowed to select freely their routes, but will also have an additional responsibility related to conflict avoidance. In [32], authors think that aircraft self route optimization is more effective than global system optimization performed by a

controller. Nevertheless, it was proven in [41], that in such situation, pilots generally try to follow relatively dangerous trajectories in order to reach the conflict point before the others. In fact, in FFC, an aircraft that reaches the conflict point after the others has to give the priority to preceding aircraft, and as a result will lose its flight efficiency. Therefore, the task of conflict avoidance is often ensured by Airborne Separation Assurance System (ASAS) [13]. ASAS is an airborne system that collects information via ADS-B (or equivalent) in order to provide pilots with procedures for traffic monitoring, conflict detection, conflict resolution and conflict prevention jointly with the surrounding traffic. Thus, aircrew with ASAS system's aid is able to detect and resolve conflicts with the surrounding traffic [61]. Nevertheless, in a complex traffic situation, the pilot's ability outperforms the automation solutions, and thus pilots must deal with the situation without automation intervention.

In the literature, several algorithms for Conflict Detection and Resolution (CD&R) are proposed, some of which are evaluated in a simulation environment, others in an operational one. Nevertheless, due to the existence of an infinite number of conflict geometries in FFC, [43] claimed that the safety level of a CD&R algorithm applied in FFC is very difficult to ensure. As a result, choosing an appropriate and performing CD&R algorithm to be implemented in cockpit that deals with all the conflict situations remain a challenging task for the designers of future ATM systems.

Within FFC applied to continental airspaces, each aircraft reserves, at any given point of its trajectory, a cylindrical volume of airspace called protected zone [32] in order to detect potential conflicts. The protected zone is defined by a cylinder with a radius of 5 NM (equal to the horizontal separation standard within en-route radar separation) and height equal to 2,000 feet (equal to the double of the vertical separation), as shown in Figure 2.2. A conflict is detected when an aircraft intrudes into this protected zone within

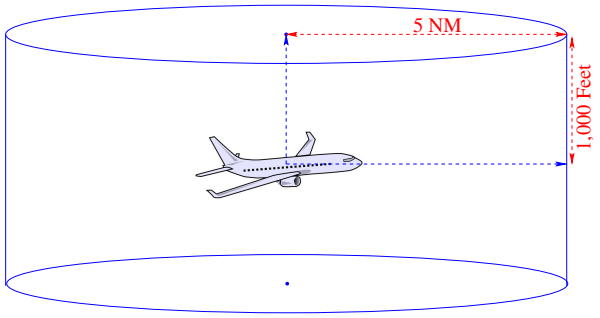

FIGURE 2.2 – An aircraft protected zone

a predetermined look-ahead time. According to how aircraft position is predicted in the future, Conflict Detection (CD) methods can be roughly classified into three fundamental categories: nominal, worst-case and probabilistic [62].

— In the **nominal approach**, aircraft position is projected into the future based on its current velocity vector. This method does not consider any uncertainty or eventual deviation from the aircraft's assigned trajectory. Thus, this method is straightforward and provides the best estimate of the aircraft's future position in

the short-term. However, it does not consider the long-term propagation trajectory errors. In the majority of the studies applying such a method, such as in [9, 20, 21, 28], an additional safety buffer or an enlarged separation norms are used.

— In the **worst-case approach**, an aircraft is predicted to perform any range of maneuvers. In the case where one of these maneuvers generates a conflict, then a conflict is predicted. Evidently, worst-case CD approach is considered as the most robust method of CD. Nevertheless, it can cause excessive false-alarm rates by predicting conflicts that will never happen. To reduce this side-effect, worst-case trajectory propagation is mainly limited to a specific look-ahead projection time. Several studies considered this approach such as [14, 79, 82, 97, 108].

— In the **probabilistic approach**, the deviation from the aircraft future assigned trajectory is considered by modeling the uncertainty affecting the aircraft motion. It is mainly performed via two different methods. The first method consists on summing up the position errors and the nominal trajectory, thereby the conflict can be detected from the probabilistic trajectories. The second method develops a set of all the possible future trajectories, while affecting an occurring probability to each. Then, the probability of conflict is determined from the propagated trajectories. This method represents a compromise between nominal and worst-case CD, whereby it avoids the conservativeness of the worst-case approach, but is still robust with respect to uncertainty. Thus, probabilistic CD approaches can be applied in a large-scale traffic scenario involving high level of uncertainties such as in strategic flight planning. This CD method is used for instance in [45, 65, 71, 84].

Because of the chaotic behavior of trajectories resulting from FFC and the lack of predictability of potential conflicts in the distributed control, more complex conflict scenarios may arise [11, 69], thus the need for more robust methods.

In [46], an intent-based probabilistic conflict detection algorithm is proposed as an automation tool. The proposed algorithm gathers the nominal information into a probabilistic framework by applying an aircraft dynamics model for short-term prediction and an aircraft navigation model for long-term prediction.

[5] investigates the potential of a set of CD algorithms for detecting conflict in FFC. The main objective of this work is to detect patterns in the behavior of CD algorithms, based on conflict characteristics, then to implement these patterns in a learning system to improve CD process. Three CD algorithms where tested, one of each methodology: nominal, worst-case and probabilistic. First, fast time simulations has been conducted to evaluate the three CD algorithms with an increasingly complex conflict scenarios, and thus to detect probe characteristics. Then, data mining techniques are used to implement patterns in the probe characteristics. Finally, a switch mechanism is applied to select the appropriate algorithm to assess a probe for potential conflicts.

Furthermore, [58] presents a system, referred to as User Request Evaluation Tool (URET), capable of accomplishing the CD tasks automatically. It collects the filed Flight Plans, the aircraft performance data and meteorological information in order to construct 4D-ATs. Then, these trajectories are used to detect potential conflicts up to 20 minutes

in the future.

A recent approach proposed by [68] for CD, under the FFC, based on Gauss-Hermite particle filter (GHPF). The proposed algorithm presents two aspects. First, data from observations are integrated into a system state transition probability, then Gauss-Hermite Filter (GHF) is applied to generate the density function. Second, GHPF is used in order to predict flight trajectory and calculate flight conflict probability. This method is found to be accurate and suitable for early-CD in free flight.

Conflict Resolution (CR) process takes place immediately following the CD process. There exist large amount of research that has been proposed in the literature to deal with CR problems in a *centralized* and *decentralized* manner. Since we are tackling FFC, we are interested only in *decentralized* or *cooperative* CR approaches, among which we will present some previous works.

For example, Pallottino *et al.* investigated in [80] a centralized cooperative approach to CD&R, in which the problem is formulated as local centralized optimization problem and cooperative maneuvers are adopted to avoid conflicts between aircraft. Here, a set of aircraft flying with constant speed and constant flight level in 2-Dimensional airspace is considered. The CR approach is modeled as a set of linear constraints and solved via a Mixed-Integer Programming (MIP) optimization, where two independent maneuvers for conflict avoidance are performed: either velocity or heading changes. In [79], the same authors demonstrate that a decentralized adaptation of the algorithm is conceivable given an appropriate look-ahead distance. In this case, the constraints imposed to an aircraft take into account its position with respect to nearby surrounding aircraft. The safety of such a decentralized scheme is proven by considering a worst-case CD algorithm.

In [23], the method presented in [80] is extended to the 3-dimensional case. The authors apply only velocity changes aimed at minimizing the total flight time using Mixed-Integer Non-Linear Programming (MINLP). Several test cases have been performed to illustrate the efficiency of this approach in dealing with the CD&R problem. However, this method suffers from high computational time.

A similar problem to that presented in [80] is introduced in [10], whereby the CR problem is modeled as an optimal control problem. Here, a decentralized cooperative method is implemented, and CR is performed via a heuristic heading change, in the case of bounded steering radius maneuvers, in order to avoid conflicts and to minimize the total time of the flight. Alejo *et al.* [6] proposed a real time decentralized change of the velocity profile in 3-dimensions to ensure that the required separation norms are maintained

Mao *et al.* [70] investigated the stability of two intersecting flight flows under decentralized conflict-avoidance and resolution rules. In this model, aircraft flying at a constant speed and following a constant altitude are organized into two flows. Conflict-avoidance is performed via a single one time bounded lateral maneuver for each aircraft (bounded

heading change). The stability of the method is proven. However, it was found that considering intersecting flows stresses a difficult problem such as the *domino effect*[1]. This problem is resolved further in [26] by solving local conflicts between every pair of intersecting aircraft flows. The necessary and sufficient conditions to decouple conflicts within intersecting flows are defined. Then, authors proved the existence of a decentralized CR rules that satisfy the decoupling requirements for each local conflict in order to converge to a global CD.

In [34], an optimization approach for CD&R for multi-aircraft is presented. Here, a relaxation approach that combines the decentralized aircraft speed vector preferences with centralized conflict resolution rules in order to limit aircraft deviations from their trajectories. Thus, the collision avoidance problem is turned into a semi-definite program, which is solved afterwards using convex optimization with a randomization scheme to generate conflict free trajectories. The important contribution of the paper is the highly non-convex nature of the collision avoidance algorithm.

Other studies are devoted to investigating ATC efficiency under the frame of FFC. In [44] for instance, the effectiveness and the robustness of a distributed ATM system in the FFC is demonstrated within high air traffic density, up to 3 times the Western European air traffic in 2000. In this study, several simulations are conducted to prove that, despite of the appearance of a chaotic traffic pattern, distributed FFC implementing appropriate airborne systems, enables safer and more efficient airspace management than the current ATM system. Furthermore, [24] demonstrates that flight trajectory distances could be reduced by almost 25% when following free flight routes compared to flying along ATC routes, and thus proved that FFC have the potential to offer great economic benefits.

To sum up, all the above-mentioned distributed CD&R approaches dedicated to the FFC require balancing the global considerations and the local goals. Particularly, the overall safety of the airspace is a global interest that all ATM operators have to consider in the search for an appropriate CR maneuvers. Nevertheless, at the local level, individual pilot interests can conflict. Thus, the need for addressing cooperative approaches combined with the distributed process. In the literature, this problem was widely solved via multi-agent systems, subject of the next section.

2.1.2 Multi-agent systems applied to ATM

Multi-agent systems (MASs) consist of multiple interconnected sub-systems able to cooperate, communicate, act flexibly, and solve problems within the frame of their objectives. This concept received overwhelming interest from researchers over the past decade and arises in several applications such as parallel optimization [98], smart-grids [63], security applications [86], and so on, ranging from industrial manufacturing to e-commerce and health care [112, 120].

Self-organization, which is a key element of MASs, is a process initially inspired from nature. It describes a mechanism that functions without central control and operates

1. Domino effect illustrates a situation where the resolution of a local conflict between a small number of aircraft leads to a propagation of new conflicts among other aircraft

based on local interactions. The strength of self-organizing systems lies in their capability to spontaneously generate a new organization in case of environmental changes.

In the case of complex systems, the easiest and most reasonable way to resolve the problem is to divide it into a number of functionally modular components, referred to as agents, which are in charge of solving a particular problem aspect. Each agent applies an appropriate paradigm for solving its particular problem. Then, when a problem arises, agents must coordinate together to ensure that the problem resolution is properly managed. Thereby, agent behaviors can help to find an overall solution to the problem at system level, by only using local rules at agent level.

As ATM represents an example of a complex system with a large number of interacting, heterogeneous individuals (e.g., operators, ATC, passengers, etc.) operating in a linked and constrained environment (air routes, delays, conflicts, international regulations, etc.), numerous application have been conducted in order to automate ATM systems via MASs, and some of which have been already implemented. An example of these systems is the Optimal Aircraft Sequencing using Intelligent Scheduling (OASIS) system [66], which is currently used at the Sydney airport, and aims to provide an efficient sequencing of arriving, departing and approaching air traffic. Further, MASs has been used to evaluate safety issues in ATM [60, 85]. However, MAS based applications are mostly oriented to address air traffic regulation in Free Flight zones. In fact, aircraft operating in Free Flight areas must be able to find by themselves conflict-free trajectories while respecting the required separation norms between neighboring aircraft. Thus, MASs was found to be a powerful tool to tackle these problems.

In [42], Harpert et al. have successfully developed a multi-agent collaborative decision-making model of pilots and air traffic controllers in a free flight concept. In this work, the resulting agents are responsible for collaborating to resolve air traffic conflicts and avoid regions of airspace, such as convective weather cells or special use airspace, in an efficient and safe manner. The decision making process for the resolution of conflicts is a distributed process including a negotiation model for selecting the leader agent for the first resolution maneuver based on a set of criteria. Then, the considered agent constructs avoidance maneuvers using velocity changes and/or a lateral shift taking into consideration all the constraints of involved agents. Then, the solution is distributed to all participant agents in order to verify that it is best suited to their preferences. This process continues until all the participating agents accept the candidate solution. Simulations prove that the deployment of conflict resolution strategies through multi-agent negotiation and collaboration produce effective conflict avoidance maneuvers for two-aircraft conflicts in a single ATC environment, with a subset of spatial and performance constraints. Basically, a solution for two-aircraft conflicts seems to be insufficient especially regarding the recent growth of air traffic density, whereby conflict situations involving more than two aircraft is more likely to occur, and resolving them is intrinsically more difficult than dealing with the two aircraft case.

Another similar conflict detection and resolution (CD&R) method is proposed by Wollkind et al. in [119]. Here, a simple conflict resolution system based on multi-agent

cooperation and negotiation among two aircraft is proposed. The process is based on monotonic concession protocol (MCP) [96, 122]. The MCP captures the incremental bargaining process that takes place between negotiating parties. Initially, each involved agent (aircraft) makes a proposal that is beneficial to its preferences. Then, they incrementally revise their proposals and propose suggestions of progressively less value until a middle solution is reached upon agreement by both agents. Findings prove that such CD&R method can get successful results with minimum safety requirements, and aircraft are able to efficiently and safely resolve their conflicts without interaction with ATC. Thus, the robustness of the system is improved when applying a decentralized method rather than using a centralized one. Indeed, having each aircraft running as an agent in a coordinated system between all aircraft reduces the dependency on a single ground-based system. However, nothing guarantees that the obtained solution is optimal, and thereby an approved proposal can be costly for an aircraft compared to the one making the proposal.

Likewise, [99] proposed an Iterative Peer-to-Peer Collision Avoidance (IPPCA) algorithm as an extension of the CD&R via MCP approach [119] to multi-aircraft conflict situations. Each aircraft is controlled by an agent and the agents are able to communicate with each other. Then, conflicts between multiple aircraft are solved iteratively in pairs. For each pair of conflicting aircraft, the algorithm starts a negotiation of conflict resolution via progressively stronger maneuvers for both aircraft, such as heading, altitude or cruise speed, until a successful resolution is achieved. In contrast, since the method relies on pairwise conflict resolution, a solution with two aircraft may cause other conflicts with other aircraft, and this problem becomes more serious with very high traffic density which leads to a very high level of dependencies between aircraft trajectories.

In [3], Agogino et al. proposed a coordinated multi-agent algorithm for air traffic flow management in order to reduce congestion. Contrary to the work proposed by [99], here an agent is associated to a fixed location in 2D space, rather than to one aircraft. An agent's mission is to decrease the congestion around its location. Thus, each agent controls aircraft around its location with one of these three actions: setting separation between aircraft, ordering ground delays, or performing reroutes. To choose the best control, the agents use reinforcement learning.

In [74], Molina et al. presented a multi-agent approach to model air traffic flow management under the CASSIOPEIA project, which is a project developed according to the goals of the SESAR program. The proposed approach considers almost all the ATM features, whereby agent models are used for different ATM stakeholders and collaborative decision processes are modeled for network managers, airlines, airports and aircraft in order to generate a collaborative decision-making process. It was successfully applied with three different ATM studies in the European airspace (with hundreds of airports and longer temporal scales), including algorithms for distributed-collaboration decision making for strategic decision levels and stochastic approaches for simulations. This work emphasizes improvements in information sharing and communications between ATM components to alleviate the ATM system complexity, which is the main goal of SESAR and

NextGen programs.

Regarding Free Flight and TBO achievements (Section 1.1.5), [12] investigates the capability of airborne self-separation to safely accommodate very high traffic demand. To this end, a MAS model has been developed in which each aircraft acts as an independent agent that manages its intended conflict-free 4-D AT (Section 1.1.5) then broadcasts it to other aircraft via ADS-B, whereby all involved aircraft are supposed to be equipped with ADS-B system or equivalent. Further in tactical level, each aircraft applies a medium-term and short-term conflict detection and resolution layer aiming to resolve any remaining problems, such as significant deviations from 4-D AT due to wind prediction errors. First, a priority is affected to each aircraft which is determined by the remaining distance to destination. Then, when a medium-term conflict is detected, the aircraft having the lowest priority has to resolve the medium-term conflict by rerouting its trajectory, while the aircraft with higher priority simply sticks to its trajectory. Simulations conducted in random traffic scenarios shows that a three-times-as-high 2005 en route traffic demand can safely and efficiently be accommodated by the airborne self-separation TBO concept. These findings prove that there is good reason for future ATM to strengthen development of airborne communication system towards self-automated traffic.

Another recent approach was performed by Breil et al. in [15] aiming at constructing self-organized air traffic via applying MASs. In this approach, aircraft represent agents exchanging ADS-B messages and are in charge, based on the exchanged messages, of resolving conflict between each other. Three decentralized algorithms have been presented in order to reduce air traffic complexity. The first algorithm assumes that aircraft agents are operating on a route network, and conflict resolution is performed via speed regulation. As route networks are not so efficient for dense traffic, the second algorithm proposes that aircraft adapt speed to avoid conflicts without the high structuring level imposed by route network, whereby flights can follow either 4D trajectory or a route network or flying along Free Flight routes. The third algorithm aim at creating temporary local route networks allowing to structure traffic with high density. Tests on real flight data proved that the three methods succeeded in structuring the air traffic and decreasing its complexity. This work reveals evident benefits from sharing the ATC missions with pilots in order to alleviate ATC workload on the one hand, and consider aircraft preferences on the other hand. Furthermore, the implementation of ADS-B systems enable the set up of such a decentralized control process delegated to inter-connected aircraft.

2.1.3 FFC and MASs in the frame of the present thesis

All the previous studies discussed in this section, reveal significant benefits from allowing aircraft to follow Free Flights, and sharing the conflict resolution process between controllers and pilots. However, for all of the mentioned studies, the problem was considered in the domestic airspace, and to our knowledge, no studies were conducted for applying MASs and FFC in oceanic airspaces.

Thanks to ADS-B, air traffic situation in the oceanic airspace is improved and flights are allowed to follow more flexible and direct routes from the departure to the arrival

airport. In this work, we propose a method for strategic planning of aircraft trajectories while transiting flights off the predefined OTS route structure to use almost direct routes between their NAT entry and exit points.

The idea of the present approach is inspired roughly from two particular behavior of the NAT flights:

— within NAT flights, we do not confront the problem of intersecting flights. In fact, eastbound and westbound traffic are treated separately and do not operate in the same flight levels.

— eastbound traffic, the subject of our study, would prefer to fly in the direction of wind and exploit the jet stream strong winds, as it offers an optimal fuel consumption.

As a consequence, we got the idea to consider the eastbound traffic as a set of birds flying in the same direction, forming a swarm behavior, and searching for the optimal paths to reach a destination, while maintaining a separation distance between each other.

This corresponds to the Flocking swarm model named *Boids Flocking* which is a model introduced by *Craig Reynold's* in the 1980*s* [87]. *Reynold's* implemented an algorithm, that simulates animal motion such as bird flocks and fish school, where *boids* refer to the generic flocking simulated creature. The aggregate motion represents the result of interactions between the simple behavior of each *boid*.

Flocking principles: In nature, flocks could be considered as a self-organized networks of mobile agents that cooperate with each other to form a group behavior. The flocking model was introduced by Craig Reynold's in 1986 [87]. It represents the form of collective behavior of large number of interacting agents with a common group objective. It's especially exploited for providing realistic representations of the aggregate motion of animal groups such as birds, fish and sheep. In Reynold's model, each agent was called "boid". The boid model has three heuristic rules applied to the *boids* at each time sample which are:

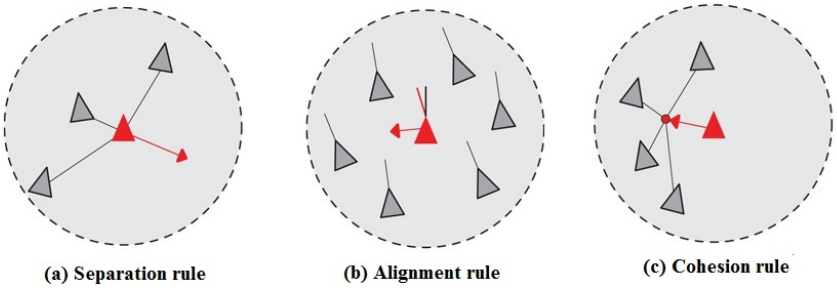

FIGURE 2.3 – The *boids* model rules

— Separation (see Figure 2.3 (a)): this rule is applied in order to maintain a specific separation distance between agents. Each boid is required to ensure a separation distance with his flock mates to avoid collision and prevent crowding.
— Alignment (see Figure 2.3 (b)): this rule is performed in order to oblige *boids* to follow each other in a quasi parallel trajectories. Each boid matches the direction and the speed of its neighbors.
— Cohesion (see Figure 2.3 (c)): this rule is performed in order to ensure the swarm behavior. Each boid moves to the average position of its neighbours.

It is important to note that the separation rule acts as a complement of the cohesion rule. In fact, if only cohesion is applied, all *boids* will merge into the same point. Figure 2.3 illustrates the behavior of an agent when applying the three flocking forces.

Flights have certainly several particularities compared to birds, this will be discussed further in section 2.3.

Furthermore, we suppose that all aircraft are equipped with ADS-B system, we are taking advantages from the reliable information that can be transmitted between flights to construct a full swarm behavior. Thus, each aircraft is considered as an agent and all agents communicate with each other and adjust their headings in order to avoid conflict while maintaining the swarm behavior.

To sum up, we propose to allow NAT flights to operate on Free Flight trajectories and to apply MASs methods based on the Flocking Model in order to generate conflict free trajectories. The proposed approach is detailed in the next section.

2.2 Problem formulation

In this section, we formulate our optimization problem that aims to provide a conflict-free configuration for a set of NAT flights. First, the given data and the assumptions made are presented. Next, we introduce our flight model as well as the conflict detection model adopted to our problem. Finally, a mathematical formulation of our optimization problem is illustrated.

2.2.1 Input data

In this section, we present our input data as well as the assumptions we made to tackle our problem. These data includes 2D Wind-Optimal eastbound NAT flight trajectories generated using the optimization approach from [103]. We got these data from the research team from NASA Ames Research Center (Mountain View, CA, USA) (refer to Section 1.4.3).

Based on these data, the input flight parameters are the following:

— Desired entry and exit points to the NAT airspace which are given by its latitude and longitude coordinates,
— Desired cruise altitude in feet,
— Desired entry time,
— Desired airspeed in knots.

Furthermore, each given flight trajectory is performed with a constant desired airspeed and a constant flight level for the entire trajectory. These parameters are constructed so as to be optimal in terms of cruising time. Based on these data, the following assumptions are made in order to simplify our model:

— Since we assume that the flight's altitude profile does not change for their entire trajectory, we can work in $2D$ airspace. We consider the airspace as an *Euclidean* space. Latitudes and Longitudes in the earth space are projected in $2D$ space by a *Lambert azimuth* projection with the center of projection located at the NAT's center.

— The flight trajectory is represented as a set of discrete points from the departure to the destination. The range between two consecutive points represents 1 minute navigation with the given data.

Furthermore, input data also includes the wind data of the considered day as described in Section 1.4.3. It consists of a $3D$ grid covering the NAT airspace. Each cell grid is a $3D$ rectangle having an horizontal dimension of $(0,5°, 0,5°)$ and vertical dimension of 1000 feet. We assume that the wind field is constant within each grid cell and at each 6-hour time step: from 00:00 UTC to 06:00 UTC, from 06:00 UTC to 12:00 UTC, from 12:00 UTC to 18:00 UTC and from 18:00 UTC to 24:00 UTC. The wind field is defined for each grid cell and at a given time and altitude by :

— west-east component, W_u, and,

— south-north component, W_v.

Then, wind data are extracted as $2D$ data for each particular flight level.

2.2.2 Flight model

For each flight f, the above mentioned input data are represented as follows:

— P_{In}^f the desired entry point to the NAT given with latitude and longitude coordinates,

— P_{Out}^f the desired exit point of the NAT given with latitude and longitude coordinates,

— FL^f the desired flight level,

— T_{In}^f the desired entry time to the NAT,

— V^f the desired aircraft airspeed.

In the current work, some of the flight parameters can be changed and represent the decision variables of our problem in order to find a conflict-free solution. For instance, entry delay less than 20 minutes is allowed. Moreover, both entry and exit points are not restricted to exact point. Indeed, if we consider that the desired entry/exit point is the center of a circle having a radius of 5 NM, any point of its surface is an allowed entry/exit point. Thus, we define the following decision variables:

— $\theta_i^f, i \in \{1, 2, .., N^f\}$ the heading of the aircraft f at each point i of its trajectory.

— D_{In}^f the time delay at entry point

— p_1^f the assigned entry point

— $p_{N^f}^f$ the assigned exit point

These variables must be determined to guarantee a set of conflict-free trajectories while respecting the limit of permitted-delay and the allowed deviation from the desired entry and exit points. In our case, the deviation from the desired entry and exit points has to be less than 5 NM. Note that based on the aircraft headings computed in each time simple, we can represent each flight trajectory with a set of sampling points referred to as $p_i^f(x_i^f, y_i^f, FL^f, t_i^f)$. The first point p_i^f results from the projection of the aircraft entry position P_{In}^f on the plane.

2.2.3 Conflict model

By definition, a conflict is a violation of the separation norms. In this work, aircraft are allowed to follow nearly their direct routes under the frame of FFC. Since we assume that all aircraft are equipped with ADS-B system, it's possible to reduce the separation standards. Thus, we define the following separation norms:

— vertical separation norm, V_{sep},
— lateral separation norm, Lat_{sep},
— longitudinal separation norm, Lon_{sep}.

In this study, the aircraft are prescribed to fly at a constant predefined FL. Thus, aircraft cruising on different FLs systematically maintain the vertical separation norm. Therefore, the conflict detection process for a set of flights can be performed separately for each FL, and consists of verifying if lateral and longitudinal separation are maintained for a given set of aircraft trajectory on each single FL, thereby the possibility of simplifying our model into $2D$ space.

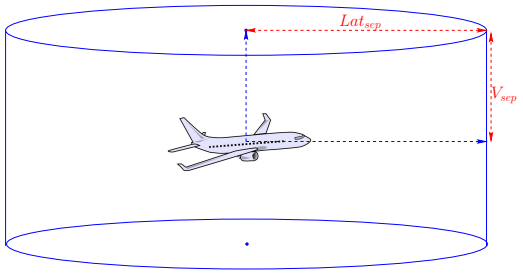

FIGURE 2.4 – The protected zone

Thus, we can define a protected zone, for each aircraft, represented as a cylinder with radius equal to lateral separation and half-altitude equal to the vertical separation norm as in Figure 2.4. Then, a conflict is detected when the protection zone of an aircraft is crossed by an other aircraft.

In our study, trajectories are sampled with a time step of Δt second. This time step has to be small enough to ensure that all potential conflicts are identified. Thus, a flight trajectory is a set of points $p_i^f(x_i^f, y_i^f, FL^f, t_i^f)$ where (x_i^f, y_i^f, FL^f) are the position coordinates at time $t_i^f = i \times \Delta t$ (where $i < N^f$ is a positive integer)of flight f projected on a *Cartesian* space.

Let us consider a set of flights S, we can distinguish two types of conflicts:

— point-to-point conflict,
— flight-to-flight conflict.

If we consider two flights f and g and their trajectories respectively $({p_i}^f)_{i\in\{1,2,..,N^f\}}$ and $({p_j}^g)_{j\in(1..N^g)}$. A *point-to-point* conflict is detected between f and g at $({p_i}^f)$ and $({p_j}^g)$, respectively, if:
— $FL^f = FL^g$, and
— $t = |t_i^f - t_j^g| < Long_{sep}$, and
— $dist(p_i^f, p_j^g) < Lat_{sep}$.
which means, in practice, that the three separation norms are violated simultaneously. In other words, a *point-to-point* conflict is detected when, at p_i^f, the flight f intrudes the protected zone of g at p_j^g.

Let us consider a binary variable, denoted $\triangle(p_i^f, p_j^g)$, defined as:

$$\triangle\left(p_i^f, p_j^g\right) = \begin{cases} 1 & \text{if a } \textit{point-to-point} \text{ conflict is detected between } p_i^f \text{ and } p_j^g \\ 0 & \text{otherwise} \end{cases} \tag{2.1}$$

Thus, the total number of *point-to-point* conflicts at point p_i^f, denoted Φ_i^f, which is defined as the number of aircraft that intrude the protected zone of f at ${p_i}^f$, and is calculated as:

$${\Phi_i}^f = \sum_{g\in S\setminus\{f\}} \sum_{j=1}^{N^g} \triangle(p_i^f, p_j^g) \tag{2.2}$$

We can, further, calculate the total number of *point-to-point* conflicts associated with the trajectory of a flight f, denoted Φ^f as follows:

$$\Phi^f = \sum_{i=1}^{N^f} \Phi_i^f \tag{2.3}$$

The total number of *point-to-point* conflicts generated by the set of flights S, referred to as Φ_{tot}, is defined as follows:

$$\Phi_{tot} = \frac{1}{2} \sum_{f\in S} \Phi^f \tag{2.4}$$

Further in this work, we use only the *point-to-point* conflicts for calculations, which we simply refer to as the number of conflicts. However, *flight-to-flight* conflicts are more understandable for displaying results. Note that *point-to-point* conflicts take into account the conflict duration which is not the case of *flight-to-flight* conflicts.

A *flight-to-flight* conflict between f and g is detected if there exists at least one *point-to-point* conflict detected between $(p_i^f)_{i\in\{1,2,..,N^f\}}$ and $(p_j^g)_{j\in\{1,2,..,N^g\}}$. To this end, we calculate, first, the number of conflict involved by the flights f and g, $C(f,g)$, as:

$$C(f,g) = \sum_{i=1}^{N^f} \sum_{j=1}^{N^g} \triangle(p_i^f, p_j^g) \tag{2.5}$$

Then, the flight-to-flight conflict between f and g, $\widetilde{\Phi}(f,g)$, is calculated as follows:

$$\widetilde{\Phi}(f,g) = \begin{cases} 1 & \text{C(f,g)} > 0 \\ 0 & \text{C(f,g)} = 0 \end{cases} \tag{2.6}$$

Finally, the total number of flight-to-flight conflicts, $\widetilde{\Phi}$, induced by the set of flights S is:

$$\widetilde{\Phi} = \frac{1}{2} \times \sum_{f \in S} \sum_{g \in S \setminus \{f\}} \widetilde{\Phi}(f,g) \tag{2.7}$$

The main objective of the present work is to find a flight set configuration that verifies the following equation:

$$\Phi_{tot} = 0 \tag{2.8}$$

2.2.4 Optimization problem formulation

In this section, we summarize all the notations, decision variables and constraints previously mentioned in order to present an optimization formulation of our problem.
A problem instance is given by the following data:

- A set S of Nb eastbound NAT flights on a specific day.
- The wind data given by:
  - west-east component, W_u, and
  - south-north component, W_v.
- For each flight f:
  - P_{In}^f the desired entry point in the NAT given with latitude and longitude coordinates,
  - P_{Out}^f the desired exit point in the NAT given with latitude and longitude coordinates,
  - FL^f the desired flight level (assumed to be constant throughout the overall trajectory),
  - T_{In}^f the desired entry time to the NAT,
  - V^f the desired flight airspeed (assumed to be constant throughout the trajectory).

For each flight f, we have the following decision variables:

- $\theta_i^f, i = 0, 1, 2, ..., N^f$ the heading of aircraft f at each point i of its trajectory.
- D_{In}^f the time delay at entry point,
- p_1^f the assigned entry point, and
- p_{Nf}^f the assigned exit point.

All these variables can be regrouped together into a specific vector, Ω^f, for each flight f as follows:

- $\Omega^f = ((\theta_i^f)_{i \in \{1,2,..,N^f\}}, D_{In}^f, p_1^f, p_{N^f}^f)$.

Thus, the decision variables related to a set of flights, S, are defined by the vector Ω as follows :

- $\Omega = (\Omega^f)_{f \in S}$

The decision variables must satisfy the following constraints for each flight f:

$$\Delta\theta_i^f = \mid \theta_i^f - \theta_{i-1}^f \mid \leq \Delta\theta_{max} \tag{2.9}$$

$$0 \leq D_{In}^f \leq Delay_{max} \tag{2.10}$$

$$dist(P_{In}^f, p_1^f) \leq Dev_{max}^{In} \tag{2.11}$$

$$dist(P_{Out}^f, p_{Nf}^f) \leq Dev_{max}^{Out} \tag{2.12}$$

Constraint 2.9 is used in order to limit the heading change maneuvers. In fact, an aircraft is not allowed to perform a heading change that exceeds $\Delta\theta_{max}$. For instance, in Figure 2.5 the maximum allowed heading is represented with red dotted line and the following point of the flight trajectory can be any point of the green bow. Constraint 2.10 represents the

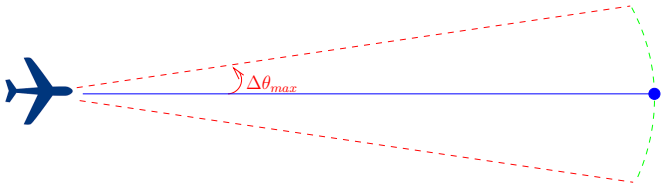

FIGURE 2.5 – Maximum allowed heading deviation

allowed departure time delay. Furthermore, constraints 2.11 and 2.12 define the tolerance with regards to the desired entry and exit NAT points respectively.

On the other hand, the decision variables should provide a conflict-free solution, therefore, the constraint 2.8 must be satisfied.

The **objective function** should take into consideration all the desired criterion of optimality. The main objective of our work is to find the optimal trajectory, for each aircraft, between its departure and destination points while avoiding conflicts. There exist different criteria of trajectory optimality, such as :

— minimizing the total cruising time,
— minimizing the fuel consumption,
— minimizing aircraft emissions.

In this work, we focus on optimizing the total cruising time. It is worth mentioning here that our model is a simplified model since we optimize a global parameter which raises the problem of equity, namely the cost delay is not a linear function. Nevertheless, minimizing the cruising time implies directly minimizing the fuel consumption as in our case aircraft have constant speeds ($\| \vec{V}^f \| = cte$) and FLs. Therefore, the **objective function**, referred to as F_{obj}, is defined by summing up the cruise time of all flights. It is calculated as follows :

$$F_{obj}(\Omega) = \sum_{f \in S} (t_{Nf}^f - t_0^f) \tag{2.13}$$

To sum up, our optimization problem can be formulated as follows :

$$\begin{aligned} \underset{\Omega=(\Omega^f)_{f\in S}}{\text{minimize}} \quad & F_{obj}(\Omega) \\ \text{subject to} \quad & \Phi_{tot}(\Omega) = 0, \\ & \Delta\theta_i^f = \mid \theta_i^f - \theta_{i-1}^f \mid \leq \Delta\theta_{max} \\ & 0 \leq D_{In}^f \leq Delay_{max} \\ & dist(P_{In}^f, p_1^f) \leq Dev_{max}^{In} \\ & dist(P_{Out}^f, p_{Nf}^f) \leq Dev_{max}^{Out}. \end{aligned} \tag{2.14}$$

2.3 Flight trajectory construction

In this section, we present the process applied in order to construct aircraft trajectories for a set of NAT flights. Afterward, we illustrate the objective function computation method of our optimization problem described in the previous section.

2.3.1 Adaptation of the flocking model

In this work, we aim to adopt the Flocking Principles, aforementioned in Section 2.1.3, to construct conflict-free trajectories. To this end, each flight, in our model, represents an agent (*boids*). Each agent has to apply flocking rules (Section 2.1.3) in order to accomplish an overall swarm behavior while automatically resolving conflicts.

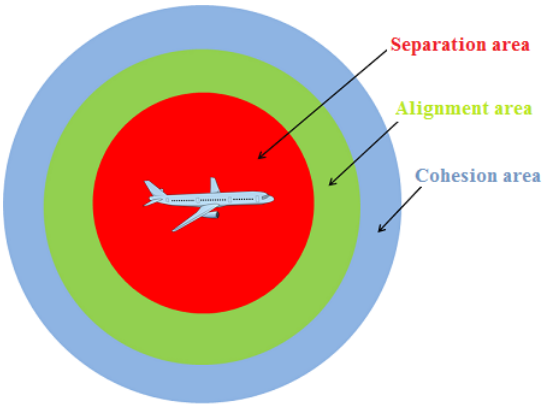

FIGURE 2.6 – Neighborhood areas

Let us start by defining the flight neighbors characteristics. In fact, in our study, the outline of neighborhoods depends on the flocking rule that has to be applied. As it is illustrated in the Figure 2.6, the separation area is the red circle space that directly surround the aircraft. In this area, the separation force is performed in order to avoid conflicts, namely with a radius R_{Sep}. It is necessary to point out that a separation force is applied before any conflict is detected, thus we are involving here a conflict avoidance maneuver. Figure 2.7 illustrates a case where two flights are within the predefined separation distance R_{Sep}. Thus, the separation rule is performed, and both involved aircraft

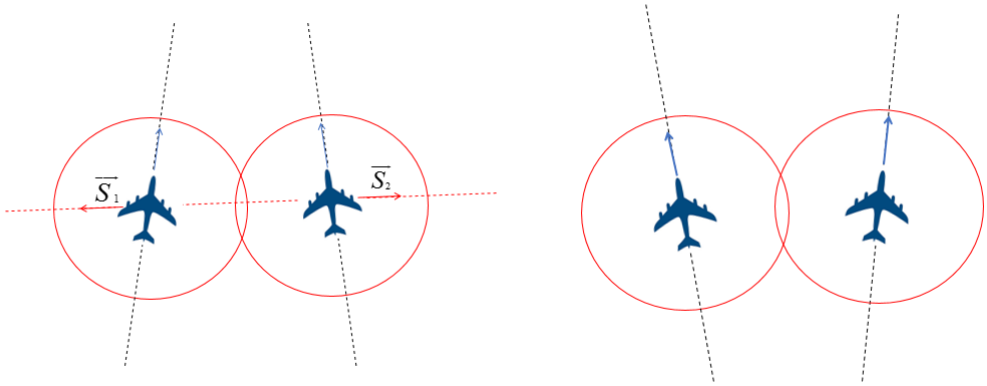

(a) Two flights within the separation radius

(b) Resulting trajectory after applying the separation vector

FIGURE 2.7 – Separation rule

are required to apply an opposite separation force ($\vec{S_1}$ and $\vec{S_2}$) as shown in Figure 2.7(a). This force yields to briefly steering each aircraft away from the other. As a result, the heading of each aircraft is adjusted in order to avoid a possible conflict, as illustrated in Figure 2.7(b).

The green circle space of radius R_{Align} represents the area where we apply the alignment force. It is applied to the flights located within the separation area as well. We recall that this force is used in order to organize the traffic into parallel or semi-parallel routes. This rule is performed by applying a force to steer a particular aircraft towards the aggregate headings of all the surrounding aircraft existing in the alignment area. An example with four aircraft, where each one is in the alignment area of the others, is shown in Figure 2.8. The alignment forces applied to each aircraft, referred as $\vec{A_1}$, $\vec{A_2}$, $\vec{A_3}$, $\vec{A_4}$, are drawn with green vectors.

The blue circle space of a radius R_{Coh} corresponds to the area where we apply the cohesion force. Recall that this force has an action opposite to that of the separation force. The cohesion force is applied to aircraft outside the separation radius, so that they stay within the group. A force is applied to aircraft far from the group in order to steer it towards the center of gravity of the swarm, such as force $\vec{C}$ in Figure 2.9.

2.3.2 Flight trajectory model

In order to build aircraft trajectories, we start with the first point of each trajectory, starting with the earliest aircraft in the set. We calculate the motion vector $\vec{V_i}^f$ to construct the next point in its trajectory. The motion vector is defined as follows (2.15):

$$\vec{V_i}^f = 60 * V^f * \frac{\vec{U_i}^f}{|| \vec{U_i}^f ||} \tag{2.15}$$

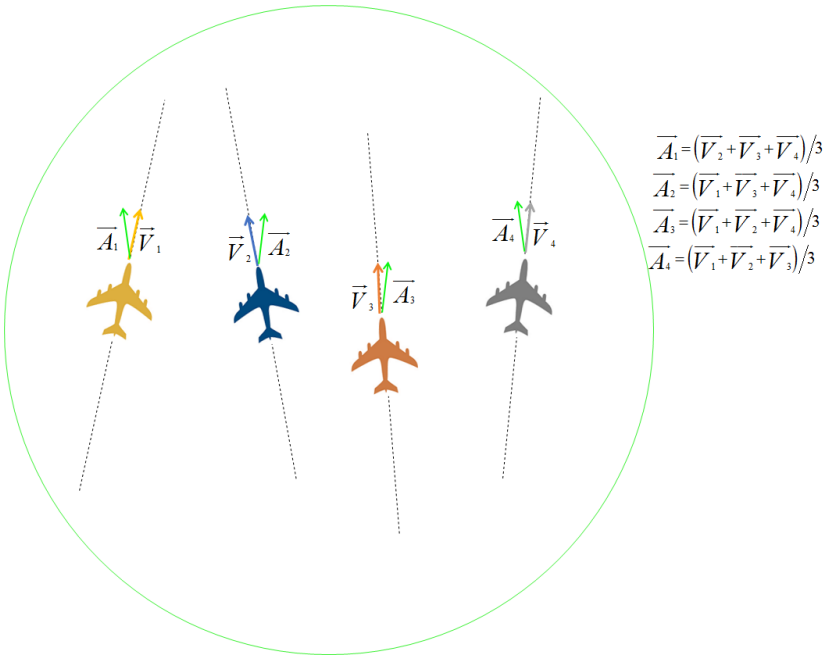

FIGURE 2.8 – Alignment rule

where i refers to the flight trajectory point, V^f is the desired aircraft airspeed expressed in meter per second. We multiply by 60 seconds to have the distance covered in 1 minute. The vector $\vec{U}_i^f$ correspond to the weighted sum of the five following vectors.

2.3.2.1 Flocking model alignment force

The *alignment* vector enables to line up an aircraft with its neighbors. Thus, the alignment vector, $\vec{A}_i^f$, of each flight f in each position i of its trajectory is calculated as the displacement vector in (2.16).

$$\vec{A}_i^f = \frac{\sum_{g \in FS_1} \vec{V}^g}{N_1} \tag{2.16}$$

where FS_1 is the set of neighbors in the alignment region for flight f, N_1 the number of flights in the set FS_1 and $\vec{V}^g$ is the motion vector of aircraft g.

2.3.2.2 Flocking model separation force

The *separation*, $\vec{S}_i^f$, vector prevents conflicts between aircraft. It is calculated for each flight f in each trajectory point i by applying (2.17).

$$\vec{S}_i^f = \frac{\sum_{g \in FS_2} ((\vec{P}_i^f - \vec{P}^g)/dist^2(\vec{P}_i^f, \vec{P}^g))}{N_2} \tag{2.17}$$

where FS_2 is the set of neighbors in the separation region for flight f, N_2 the number of flights in the set FS_2 and $\vec{P}_i^f$ is the position of flight f at the trajectory point i. $\vec{P}^g$ is the position of its neighbor aircraft g and the function $dist()$ calculates the distance between

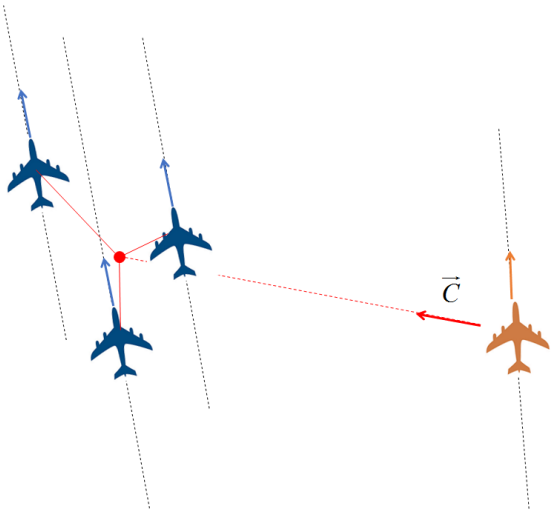

FIGURE 2.9 – Cohesion rule

two points. If we only apply the separation rule, aircraft will disperse. Thus, we need to apply the cohesion rule.

2.3.2.3 Flocking model cohesion force

The *cohesion* vector is in charge of gathering the flights to create a swarm behavior. Cohesion of flight f at point i is calculated in two steps. First, we calculate the barycenter $\vec{Fc}_i^f$ of its neighbors' positions, as in (2.18). Then we need to steer the flights toward that barycenter by calculating the cohesion displacement vector, $\vec{C}_i^f$, as in (2.19).

$$\vec{Fc}_i^f = \frac{\sum_{g \in FS_3} \vec{P}^g}{N_3} \tag{2.18}$$

$$\vec{C}_i^f = \vec{Fc}_i^f - \vec{P}_i^f \tag{2.19}$$

where FS_3 is the set neighbors in the cohesion region for flight f, N_3 the number of flights in the set FS_3, $\vec{P}^g$ is the position of the neighbor g and $\vec{P}_i^f$ represents the position vector of the flight f at the trajectory point i.

However, we noticed some issues when only applying the Flocking rules. In fact, all aircraft merge to the same destination point rather than their desired ones, as Flocking rules are originally designed for birds traveling towards the same destination. As a result, we add a Destination Vector that steers each aircraft to its destination. Nevertheless adding only this force does not solve the entire problem. Indeed, we notice that the aircraft trajectories are widely sinuous. This behavior is expected since birds are flexible in their movements which is not allowed for aircraft. Thus, we add another force that represents the Previous Motion Vector in order to establish a certain stability in the resulting trajectory. The two additional forces, that we should take into account in our problem, are presented in the following paragraphs.

2.3.2.4 Destination force

The *destination* vector is introduced in order to force each aircraft to navigate towards its destination point. Thus, it is a vector that links the current position of the flight with the destination position. It is referred to as $\vec{D}_i^f$ at each point i of the trajectory of flight f.

2.3.2.5 Previous motion force

The *previous motion* vector is introduced in order to avoid oscillations of the trajectory. It corresponds to the displacement vector applied in the previous point of the trajectory. Obviously, we do not add this vector at the first point of the trajectory. This vector is labeled $\vec{U}^f_{pred_i}$. For example, at position i, .

Finally, the resulting vector, $\vec{U}_i^f$, applied in each trajectory point i of the flight f, is calculated as the weighted sum of the five aforementioned vectors as in (2.20).

$$\vec{U}_i^f = w_{i1}^f * \vec{U}^f_{pred_i} + w_{i2}^f * \vec{D}_i^f + w_{i3}^f * \vec{A}_i^f + w_{i4}^f * \vec{S}_i^f + w_{i5}^f * \vec{C}_i^f \tag{2.20}$$

where $(w_{ij}^f)_{i\in\{1,2,..,N^f\},j\in\{1,2,...,5\}}$ are the coefficients to balance the five forces in each trajectory point i and represent the influence of each steering force. We recall here, that the displacement vector $\vec{V}_i^f$ of the flight f at each point i of its trajectory is given by 2.15.

2.3.3 Flight time computations in wind fields

To simulate each flight trajectory, we need to compute passing time at each trajectory point. These passing times depends on aircraft true airspeed and the wind direction and speed which are given data in our problem. To do so, we calculate the wind vector at each trajectory point using a grid of wind data (described in Section 1.4.3). For each trajectory point, we extract the east wind component W_u and the north wind component W_v and calculate the wind norm $||\vec{W}|| = \sqrt{W_u^2 + W_v^2}$ and the associated wind bearing $\theta_W = arctan(W_u/W_v)$ (see Figure 2.10).

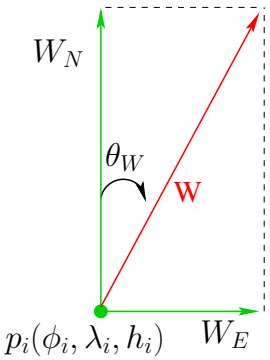

FIGURE 2.10 – Wind information in each flight trajectory point ($p_i{}^f$)

Once we get the wind information for each trajectory point, we can calculate the tail wind for each link connecting two successive trajectory points. Let (ϕ_i, λ_i, h_i) and

$(\phi_{i+1}, \lambda_{i+1}, h_{i+1})$ be the spherical coordinates (latitude, longitude and altitude) of the link origin point p_i and the link destination point p_{i+1} respectively. As we are working on 2D airspace and all the trajectory points have the same altitude we have $h_i = h_{i+1}$. Thus, computation are performed without considering the altitude and wind data are extracted for the particular flight level.
The associated bearing θ_l (see Figure 2.11) of each link l is given by the following formula:

$$\theta_l(p_i, p_{i+1}) = arctan(\frac{sin(\Delta_\lambda).cos(\phi_{i+1})}{cos(\phi_i).sin(\phi_{i+1}) - sin(\phi_i).cos(\phi_{i+1}).cos(\Delta_\lambda)}) \tag{2.21}$$

where $\Delta_\lambda = \lambda_{i+1} - \lambda_i$.

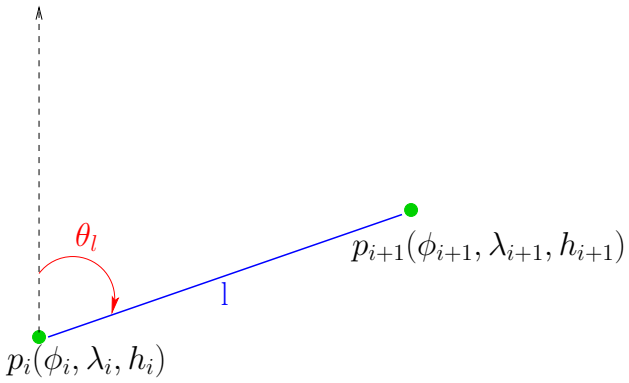

FIGURE 2.11 – The link bearing angle

Then, the tail wind at each extremity of the link TW_i and TW_{i+1} is given by:

$$TW_i = ||\overrightarrow{W_i}||.cos(\theta_l - \theta_{W_i}) \tag{2.22}$$

$$TW_{i+1} = ||\overrightarrow{W_{i+1}}||.cos(\theta_l - \theta_{W_{i+1}}) \tag{2.23}$$

We associate to each link the average of these two tail winds:

$$TW_l = \frac{TW_i + TW_{i+1}}{2} \tag{2.24}$$

The time needed for a flight to reach the trajectory point p_{i+1} from the point p_i can be now deduced by:

$$t_i = \frac{d_l}{V^f + TW_l} \tag{2.25}$$

where d_l represents the length of the considered link along the great circle and V^f is the true airspeed of the aircraft. Finally, the passing time of each flight through each point of its trajectory is updated with regards to the new computed times considering the wind.

Thus, we construct here the sequence points $(p_i{}^f, \vec{V}_i^f), i = 1, 2, .., N^f$ of each trajectory. Actually, the number of trajectory points N^f is not predefined, however, it is computed once the trajectory construction is achieved.

2.3.4 Trajectory construction method

Recall that we have defined, in section 2.2.4, the set of the following decision variables related to each flight f :

— $\Omega^f = ((\theta_i^f)_{i\in\{1,2,..,N^f\}}, D_{In}^f, p_1^f, p_{N^f}^f)$.

More precisely, the sequence of headings $(\theta_i^f)_{i\in\{1,2,..,N^f\}}$ is fully determined by the coefficients $(w_{ij}^f)_{i\in\{1,2,..,N^f\},j\in\{1,2,...,5\}}$. Thus, we can consider instead the following decision variable:

— coefficients w_{ij}^f, where $j \in \{1, 2, ..., 5\}$ and $i \in \{1, 2, .., N^f\}$

Indeed, determining the sequence of headings $(\theta_i^f)_{i\in\{1,2,..,N^f\}}$ of each flight trajectory is equivalent to determining the coefficient w_{ij}^f. Therefore, Ω^f is also defined as :

— $\Omega^f = ((w_{ij}^f)_{i\in\{1,2,..,N^f\},j\in\{1,2,..,5\}}, D_{In}^f, p_1^f, p_{N^f}^f)$.

Furthermore, recall that we have defined the following constraints that have to be satisfied by our decision variables :

$$\Delta\theta_i^f = \mid \theta_i^f - \theta_{i-1}^f \mid \leq \Delta\theta_{max} \tag{2.26}$$

$$0 \leq D_{In}^f \leq Delay_{max} \tag{2.27}$$

$$dist(P_{In}^f, p_1^f) \leq Dev_{max}^{In} \tag{2.28}$$

$$dist(P_{Out}^f, p_{N^f}^f) \leq Dev_{max}^{Out} \tag{2.29}$$

We add a new constraint to the weighted coefficients w_{ij}^f as follows:

$$0 < (w_{ij}^f)_{i\in\{1,2,..,N^f\},j\in\{1,2,..,5\}} < 1 \tag{2.30}$$

The constraint 2.26 is implicitly established by the trajectory construction process thanks to the *Previous motion force*. This result has been also verified empirically. In fact, the resulting trajectory shapes do not present any zigzagging behavior.

Furthermore, the constraint 2.29 is also automatically verified by the trajectory construction strategy. In fact, for each flight trajectory, the point p_d^f is the projection of the destination point P_{Out}^f on a plane. Then, at each iteration i, we check the two following equations:

$$dist(p_i^f, p_d^f) \leq dist(p_i^f, p_{i+1}^f) \tag{2.31}$$

$$dist(p_{i+1}^f, p_d^f) \leq Dev_{max}^{Out} \tag{2.32}$$

If the equation 2.31 is verified, then the process stops at the i^{th} iteration and the last point of the considered trajectory is p_d^f. Otherwise, if the equation 2.32 is verified, then the process stops at the iteration $(i + 1)$ and the last point of the considered trajectory is p_{i+1}^f. If neither of the two aforementioned equations, 2.31 and 2.32, are verified then the process continues. As a consequence, based on this process, we make sure that the destination point is either the desired one, or within a distance of Dev_{max}^{Out} from the desired one. Therefore, constraints 2.26 and 2.29 are not considered in our optimization process.

As the flight trajectory points are computed gradually in each algorithm iteration, the objective function, F_{Obj}, defined in 2.13 can not be explicitly determined in each iteration

because it depends on the flight arrival times. Therefore, we reformulate our objective function so that it appropriately fits within our resolution process.

Our optimization process is divided into two steps. First, the possible initial conflict at the point p_1^f of each flight f, must be resolved before the start of the algorithm. These initial conflicts can be resolved either by shifting the desired entry point or by delaying the flight. To do so, we define first the sub-set of decision variables relative to this sub-problem such as:

— $\sigma^f = (D_{In}^f, p_1^f)$.

— $\sigma = (\sigma^f)_{f \in S}$

Then, let us consider the total induced delay D_{tot}, over all flights which is calculated as follows:

$$D_{tot} = \sum_{f \in S} D_{In}^f \tag{2.33}$$

Furthermore, the time necessary for each aircraft to reach its desired entry point from its assigned entry point T^f, is deduced from the following equation:

$$T^f = \frac{dist(P_{In}^f, p_1^f)}{V^f} \tag{2.34}$$

Thus the total deviation time, over all aircraft, induced from the entry position shift, denoted T_{tot} is calculated as follows:

$$T_{tot} = \sum_{f \in S} T^f \tag{2.35}$$

As the two above-mentioned criteria, D_{tot} and P_{Nb}, are expressed in terms of time, they can be gathered using appropriate weighting coefficients to form the following objective function F_{obj_1} for the first process.

$$F_{obj_1}(\sigma) = \alpha_1 \times D_{tot}(\sigma) + \alpha_2 \times T_{tot}(\sigma). \tag{2.36}$$

where α_1 and α_2 are non-negative user-defined weighting coefficients to represent the trade-off between different criteria in the objective function.
As a result, our sub-optimization problem is stated as follows:

$$\begin{aligned} \underset{\sigma=(\sigma^f)_{f \in S}}{\text{minimize}} \quad & F_{obj_1}(\sigma) \\ \text{subject to} \quad & \Phi_{tot}(\sigma) = 0, \\ & 0 \leq D_{In}^f \leq Delay_{max}, \\ & dist(P_{In}^f, p_1^f) \leq Dev_{max}^{In}. \end{aligned} \tag{2.37}$$

Once the first process is accomplished, we perform for the second one. Here, the flight entry positions and times, obtained from the first process, are fixed and are not changed in this stage. Thus, the remaining decision variables considered for generating conflict-free trajectories in this stage are:

— $\chi^f = (w_{ij}^f)_{i\in\{1,2,..,N^f\},j\in\{1,2,..,5\}}$
— $\chi = (\chi^f)_{f\in S}$

As it is previously mentioned, flight trajectories are constructed sequentially at each time step, by finding the optimal balance between different applied vectors (Section 2.3.2). Initially, we assume that aircraft headings are directly steered to the destination points. Thereafter, the heading is adjusted in each point in order to avoid conflict with neighbors while maintaining the swarm behavior. In other words, in each algorithm iteration, we compute the coefficients $(w_{ij}^f)_{i\in\{1,2,..,N^f\},j\in\{1,2,..,5\}}$ in order to find for each aircraft the shortest trajectory towards its destination, while avoiding conflicts with other traffic.

In each iteration i of the algorithm, the **objective function** F_{obj_2}, which is defined as the sum, over all aircraft, of the time remaining for each aircraft to reach its desired destination, and is calculated as follows:

$$F_{obj_2}(\chi) = \sum_{f\in S} \frac{dist({p_i}^f, P_{Out}^f)(\chi)}{V^f + TW} \tag{2.38}$$

where TW represents the mean tail wind between the trajectory points p_i^f and P_{Out}^f. It is computed as follows. First, the remaining trajectory for the aircraft f to reach its destination point P_{Out}^f is sampled with a constant sampling time step of 60 seconds. To do so, the shortest possible distance between p_i^f and P_{Out}^f (*great circle path*) is computed as a time-sequence of trajectory points. Then, the tail wind between each two successive points is calculated such as in 2.24. Figure 2.12 describes the trajectory sampling process.

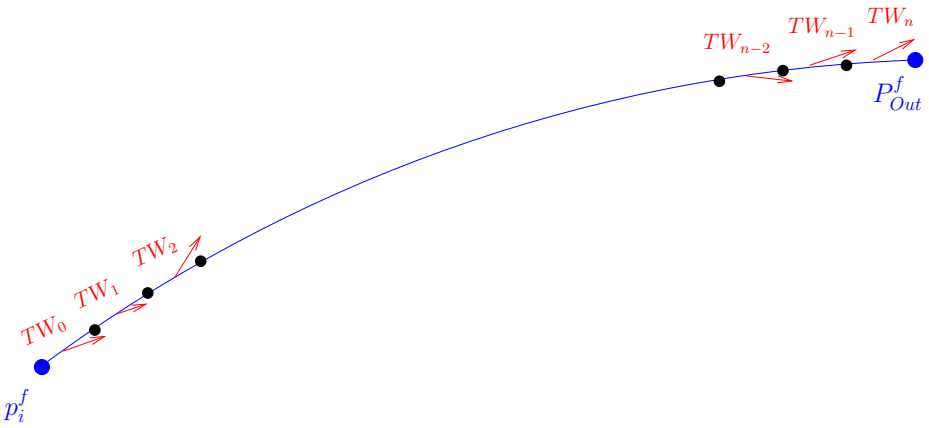

FIGURE 2.12 – Trajectory sampling

Finally, the mean tail wind TW is computed as follows :

$$TW = \frac{1}{n} \times \sum_{i=0}^{n} TW_i \tag{2.39}$$

Where n represents the number of the remaining trajectory sampling points. To summarize, the trajectory construction problem can be defined by the following combinatorial

optimization formulation:

$$\begin{aligned} \underset{\chi=(\chi^f)_{f\in S}}{\text{minimize}} \quad & F_{obj_2}(\chi) \\ \text{subject to} \quad & \Phi_{tot}(\chi) = 0, \\ & 0 < (w_{ij}^f)_{i\in\{1,2,..,Nf\},j\in\{1,2,..,5\}} < 1. \end{aligned} \tag{2.40}$$

2.4 Resolution algorithm

The two problem formulation steps 2.37 and 2.40, presented in the previous section are highly combinatorial, non-linear and with a non-explicit objective function since we cannot express it in terms of decision variables. Thus, we propose to resolve the problem via a *stochastic method*, namely the Simulated Annealing (SA) algorithm. The SA algorithm is described in details in Section 1.3.2. In this section, we present our resolution algorithm and how we adopt the SA to our problem. Then, numerical results from computational experiments are presented and discussed.

2.4.1 Adaptation of SA to our problem

The simulated annealing is applied independently for the two subproblems described in Section 2.2.4. The resolution algorithm processes as follows:

1. flights are sorted according to their entry times,
2. the first sub-process aimed at generating a set of conflict-free flights at the entry points is performed via SA,
3. the flight set obtained from the first sub-process is re-sorted according to the new assigned entry times.
4. the second sub-process takes place in order to generate a set of conflict free trajectories. This problem is also resolved with SA algorithm.

Roughly, the SA heuristic aims to minimize an energy function in an iterative process involving small changes to the current solution. The concept consists in accepting even the degrading solutions, but in a controlled manner. The process begins with an initial solution and with a pre-determined control parameter T (called temperature). The latter decreases with the number of iterations. At each step, SA calculates a neighbor solution. It associates with each solution an energy value and decides to keep either the neighbor solution or the current one. When T is large, exploration of the search space is promoted. When T is small, the system will converge towards the least energy solution.

Further in this section, the adaptation of SA algorithm to de-conflict entry points and to generate conflict free trajectories is described.

2.4.1.1 De-conflict entry points

We recall here that the optimization formulation of this sub-problem is given by 2.37. The SA algorithm is adapted to solve our sub-problem as follows:

— The search space consists of all possible configurations of the entry point parameters (entry point positions and entry times) for a set of flights. A solution is determined when we fix the decision variables (entry point positions and entry times) for each flight in the flight set.
— The energy function represents the objective function of our optimization sub-problem, as described in equation 2.37.
— The initial solution consists of the initial flight configurations obtained from the submitted flight plans.
— A neighbor solution is obtained by applying a local change to the current solution $\vec{x}_i$ in order to generate a new solution $\vec{x}_j$. It consists in changing one decision variable of an individual flight. The process of getting a neighbor solution is divided into two steps. First, the flight that generates the largest number of conflicts is selected to be modified. Then, we select the decision variable to be modified. Here, we choose randomly either to change the entry position or to delay the flight. The shift of the entry position is randomly performed within a circle having the desired entry point as a center and Dev^{In}_{max} as a radius. Also, the flight delay is randomly selected from the interval $]0, Delay_{max}]$ minutes.
— In each algorithm iteration, we consider the current solution $\vec{x}_i$, and $\Phi_{tot}(\vec{x}_i)$ its number of induced conflicts. Then, a neighborhood solution, $\vec{x}_j$, is generated and its number of induced conflicts $\Phi_{tot}(\vec{x}_j)$ is calculated. Here, we can distinguish two cases:
  — If the new solution minimizes the number of conflicts, e.i. $\Phi_{tot}(\vec{x}_i) > \Phi_{tot}(\vec{x}_j)$, then it is accepted.
  — Otherwise, the acceptance probability of the neighbor solution $\vec{x}_j$ is given by $e^{(F_{obj_1}(\vec{x}_i) - F_{obj_1}(\vec{x}_j))/T}$, where T is the temperature, $F_{obj_1}(\vec{x}_i)$ is the objective value of the current solution, $\vec{x}_i$, and $F_{obj_1}(\vec{x}_j)$ is the objective value of the neighbor solution, $\vec{x}_j$.
— The temperature decreases via a geometrical law given by $T_i = \alpha * T_{i-1}$.
— The process stops when the temperature T goes below a predefined final temperature, T_f. T_f is adjusted to be: $T_f = \beta * T_0$ (with $\beta << 1$).

Once the de-conflicting of entry points is accomplished, we perform for the second process to generate conflict-free trajectories.

2.4.1.2 Generate conflict free trajectories

The optimization formulation related to the present sub-problem is given in 2.40. The SA process applied to this sub-problem is similar to that applied for de-conflicting entry points, but with some modifications. First, we define experimentally a time step interval $T_{step} = 10$ minutes. Then, the process is iterated in each T_{step} until all flights reach their destinations. The main objective, in each iteration, is to find a conflict free sub-trajectory for each aircraft to fly in the next T_{step} minutes. Therefore, generating conflict-free trajectories is performed as follows:

— The search space consists of all possible configurations of $\chi = ((w_{ij}^f)_{i\in\{0,1,..,N^f\},j\in\{1,2,...,5\}})_{f\in S}$. A solution is determined when we fix the decision variables $((w_{ij}^f)_{i\in\{1,2,..,N^f\},j\in\{1,2,...,5\}})$ for each flight in the flight set.

— The energy function represents the objective function of our optimization sub-problem, as described in equation 2.40.

— The initial solution consists of a random configuration of $(w_{ij}^f)_{i\in\{1,2,..,N^f\},j\in\{1,2,...,5\}}$ for each flight.

— A neighbor solution is obtained by applying a local change to the current solution $\vec{x}_i$ in order to generate a new solution $\vec{x}_j$. The neighbor solution is generated by changing one decision variable of an individual flight, and the process is divided in two steps. First, we select the flight f that generates the largest number of conflicts to be modified. Then, we randomly change the configuration of $(w_{ij}^f)_{i\in\{1,2,..,N^f\},j\in\{1,2,...,5\}}$.

— The solution acceptance process, the temperature decrease law and the stopping criterion are performed the same as what was described in the first sub-process of de-conflicting entry points.

The overall approach we used in this work is described in Figure 2.13.

2.4.2 Computational results

First, detailed results for a sample flight set are discussed. Then, we display results for larger flight set samples. In this work, it is assumed that all aircraft are equipped with ADS-B. Thus, reduced separation norms are considered as follows :

— the vertical separation norm $V_{sep} = 1000$ feet (1 FL),

— the lateral separation norm, $Lat_{sep} = 30$ NM,

— the longitudinal separation norm, $Lon_{sep} = 3$ minutes .

We stress here that 3 minutes in longitudinal separation is approximately equal to the time required by the fastest commercial aircraft ($v_{max} \approx 600kts = 10NM/min$) to overfly 30 NM. Thus, it is conceivable to combine lateral and longitudinal separation to a horizontal separation of 30 NM.

Furthermore, the radius of the flocking rules application are set experimentally as follows:

— the radius of the separation area $R_{Sep} = 2 \times Lat_{sep}$

— the radius of the alignment area $R_{Align} = 5 \times Lat_{sep}$

— the radius of the cohesion area $R_{Coh} = 8 \times Lat_{sep}$

Moreover, the algorithm parameters are set as follows:

— the weighting coefficients in equation 2.36: $\alpha_1 = \alpha_2 = 1$, in order to give the same priority to decreasing the total delay and the total deviation time.

— the maximum heading deviation $theta_{max} = \frac{\pi}{6}$

— the maximum delay $Delay_{max} = 20$ minutes.

— the maximum deviation from the desired entry point $Dev_m^{In}ax = 5$ NM.

— the maximum deviation from the desired exit point $Dev_m^{Out}ax = 5$ NM.

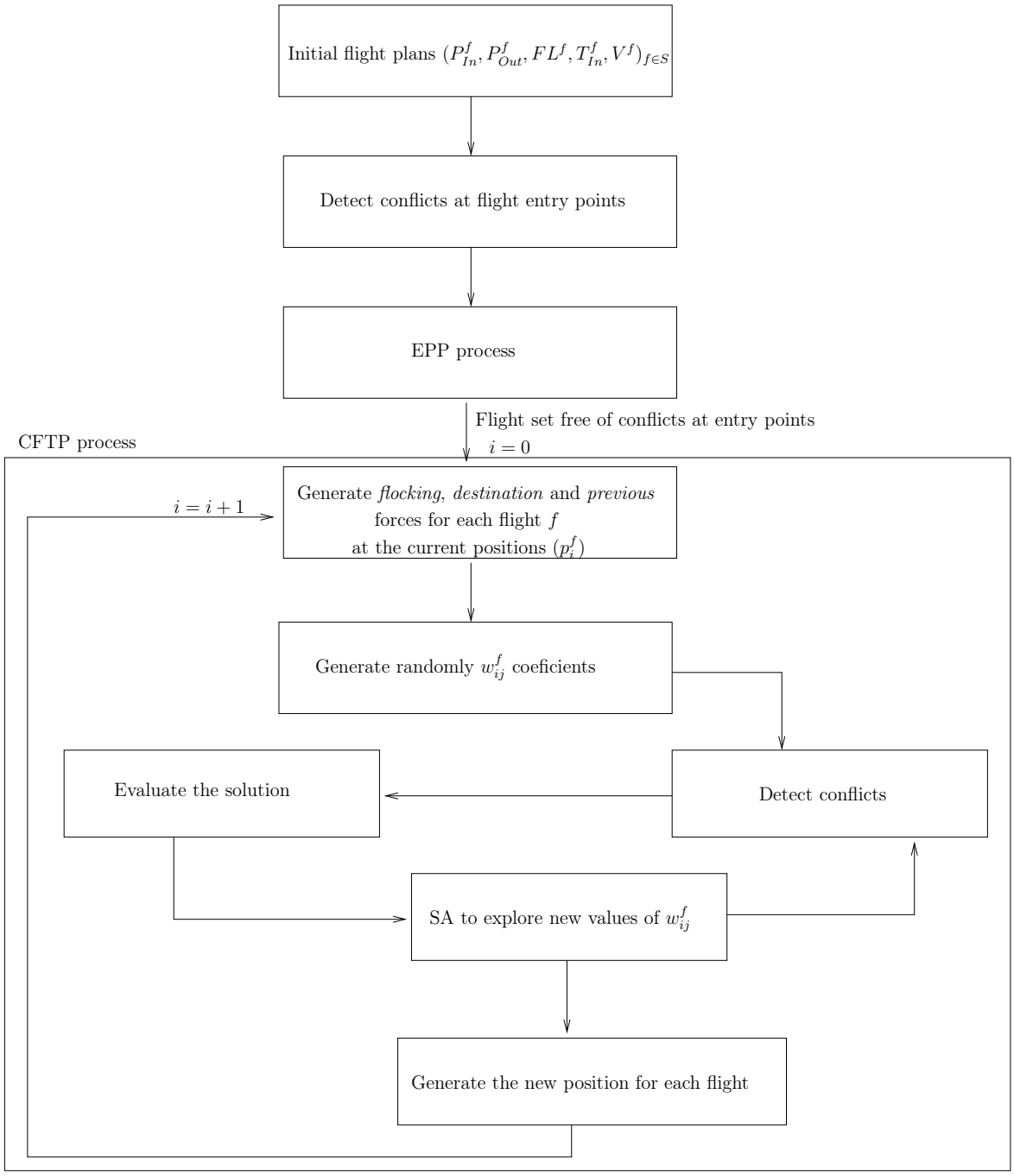

FIGURE 2.13 – Proposed approach

2.4.2.1 Results for a small flight set sample

We perform simulations with a small set containing $Nb = 200$ flight extracted from real NAT traffic for July 15^{th}, 2012. Initially, the considered flight set generates 199 aircraft pairs in conflict, among which 18 aircraft pairs are in conflict at their entry points. We start with de-conflicting the entry points then we generate conflict-free trajectories.

Results of de-conflicting entry points As described in 2.4.1, this process is aimed at resolving conflicts at the flight's entry point. The configuration of the SA is displayed in Table 2.1.

Algorithm parameters	value
Number of iterations at each temperature step, N_{iter}	500
Geometrical temperature decrease law, α	0.95
Final temperature, T_f	$0.0001 * T_0$

TABLE 2.1 – Empirically set parameters of the SA algorithm

After resolving conflicts at entry points, the resulting flight set is free-of-conflict at each entry point. This result is obtained by only delaying flights, while keeping the desired entry points for all flights without any deviations. Figure 2.14 displays the distribution of assigned delays among the 200 considered flight.

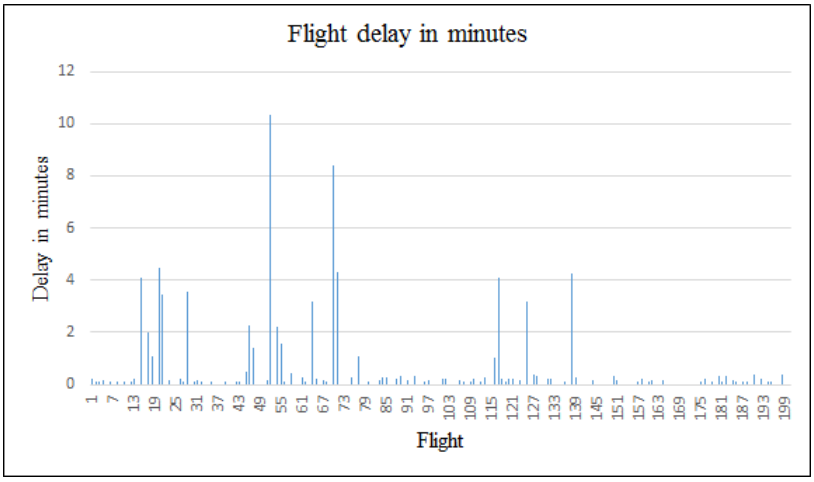

FIGURE 2.14 – The assigned delays in minutes

The resulting solution is obtained by delaying 100 flight, which represent a rate of 50%. As displayed in Figure 2.14 the majority of assigned delays does not exceed 2 minutes. In fact, the assigned delay of 86 flight is less than 2 minutes, which represents a rate of almost 86% of all delayed flights. The maximum assigned delay is 10.33 minute and only one flight is delayed by more than 10 minutes. Once the departure conflict are resolved, we start with generating conflict-free trajectories.

Results of generating conflict-free trajectories Starting with the conflict-free entry points, the trajectory of each flight is constructed iteratevely based on the displacement vector calculated as in Section 2.3.2. The configuration of the algorithm is displayed in Table 2.2. These parameters are set experimentally. After applying the algorithm, the resulting flight trajectories are conflict-free. This result is very important, but we also have to verify the trajectory length. For this reason, we compare our resulting trajectories

Algorithm parameters	value
Separation radius	$2 * Lat_{sep}$
Alignment radius	$5 * Lat_{sep}$
Cohesion radius	$8 * Lat_{sep}$
Number of iterations at each temperature step, N_{iter}	500
Geometrical temperature decrease law, α	0.95
Final temperature, T_f	$0.0001 * T_0$

TABLE 2.2 – Parameter values of the algorithm of generating conflict-free trajectories

with the reference trajectories which are wind-optimal (Section 1.4.3). The considered wind-optimal trajectories are believed to be the shortest paths for flights taking into account the wind direction and without considering the trajectory conflicts. In other words, it designs the shortest path for each flight supposing that it is flying alone in the airspace. Thus, the wind-optimal trajectories are operationally not realistic. As such, we consider that a flight trajectory 5% longer than the wind-optimal one is satisfying, since we consider the conflict resolution pattern. In our case, the trajectory elongation is calculated in terms of time, and represents the rate of extra time needed to reach the destination point following the resulting trajectory compared to the wind-optimal cruising time when following wind-optimal trajectory.

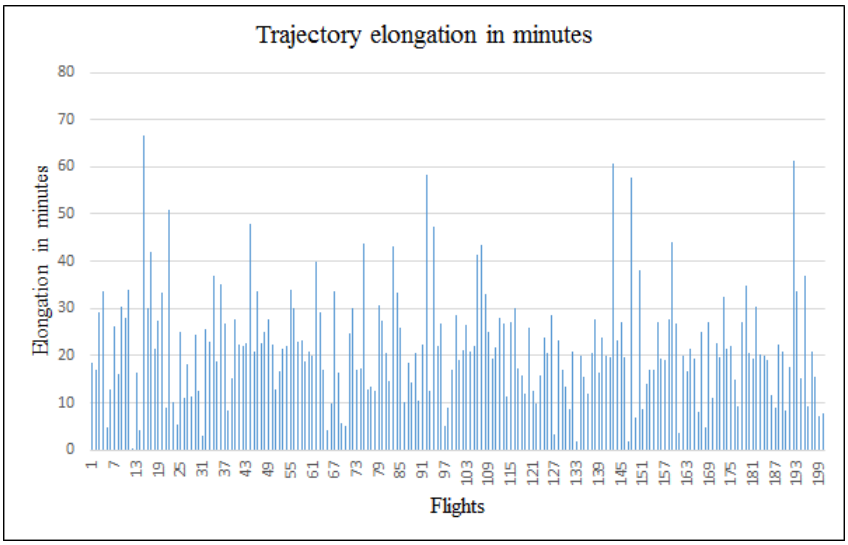

FIGURE 2.15 – Cruise time elongation in minutes

Figure 2.15 displays the cruise time elongation in terms of minutes for each flight. We observe that for 163 flight (which represents $81,5\%$ of all flights) the trajectory cruise time increase does not exceed 30 minutes. However, some flights experience a cruise time elongation that exceeds 50 minutes. Note here that we are tackling very long flights with a total flight cruise time that ranges between 6 to 8 hours. Thus, a cruise time increase of 30 minutes represents between 6.2% to 8.3% of the total flight cruise time while a cruise

time increase of 50 minutes elongation represents between 13, 8% and 10.4%. Figure 2.16

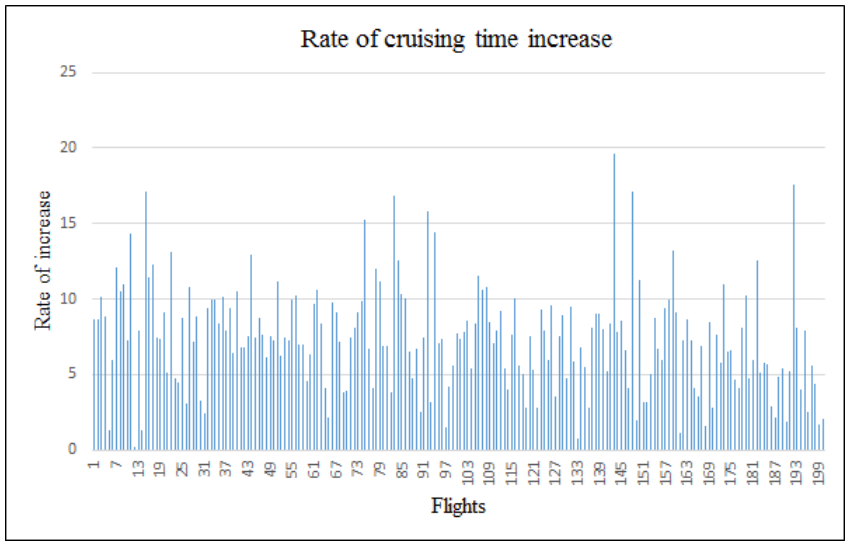

FIGURE 2.16 – Rate of cruise time increase (%)

illustrates the rate of cruising time increase for each flight. To determine this rate, we first compute the cruising time for each flight following the wind-optimal trajectory, denoted t_{crui_1}. Then, we compute the cruising time for the flight following our resulting trajectory, t_{crui_2}. The rate of cruising time increase is given by: $\frac{t_{crui_2} - t_{crui_1}}{t_{crui_1}} * 100$.
The average of cruising time increase rate for the 200 considered flight is almost 7%. As we aforementioned, the wind-optimal trajectory do not consider the conflict resolution and are operationally not realistic. For this reason, we can consider that our result is satisfying. Nevertheless, the increase in cruising times is, in our case (with constant velocities and flight levels), directly related to the increase of fuel consumption. Therefore, flying the resulting trajectories will require on average 7% more kerosene for the considered flights.

Table 2.3 summarizes the performance results of the conflict resolution algorithm. The number of initial conflicts, being excessively large, is totally reduced with our resolution algorithm. Furthermore, even though the percentage of delayed flights is large, however, the mean delay is considerably small (0.8 minutes), which results on an almost equitable distribution of rather small delays between flights.

The obtained results leads us to the following conclusions:

— The number of conflicts induced by the set of wind-optimal trajectories is very large due to the restrictive separation norms applied in oceanic airspaces (Lateral separation of 30NM).

— Our conflict resolution algorithm enables to resolve conflicts in the considered set of 200 flights.

— The trajectory set, though conflict-free, presents a considerable cruising time increase compared to wind-optimal trajectory. This is due to the *cohesion force* which influences the aircraft to stay on the group even though the resulting trajectory is longer than the direct trajectory to the destination.

	Before	De-conflict entry points	Generate conflict-free traje
Number of *point-to-point* conflicts	35148	35130	0
Number of *flight-to-flight* conflicts	199	189	0
Percentage of delayed flights, %	-	50%	50%
Mean delay, minutes	-	0.8	0.8
Percentage of entry point deviation, %	-	0%	0%
Percentage of exit point deviation, %	-	-	0%
Mean cruising time increase, minutes	-	-	21
Mean rate of cruising time increase, %.	-	-	7%

TABLE 2.3 – Summary of the conflict resolution results

The next section presents similar results, but for larger flight sets.

2.4.2.2 Results for a real traffic day

In this section, we examine results for real traffic in the NAT on July, 15^{th} 2012. The flight set contains 668 eastbound flights. Similarly to the previous section, we start with de-conflicting entry points then we generate conflict-free trajectories. In this section, we will only present the results as the two algorithms have been described in the previous section.

Results of de-conflicting entry points To perform this process, we keep the same algorithm configuration described in Table 2.1. The resulting flight set is free-of-conflict at entry points. This result is obtained by only delaying flights, while keeping the desired entry points for all flights without any deviations. Table 2.4 summarizes the obtained

	Before	De-conflict entry points
Number of conflicts at entry points	61	0
Maximum delay, minutes	-	16
Percentage of delayed flights, %	-	73%
Mean delay, minutes	-	1.2
Percentage of entry point deviation, %	-	0%

TABLE 2.4 – De-conflicting entry points results for a day traffic

results de-conflicting entry points. Results here are similar to those found with a small set of flights. In fact, we notice a large number of delayed flights but with a very small assigned delays. Note that reducing the number of delayed flights is possible with our model by including this number to the objective function. Nevertheless, in this case, we penalize some flights much more than others. For this reason, we think that distributing assigned delays between flights is a rather fair solution.

Results of generating conflict-free trajectories The same algorithm parameters described in table 2.2 are applied here to generate conflict-free trajectories. Findings

are summarized in Table 2.5. The first observation that can be made, based on these

	Before	De-conflict entry points	Generate conflict-free trajecto
Number of *point-to-point* conflicts	119078	119017	65
Number of *flight-to-flight* conflicts	781	775	32
Percentage of delayed flights, %	-	73%	73%
Mean delay, minutes	-	1.2	1.2
Percentage of entry point deviation, %	-	0%	0%
Percentage of exit point deviation, %	-	-	10,7%
Mean cruising time increase, minutes	-	-	16.18
Mean rate of cruising time increase, %.	-	-	5.6%

TABLE 2.5 – Summary of the conflict resolution results for a day traffic

results, is that the number of conflicts is significantly decreased. Nevertheless, it is not possible to find a conflict-free solution. The number of conflicts between flight trajectories is decreased from 781 to 32 conflicts. This result is considered as a good result in our case. In fact, we are considering strategic conflict resolution, and any remaining conflicts can be treated further in tactical and pre-tactical phases.
Moreover, the average increase in cruising time in comparison with wind-optimal trajectories is very satisfying (16.18 minute). However, the mean value does not give an accurate view of the overall flight trajectories. For this reason, more detailed results are given in table 2.6.

	values
Nb. flights with cruising time increase < 5 minutes	63
Nb. flights with cruising time increase < 30 minutes	540
Nb. flights with cruising time increase > 60 minutes	29
Nb. flights with cruising time increase > 90 minutes	7
Maximum cruising time increase, min.	119

TABLE 2.6 – Results on flight cruising time increase

The first conclusion drawn from these results is that a large number of flights, almost 80%, are within 30 minutes from their wind-optimal trajectories. This is a very important result since the wind-optimal trajectories, that we refer to, do not take into account the conflict resolution. Furthermore, about 10% of flights follow almost their optimal trajectories (with cruising time increase under 5 minutes). Nevertheless, we notice that 29 flights, which represents almost 4% of all flights, are penalized with a very large extension compared to optimal trajectories, and their flight time increase exceeds an hour. This result reveals the downside of our methodology which stems mainly from two causes. First, in our approach, we are more interested in the conflict resolution process, and the quality of the trajectory is a secondary interest. Second, the considered objective function to be minimized includes the sum of flight cruising times, and as a result the cruising time

is not minimized for each individual flight. The main drawback here is that the decrease of a global parameter can be favorable for some flights, but very penalizing for others.

In addition to this, we propose to re-evaluate the resulting set of trajectories under wind uncertainties. For this reason, we perform the conflict detection with different wind scenarios. The four considered wind scenarios are described in detail in Section 1.4.3. The results are presented in table 2.7.

	values
Initial number of conflict	781
Residual conflicts	32
Residual conflicts with scenario s1	65
Residual conflicts with scenario s2	102
Residual conflicts with scenario s3	122
Residual conflicts with scenario s4	175

TABLE 2.7 – Re-evalute the resulting solution with different wind scenarios

These results prove that a big number of conflicts reappear once the resulting flight set is evaluated with different wind fields that take into account wind uncertainties. The number of conflicts that reappear in some cases (s4) can be up to 5 times the initial residual number. We recognize here the main drawback of strategic trajectory planning, i.e. its robustness regarding changing flight conditions, in particular, meteorological conditions especially for oceanic airspace that are subject to very strong winds. Therefore, this problem encourages us to investigate more robust flight trajectories in NAT, and that is a good challenge for our following work.

2.5 Conclusions

In this chapter, we propose a new trajectory planning method for NAT flights based on the Free Flight Concept and Multi-agent systems. Assuming that all aircraft are equipped with an ADS-B system, the proposed approach adopts the Flocking rules in order to construct a set of conflict-free flight trajectories. The trajectory construction process and the flight parameter allocation was modeled as an optimization problem that we solve using a simulated annealing algorithm.

The algorithm was tested with a real traffic data from July 2012. The computational results show that we can considerably reduce conflicts with reasonable assigned delays and elongation compared to the direct path. The remaining number of conflicts between flights is not a big problem in our case since we are considering the strategic phase. Nevertheless, results for some flights are disappointing. Indeed, even though the majority of flight trajectories are close to the optimal ones, we notice that some flights experience a large elongation from their optimal trajectories. Furthermore, our study was unsuccessful in finding robust flight trajectories with respect to changing wind. In fact, when we re-evaluate the resulting flight set with different wind data new conflicts re-appear. This is

a very big problem when considering the NAT traffic. Indeed, NAT flights are subject to very changing and strong winds caused by the jet streams.
For this reason, it is primordial to find new robust solutions for the NAT trajectory planning problem. This will be the main focus of the next chapter.

Chapter 3

Flight planning based on wind-optimal route structure

In this chapter, we present a new route structure that we propose to replace the OTS, in order to organize the NAT traffic. The chapter starts with a discussion of existing works devoted to improving the air traffic situation in oceanic airspaces. Then, we describe in detail the proposed route structure as well as its construction procedure. After that, we propose a mathematical model to organize the NAT traffic inside the route structure, by formulating it as an optimization problem and resolve via a simulated annealing algorithm. Finally, computational results for real NAT traffic are presented, and a comparison with wind-optimal NAT trajectories is made.

3.1 Literature review

In this section, we discuss existing approaches from the literature that address improving air traffic situation in oceanic airspaces. As we propose to take advantage from the reduced separation standards in NAT trajectory planning, we start by investigating its induced benefits. Then, we highlight previous works proposing wind-optimal flight trajectories rather than the nominal oceanic route structure.

3.1.1 Separation standards reduction in oceanic route structures

In this section, we present some previous works that investigate benefits from applying reduced separation norms (vertical, lateral and longitudinal) within the route structure established in oceanic airspaces.

[73] is among the earliest studies to investigate the benefits of reducing the vertical, lateral and longitudinal separation norms in North Pacific oceanic airspace in 1993. The North Pacific oceanic airspace accommodates traffic between North America and the Far East, and a route structure, referred to as NOPAC, presents the primary link between these two continents. In the early 90's, separation norms in oceanic airspaces were even greater than the current standard separation norm, and about 40% of Pacific traffic was required to fly at constant Flight Levels. In [73], simulations were conducted for real Pacific traffic in 1993, and also for the traffic growth predicted for year 2000. Important conclusions are drawn based on these simulation results. First, reduction of longitudinal

separation significantly improves the system efficiency by increasing the capacity of preferred tracks. Second, reduction in lateral separation leads to upgrading the track system by increasing the number of tracks. For instance, seven tracks could be created in the Pacific airspace to replace the five nominal tracks. As a result, the traffic density within tracks is alleviated. At last, reduction in vertical separation, combined with allowing step-climbs, has a significant positive effect on reducing fuel consumption.

In a detailed report in 2000 [35], Gerhardt-Falk *et al.* investigate the fuel savings resulting from several scenarios of reduced separation norms applied to NAT. First, authors introduce a new model to simulate NAT traffic. Then, five scenarios with various lateral, longitudinal and vertical separation norms are played out. Simulation results reveal that reducing separation norms significantly reduces fuel consumption by attributing flights their preferred flight levels, and reduces the number of detected conflicts as well.

Williams et al. evaluate potential benefits from implementing an Airborne Separation Assurance System (ASAS) In-Trail Climb procedure in the South Pacific oceanic airspace (SOPAC) [117], then on the NAT [118]. Here, an aircraft is allowed, while climbing to a higher flight level, to apply an alternate longitudinal separation standard of 10 NM with an aircraft at an intermediate flight level, instead of a longitudinal separation of 10 minutes which is set to be equal to 80 NM in this study. This separation norm reduction is subject to the availability of ADS-B information. In this study, all aircraft are assumed to be properly equipped, and six scenarios with different separation norm reductions are discussed in the simulations. This research reveals improvements in operational efficiency through fuel savings and additional cargo revenue potential. It clearly proves that reducing the separation standards in oceanic airspaces is very beneficial.

A similar study performed by Chatrand *et al.* is discussed in [22]. The same idea as in [118] is presented here, however the investigated scenarios are not the same. For instance, the percentage of aircraft equipped with ADS-B may take different values and several aircraft densities in the NAT OTS are considered. The simulations were only performed for eastbound flights, as it has been shown that westbound traffic results in similar findings. Considering the climb-request approval rate over scenarios, Chatrand *et al.* affirm that it increases as the ADS-B equipage rate increases. Furthermore, authors affirm that ADS-B equipped aircraft achieve important savings on fuel consumption, without affecting the fuel performance of non-equipped aircraft. Therefore, the latter are not penalized by the increased number of equipped aircraft.

In [116] authors analyze the advantages of reducing the horizontal separation between appropriately equipped oceanic flights on NAT OTS. An aircraft is considered to be properly equipped when it is able to maintain a situational awareness and navigate accurately. Both lateral and longitudinal separation norms are reduced to 30 NM for properly equipped aircraft. The longitudinal separation reduction is performed by allowing reduced spacing between two consecutive well-equipped flights in the same track. The lateral separation reduction is performed by introducing new tracks among NAT OTS tracks with reduced separation norms, referred to as *segregated tracks*. As illustrated in Figure 3.1, the separation between *segregated tracks* (presented in red) is reduced (Sep

A = $30NM$). These *segregated tracks* are reserved for properly equipped aircraft. Nevertheless, the spacing between nominal tracks remains equal to the lateral separation standards (Sep B = $60NM$). These nominal tracks are available for all flights. Two

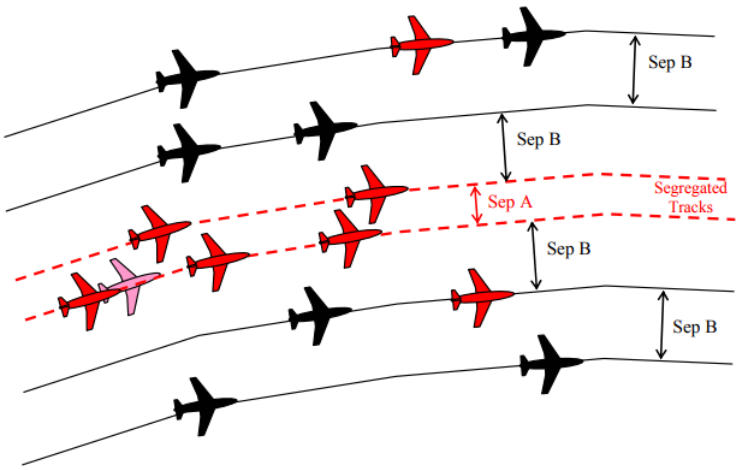

FIGURE 3.1 – Construction of segregated tracks within the OTS [116]

cases of simulations are considered. In the first case, only vertical separation reduction is considered while addressing nominal OTS tracks with mixed operations of non-equipped and equipped flights. In the second case, segregated tracks are included in the OTS. Furthermore, various aircraft equipage rates are addressed in the study, and different levels of traffic density are investigated. The most important advantages concluded from this research involve improvements in operator efficiency over time and fuel savings, additional cargo revenue potential, and system efficiency through better cruise level assignments.

To sum up, all the previous studies mentioned in this section prove significant benefits come from reducing the separation norms, including time and fuel savings, additional cargo potential, frequency of optimal FL assignments, etc. Nevertheless, none of the aforementioned studies have addressed the possibility of re-routing inside the route structure. The next section is devoted to studies that investigate the benefit from re-routing between tracks.

3.1.2 Rerouting inside oceanic route structures

In the previously discussed studies, the flights are required to follow a single track, from the entry point to the exit point, because of the large separation norms. Nevertheless, aircraft may desire to enter and exit the OTS at different tracks.

In [67], Louyot *et al.* investigate the benefits of reducing the separation norms in the case of re-routing inside a route structure. The study focuses essentially on two issues. First, it quantifies the need for flights to change their tracks inside the OTS. Second, it evaluates the frequency of such re-routings in scenarios with different separation norms and with different ADS-B equipage rates. Some assumptions are made in the simulations. For instance, only eastbound OTS traffic is considered. Moreover, flights can only be

re-routed to an adjacent track, and the *First In First Out* (FIFO) principle is applied to perform re-routing. Furthermore, re-routing was only allowed in the final portion of eastbound OTS, in the zone just before exiting the NAT, namely between longitude $20°W$ and $15°W$. In simulations, several days of NAT traffic are performed with various ADS-B equipage rates. Furthermore, two separation scenarios are considered as displayed in Figure 3.2.

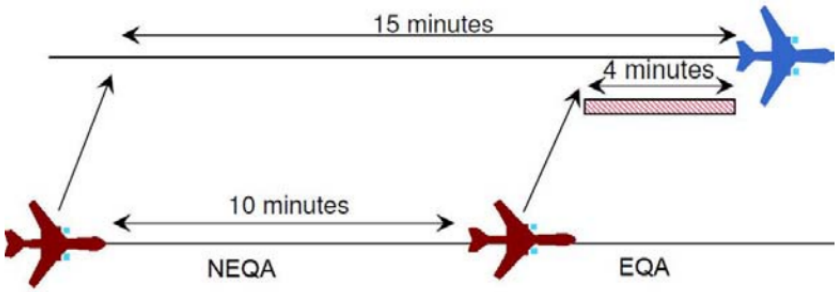

FIGURE 3.2 – Separation scenarios for re-routing OTS flights [67]

The first scenario considers procedural separation between non-equipped flights, which imposes a longitudinal spacing of 10 and 15 minutes (Section 1.2.3). The second one applies reduced separation norms, ranging from 2 to 5 minutes, between equipped flights. Based on the simulation results, the major conclusion drawn by Louyot *et al.* is that reducing the separation norms thanks to ADS-B equipage significantly favors the flights re-routing between tracks in order to join a more convenient track. This re-routing results in a strong positive effect on improving not only each single flight trajectory, but also the whole NAT traffic situation.

As an extension of [67], Rodionova *et al.* [90] investigate the possibility of performing re-routing between OTS tracks in the whole NAT OTS. Similar to all the previously discussed studies, Rodionova *et al.* consider the case where flights are equipped with ADS-B in order to benefit from reduced separation norms, and only eastbound traffic is treated. Here, the OTS is represented as a grid of waypoints (WPs) (see Figure 3.3), and flights can only perform re-routing at waypoints. Thus, at each waypoint, the aircraft has three possibilities: stay on the some track, move one track up, or move one track down. The aircraft also has the possibility of changing its flight level at waypoints. In [90], authors propose an optimization formulation of the problem that consists in providing the optimal flight plans for a set of NAT flights within the OTS and taking into account reduced separation norms. Then, the problem is resolved by Genetic Algorithm (GA). The proposed approach has been applied to real NAT traffic data containing almost 350 flights, and the influence of wind has also been taken into account in simulations. The main conclusion that can be drawn from this study is that reducing of oceanic separation standards thanks to ADS-B equipage encourages aircraft to perform re-routing within the OTS, which in turns, makes it possible for aircraft to follow more optimal trajectories towards their destination. Therefore, the total flight duration and the congestion level in

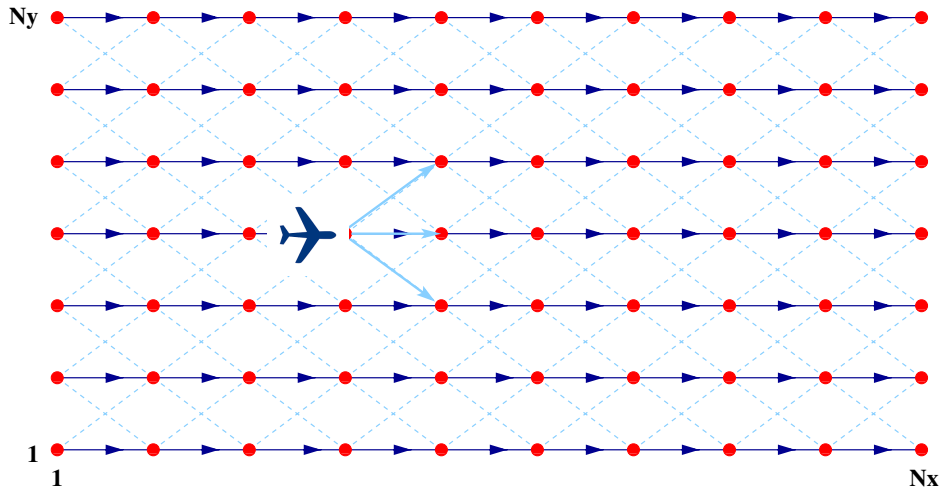

FIGURE 3.3 – OTS grid in horizontal dimension [90]

the pre/post oceanic airspace is significantly decreased.
The same authors applies the Simulated Annealing (SA) algorithm to resolve the same problem in [95]. When comparing the two algorithms (SA and GA) in terms of quality of the best solution found and the CPU time execution, Rodionova *et al.* affirm that SA finds better solutions than GA in much less time. More details on the two previously mentioned studies can be found in [91].

Works by another research group investigate the potential benefits of transitioning from the route structure to wind optimal routes. These works are addressed in the next section.

3.1.3 Wind-optimal flight trajectories

Generally, generating optimal aircraft trajectories involves not only flight and air traffic performances but also meteorological conditions. Therefore, the first important step to perform in order to construct wind-optimal trajectories consists on analyzing the weather particularities of the considered airspace.

A detailed analyses of meteorological conditions, including a classification of weather patterns in NAT airspace, our region of interest, is presented in [53]. The climate cost functions are calculated, for each weather pattern, by selecting representative days in both winter and summer. Analysis of climate impact from NAT flights were conducted in terms of CO_2 and O_3 emissions, water vapors and contrails. Authors conclude that climate impact is more influenced by long flights, and thus, affirm the importance of selecting wind-optimal trajectories especially for NAT flights.

[39] is among the first studies to discuss the potential benefits of following wind-optimal routes instead of using the Central East Pacific (CEP) airspace route structure. A backward recursion dynamic programming algorithm is used to calculate wind-optimal flight routes. The study revealed an average reduction in time and distance of 9.9 minutes and 36 NM per flight, respectively.

In [38], the same authors present a conflict-detection approach, which is based on the Conflict Grid where each grid cell can be occupied by only one aircraft at any time. In this study, the problem of conflict resolution is formulated as a job-shop scheduling problem. The approach is applied to de-conflict wind-optimal trajectories for Central East Pacific flights generated in [39]. The flight departure times are considered as the only optimization variables. The advantage here is that the resulting aircraft trajectories remain wind-optimal as their shapes are not changed. However, the resulting solution may involve very large flight delays which is an important issue from the operational point of view.

In [78], authors present an approach for cross-polar aircraft trajectory optimization and analyze its potential climate impact. The research focuses on deviating flights from fixed routes to operate on wind-optimal routes in order to reduce environmental emissions by minimizing fuel burn. Wind-optimal flight trajectories were generated by applying Pontryagin's Minimum Principle [29]. In this study, each aircraft trajectory is optimized by calculating the adequate heading that minimizes the flight travel time considering the wind, using the aircraft equations of motion at a constant altitude. A comparison between great circle and wind-optimal trajectories for cross-polar flights between three origin-destination airport pairs is performed. Findings prove a reduction of almost 0.3% to 2% in fuel consumption when following wind-optimal trajectory compared to great circle route.

The same approach is applied in [103] in order to generate wind-optimal trajectories in cruise for NAT flights. The 2D-horizontal trajectory is optimized by determining the heading that minimizes travel time in the presence of wind. The resulting wind-optimal trajectories are compared to the flight routes following NAT OTS in order to estimate the potential for fuel and time savings. First, simulations were conducted for the westbound and the eastbound flights between Newark and Frankfurt regarding the daily variations of potential wind-optimal savings during July 2012. Results, along the entire month, show mean fuel savings of 2.4% and 2.2% for the eastbound and westbound flights, respectively. Furthermore, analyses were conducted to determine the potential fuel benefits resulting from wind-optimal trajectories for the 10 busiest trans-Atlantic airport pairs over July 2012. Results reveal a rate of fuel savings ranging between 1.7% and 3.5% for both eastbound and westbound can be reached monthly.

The approach proposed in [78, 103] is extended to 3-dimensional airspace in [75]. Here, the process is divided into two stages. First, the optimal vertical profile for each aircraft is calculated. Then, optimal aircraft headings considering the wind are determined on multiple flight levels. Dynamic programming is applied to generate wind-optimal 3D aircraft trajectories in NAT. Similarly to the aforementioned studies, results also prove the importance of traveling wind-optimal trajectories in saving both travel-time and fuel.

The use of wind-optimal routes, being very beneficial especially in terms of fuel savings, generates a large number of potential conflicts between flights. As a result, the NAT becomes extremely congested. Some recent works aim to de-conflict wind-optimal routes over the oceanic airspace. For instance, both studies [93, 105] introduce strategic methods

for detecting and resolving conflicts between wind-optimal flight trajectories in the NAT airspace.

In [105], the conflict resolution is ensured by a SA algorithm and is based on two maneuvers: changing the departure time, and slightly modifying the geometrical shape of the trajectory while remaining wind-optimal. More details and results about the adopted approach are further presented in [93]. Findings show that an interesting reduction in the number of conflicts can be reached while keeping flight trajectories as close as possible to wind-optimal ones. However, the main disadvantage of this approach concerns the robustness of the resulting trajectories. In fact, when taking into account uncertainties in wind data, new conflicts appear and the proposed method does not provide any solution to this problem.

To sum up, the current route structures implemented in oceanic airspaces, though robust, are inefficient regarding the traffic density growth. Alternatives to these route structures, and in particular to the NAT OTS, are made possible by reducing oceanic separation norms. Although flying free wind-optimal trajectories significantly reduces fuel consumption, it is not a robust strategy to the strong winds encountered in oceanic airspaces. In order to benefit from both reduced separation norms and wind-optimal operations, we propose a new wind-optimal route structure, referred to as Wind-Optimal Track Network (WOTN), to replace the OTS. The proposed approach is detailed in the next section.

3.2 Mathematical model

The NAT particularities are described in detail in Section 1.2. Furthermore, the problem considered in this work is highlighted in Section 1.4. Below, we briefly describe the considered problem and we discuss some assumptions made for simplifying the problem. Next, a new route structure for the NAT is proposed, referred to as *Wind-Optimal Track Network* (WOTN). The construction of WOTN represents an improvement compared to the actual OTS that is based on two major factors. First, this WOTN allows eastbound flights following the jet stream direction which is beneficial for the en-route fuel consumption. Second, assuming that all aircraft implement the ADS-B system, reduced separation norms are considered. After that, we formulate our optimization problem expressed as input data and decision variables. Finally, we describe the optimization algorithm that we address to find optimal flight plans for a set of NAT flights.

3.2.1 Problem description

This work is aimed at improving the traffic situation in the NAT by organizing the transatlantic traffic and scheduling flights at the strategic level while ensuring that the required separation norms are maintained. The flight data are exactly the same as presented in 1.4. In this work, we aim at constructing efficient flight schedules that benefit from the wind-direction and satisfy the required separation between flights. This is done at the strategic level, i.e. several hours or days before real time operations, in order to

facilitate the controller workload during the tactical phase. To deal with this problem, we propose a new, more efficient route structure, the WOTN, to replace the OTS. The main challenge of the strategic planning is dealing with high level of uncertainty resulting, in particular, from the wind prediction errors. Thus, robustness of the proposed solution is crucial: we want to ensure that the required separation is maintained for the proposed flight schedules regardless of the changing wind conditions.
Our problem can be formulated as follows. We are given:

— Original flight schedules based on the submitted flight plans,
— Forecast wind fields,
— Separation norms.

We would like to assign a trajectory to each flight follow using a traffic organization method based on the WOTN structure.
Our main goal is to resolve all potential conflicts between such trajectories, while maintaining optimal routes in terms of cruise times. We recall here that, for the purpose of simplifying the simulations, we concentrate our effort on conflict detection and resolution within the NAT, as it is the main subject of the study. We omit the possible conflicts in the continental airspace which may be induced by our solution, considering that they are easier to resolve thanks to the relatively small continental separation norms. Thus, we end up with a conflict detection and resolution problem.

3.2.2 WOTN construction and model

In this section, we present the new WOTN route structure which we use instead of the OTS to schedule transatlantic flights. The new route structure concept was performed in two independent steps. In the first step, we construct the new WOTN based on the location of the OTS. The resulting tracks are denoted $WOTN_{OTS}$. Then, the same concept of the route structure design is adjusted to cover a larger region of NAT, the resulting route structure is denoted WOTN. In both cases, we assume that we are dealing with a system where all flights are ADS-B equipped, as this assumption will soon be a fact (Section 1.1.5). Thus, we consider a lateral separation of 10 NM for $WOTN_{OTS}$ tracks and 12 NM for WOTN tracks in some cases, namely when following parallel tracks. The construction procedure of WOTN is detailed below.

3.2.2.1 $WOTN_{OTS}$ construction

The location of OTS tracks differs daily according to weather and traffic demand. They are typically located between longitude $-50°$and $-15°$, and latitude $45°$and $55°$. Furthermore, the average distance across each OTS track is 1500 NM.
As mentioned in Section 1.2.2, OTS tracks are separated by 60 NM. In contrast, in $WOTN_{OTS}$, we keep tracks separated by 10 NM. Considering the fact that only one or two OTS tracks are completely merged in the jet stream and that these tracks are typically the middle ones (Section 1.4.1), $WOTN_{OTS}$ is constructed as follow: We keep the entry and exit points of the OTS tracks. Beginning from the first point of each

track, all tracks are merged to the center where the jet stream is located. Then, we keep tracks parallel and separated by 10 NM along 1000 NM. Finally, each track joins the corresponding exit point of the OTS system (see Figure 3.4). Furthermore, in the section of our structure where tracks are separated by 10 NM, we do not allow aircraft to change their track. Indeed, an aircraft entering the parallel track section has to keep its track until it reaches the exit point of this section. Obviously, flights crossing the OTS do not

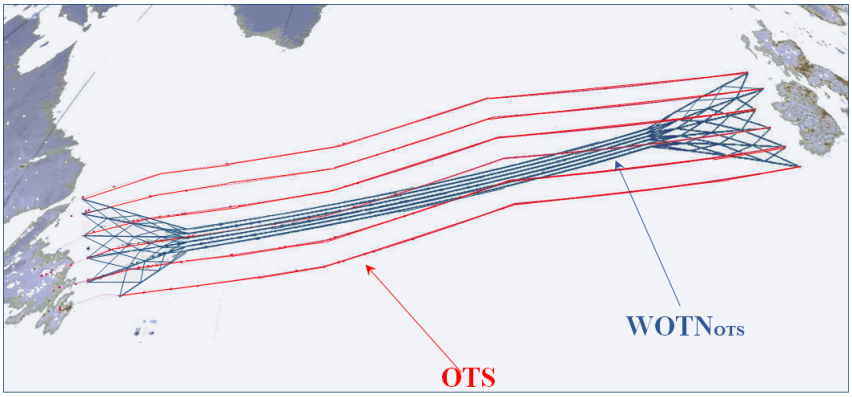

FIGURE 3.4 – Superposition of the OTS with the new route structure

keep the same track from entrance point to exit one. As a result, $WOTN_{OTS}$ has to satisfy this constraint and guarantee reliable transitions between tracks. Thus, sections before and after the parallel track region are considered as filters. In these sections each track contains waypoints. Flights are only allowed to change their tracks at these waypoints. Moreover, maintaining the preferred flights altitude profile is recommended since it guarantees optimal fuel consumption. Thus, even though we forbid transitions from one track to another inside the parallel track region, aircraft can change flight level according to their preferred altitude profiles over this region. For this reason, three waypoints per track are used to change flight levels while maintaining the same track in the parallel region. Therefore, tracks are represented as a set of waypoints connected by links.

3.2.2.2 WOTN construction

As NAT air traffic is exponentially growing, OTS tracks are insufficient to deal with this growth. Therefore, we propose to increase the number of tracks as well as the airspace covered by the route structure. For this reason, we consider the area between longitude $-90°$and $10°$, and latitude $30°$and $70°$, in order to extend the $WOTN_{OTS}$ tracks to cover the overall NAT airspace. As shown in section 1.4.3 (see Figure 1.12), jet stream are mainly concentrated around latitude $50°$. First, we construct the entry points of the new eastbound tracks: at longitude $-70°$, we put 8 virtual equally distributed points, starting from latitude $42°$and separated by 120 NM. Exit points are constructed similarly at longitude $-10°$and latitude $48°$. Then, starting from the entry point on each track, we merge all tracks to the center (around latitude $50°$), and we keep tracks parallel and

separated by 12 NM along 1600 NM (this part of the WOTN is referred to as "parallel track section"). Here, parallel tracks are separated by 12 NM unlike $WOTN_{OTS}$ tracks which are separated by 10 NM. This small increase of the lateral separation is made for design simplicity reasons and it is not inconsistent with the route structure construction principles as the parallel tracks are still immersed in the jet stream (the jet stream width is up to 100 NM).
Finally, each track joins the corresponding exit point. We do not allow aircraft to change their tracks within the parallel track section: an aircraft entering the parallel track section has to stay on the same track until it reaches the exit point of this section. However, as aircraft may desire to enter and exit the NAT from different tracks, we want to guarantee reliable transitions between tracks. Thus, sections before and after the parallel track section are used as filters.

Flight level change is allowed in all WOTN waypoints. However, re-routing between tracks is only allowed at waypoints in the filter section. Therefore, at each waypoint of the filter region, the flight can perform one of the three following maneuvers: either it continues with the same track or it changes its track to an adjacent one (north or south) or it changes its flight level.

3.2.2.3 WOTN model

WOTN can be modeled by a $N_y \times N_x \times N_z$ grid of waypoints:
— N_y is the number of WOTN tracks which is equal to 8 tracks,
— N_x is the number of waypoints in each track wich is equal to 22 waypoints in each track, and
— N_z is the number of flight levels available which is equal to 21 flight level.

Figure 3.5 illustrates the grid model in horizontal dimension in the general case. In this case, the route structure includes 8 tracks and covers an airspace of 2600×840 NM^2. Therefore, each two successive entry points, as well as each two successive exit points, are separated by 120 NM. Furthermore, the parallel track section stretches for 1600 NM. Figure 3.6 illustrates the case of restricting the route structure to the number of tracks and airspace considered within the OTS. Here, the same entry and exit points of the OTS, which are separated by 60 NM, are considered and the parallel track section extends for 1000 NM.
We define here some notations that will be used in the rest of this work:
— Tracks are labeled with j ranging from 1 to N_y, starting from the southern track.
— On each track, waypoints are labeled with i ranging from 1 to N_x, starting from the western waypoint.
— Flight levels are labeled with k ranging from 1 to N_z, starting from the lowest one.

Therefore, the vector *(i,j,k)* specifies the exact position of an eastbound flight flying on track j at waypoint i and at flight level k. Based on the constructed grid, we introduce the notion of *links* and *nodes* as follows:
— A *link* represents a straight line joining:

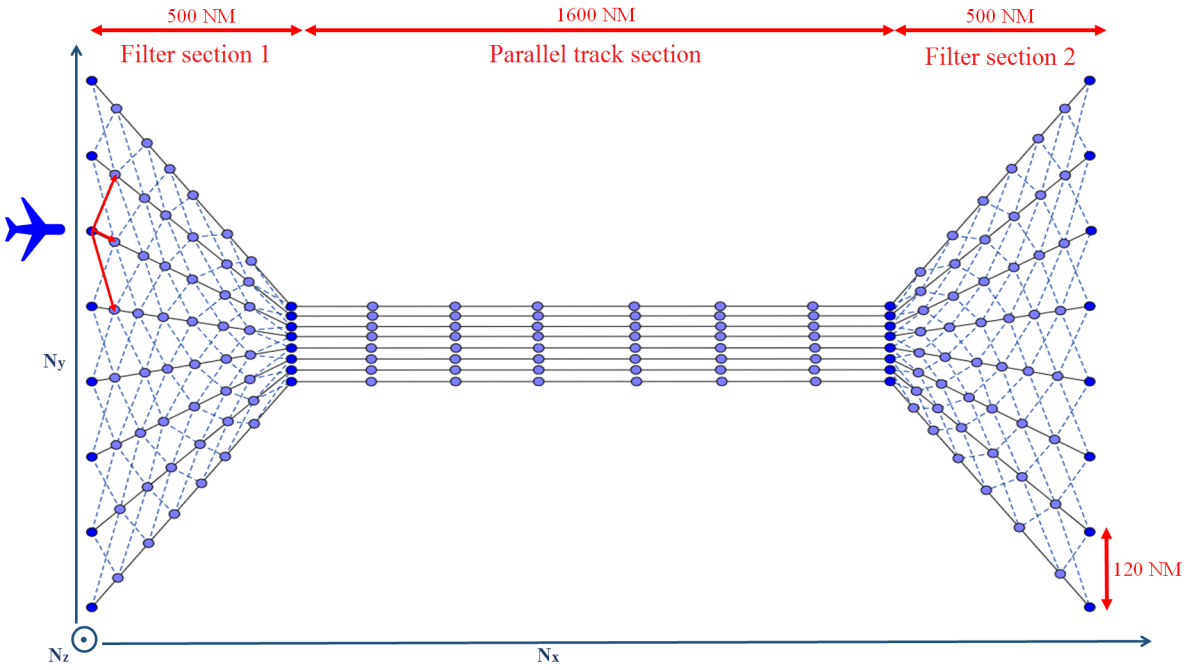

FIGURE 3.5 – Horizontal section of the WOTN grid model

— a pair of consecutive waypoints, *(i,j,k)* and *(i+1,j,k)*, on the same track j and the same flight level k,
— a pair of consecutive waypoints on adjacent tracks and on the same flight level: from *(i,j,k)* to *(i+1,j-1,k)* or from *(i,j,k)* to *(i+1,j+1,k)*.

— A *node* represents each intersection point between two links. Thus, each waypoint represents a node. Furthermore, the intersection between links connecting two waypoints from different tracks is also a node, denoted *crossing node*.

We denote L the set of all WOTN grid links and N the set of all WOTN grid nodes. In addition to WOTN waypoints, N also includes the points of intersection between links joining adjacent tracks.

3.2.3 Flight model

In this section, we describe how flights are modeled in our problem.

Based on the flight data detailed in Section 3.2.1, we start by selecting desired entry and exit tracks for each flight. The desired entry and exit tracks for each flight f are referred to as $Track^f_{in}$ and $Track^f_{out}$, respectively. These are obtained from the flight entry data. In fact, for each flight f, the $Track^f_{in}$ represents the track closest to the flight's entry point into the NAT, and $Track^f_{out}$ represents the track closest to its exit point. This choice of tracks is performed in order to reduce congestion in the pre-oceanic continental airspace.

Furthermore, in order to enlarge our state space in case of high traffic demand, we authorize the assignation of flights entry and exit tracks that are adjacent to the desired ones. As a result, the aircraft is allowed to deviate from its desired entry/exit track by one

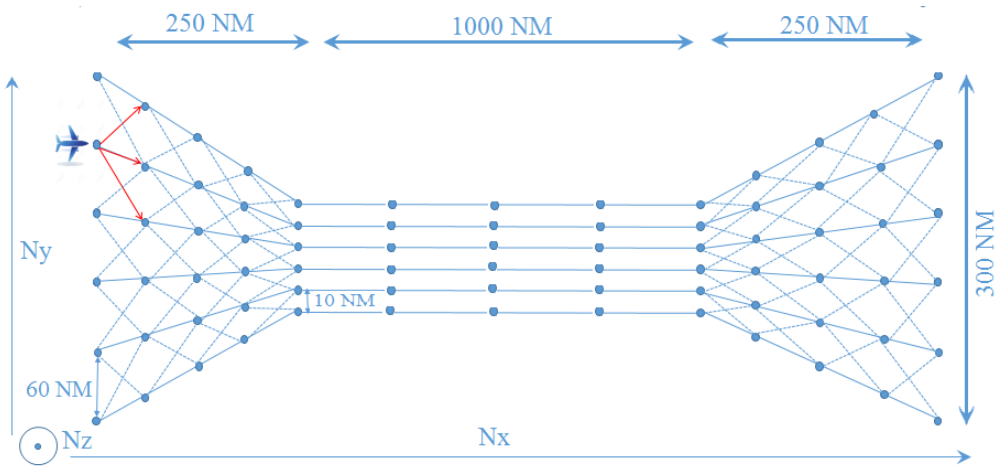

FIGURE 3.6 – Horizontal section of the $WOTN_{OTS}$ grid model

track north or south. The new assigned entry and exit tracks are denoted as $ATrack_{in}^{f}$ and $ATrack_{out}^{f}$ respectively and are part of the decision variables of our optimization problem.

Once the aircraft enters the WOTN at an assigned track, it is required to keep the same track and the same flight level unless a change of its trajectory is made. Considering an aircraft at a waypoint *(i,j,k)*, it has several possibilities to continue its trajectory:

— continue on the same track and at the same flight level, or
— re-route to an adjacent track at the same flight level, or
— change the flight level.

Re-routing between tracks is only authorized at the waypoints of the filter sections (see Figure 3.5). Furthermore, it is only allowed in one direction (either north or south) in order to conduct aircraft towards their destinations and prevent zigzagging between tracks. Therefore, the number of re-routing maneuvers is given by the difference between the assigned entry and exit tracks for each aircraft.

Thus, at waypoint *(i,j,k)*, the aircraft has three possibilities to choose its next waypoint when keeping the same flight level:

— the following waypoint is *(i+1,j,k)* if the aircraft continues on the same track, or
— the following waypoint is *(i+1,j+1,k)* if the aircraft switches to the northern track, or
— the following waypoint is *(i+1,j-1,k)* if the aircraft switches to the southern track.

To summarize, entry and exit tracks along with the re-routing profile determines the 2D trajectory of each aircraft. The 3D flight trajectory is computed by considering the vertical profile of the flight. Therefore, we also allow aircraft to perform *step climbs* in order to follow their optimal vertical profiles in terms of fuel consumption. However, *Step Descents* are not considered in our case of study since we are only tackling the cruise phase. Step climbs are performed only at waypoints, for both filter and parallel sections. In our simulations, we assume that for each flight *f*, its vertical profile FL_i^f at each waypoint $i \in \{1, 2, \ldots, N_x\}$ is a given input data recorded from the FPL. For the

purpose of extending the search space, we authorize a step climb planned at waypoint *(i,j,k)* to be performed at an adjacent waypoint on the same track (namely at *(i-1,j,k)* or *(i+1,j,k)*) if aircraft performance is compatible. In our model, we neglect the time needed by the aircraft to reach its new flight level when performing a step climb. This assumption is conceivable since the distance between waypoints is much longer than the distance between flight levels. We also assume, for simplicity, that the aircraft jumps directly from its waypoint *(i,j,k)* to the next waypoint *(i,j,k+1)* on the upper flight level. Therefore, step climbs are also included in the decision variables of our optimization problem.

Once the 3D trajectory is determined, we can compute 4D flight trajectories by computing flight passing times at waypoints. To do so, we consider first the True Air Speed (TAS) of each flight *f*, denoted V^f. We assume that V^f is an input data and is not changed for the entire trajectory. Furthermore, it is necessary to consider the desired entry time to the WOTN, denoted T^f_{In}. This is a given input data defined in the FPL based on airlines preferences. Nevertheless, it has been determined, empirically, that a conflict-free solution is almost impossible with the desired entry times. As a result, we assume that entry times can be relaxed, but in a controlled manner. Thus, we restrict the maximum allowed delay assigned to an aircraft to 20 minutes. Therefore, the assigned delay for each flight *f*, further denoted ${D_{in}}^f \in [0, 20]$ minutes, is part of the decision variables of our optimization problem.

Finally, we have also to consider wind influence on the flight progress in order to have almost exact computation of flight passing times at waypoints. In our model, we consider a simplified model of wind calculation. In fact, the wind field is supposed to be constant for each 6 hours of the day. Furthermore, the wind is defined at nodes and links and is supposed to be constant on each link. The flight passing times considering the winds in each waypoint of the flight trajectory is detailed in Section 3.2.4. As 4D flight trajectories are explicitly determined, they will be used in order to perform conflict detection in Section 3.2.5, and to formulate our optimization problem in Section 3.2.6.

3.2.4 Flight time computations in wind fields

The flight trajectory progress is simulated, for each aircraft, based on the aircraft true airspeed and the wind direction and speed which are given data in our problem. This process is performed exactly as in the approach previously proposed in Section 2.3.3. In fact, we calculate the wind vector at each waypoint of the WOTN using a grid of wind data (described in Section 1.4.3). For each waypoint, we extract the east wind component W_u and the north wind component W_v and calculate the wind norm $\| \vec{W} \| = \sqrt{W_u^2 + W_v^2}$ and the associated wind bearing $\theta_W = arctan(W_u/W_v)$.

Once we get the wind information for each waypoint, we can calculate the tail wind for each link. Let (ϕ_o, λ_o, h_o) and (ϕ_d, λ_d, h_d) be the spherical coordinates (latitude, longitude and altitude) of the link origin waypoint WP_o and the link destination waypoint WP_d

respectively. The associated bearing θ_l of each link l is given by the following formula:

$$\theta_l(WP_o, WP_d) = arctan(\frac{sin(\Delta_\lambda).cos(\phi_d)}{cos(\phi_o).sin(\phi_d) - sin(\phi_o).cos(\phi_d).cos(\Delta_\lambda)}) \tag{3.1}$$

where $\Delta_\lambda = \lambda_d - \lambda_o$.

Then, the tail wind at each extremities of the link TW_o and TW_d is given by:

$$TW_o = \parallel \vec{W}_o \parallel .cos(\theta_l - \theta_{W_o}) \tag{3.2}$$

$$TW_d = \parallel \vec{W}_d \parallel .cos(\theta_l - \theta_{W_d}) \tag{3.3}$$

We associate to each link the average of these two tail winds:

$$TW = \frac{TW_o + TW_d}{2} \tag{3.4}$$

The time needed by a flight to reach waypoint WP_d from waypoint WP_o can be now deduced by:

$$t = \frac{d_l}{V^f + TW_l} \tag{3.5}$$

where d_l represents the length of the considered link along the great circle and V^f is the true airspeed of the aircraft.

3.2.5 Conflict detection strategy

Based on our WOTN model, conflicts between flights can occur either at links or at nodes, which includes both waypoints and crossing nodes. At each node, conflict is detected if two successive flights are within a longitudinal separation, denoted further Lon_{sep}. It is assumed to be 2 minutes for aircraft in the same track, and 3 minutes for aircraft changing tracks. Figure 3.7 shows the longitudinal separation norms.

Besides, an aircraft has also the possibility to change its flight level (only by climbing). The aircraft position deviation in the horizontal plane is neglected, as well as the time required to reach the new flight level. This assumption is reasonable since the distance between successive waypoints (about 1.5°≈ 75 Km between waypoints in the filter section and about 5°≈ 250 Km between waypoints of the parallel section) is much longer than the distance between flight levels (1,000 feet, equal to 0.3048 Km). However, when changing its flight level, an aircraft has to maintain a new separation norm with aircraft flying on the same track at the new flight level. The separation standards, in this case, become 2.2 minutes (refer to Section 1.2.3).

Considering our WOTN, we can distinguish two type of conflicts:

— Φ_N conflict at nodes, and

— Φ_L conflict at links.

At node level, conflicts are detected by:

1. sorting flights passing through a given node according to their arrival times, then

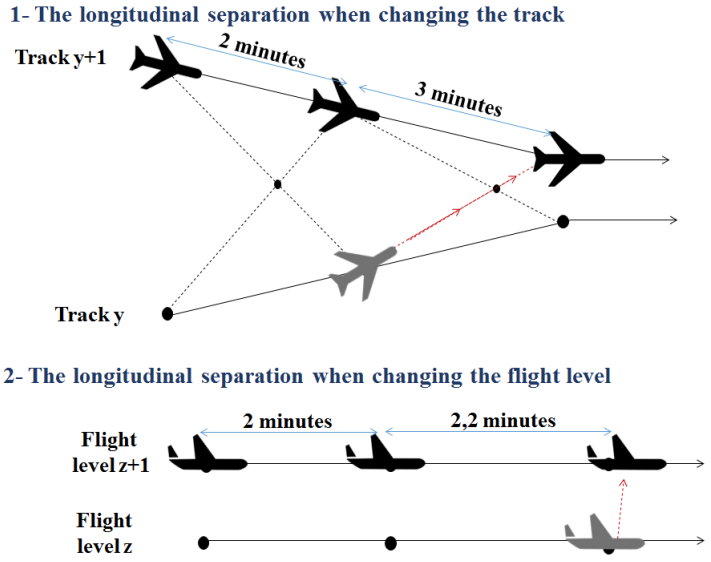

FIGURE 3.7 – Longitudinal separation norms

2. computing the difference in arrival times between each two successive flights in the sorted list, and thus
3. a conflict is detected when this difference is less than the longitudinal separation norm.

An example of a conflict avoidance maneuver between two aircraft at a common crossing node is illustrated in Figure 3.8. For instance, let us consider two aircraft, f_n^1 and f_n^2,

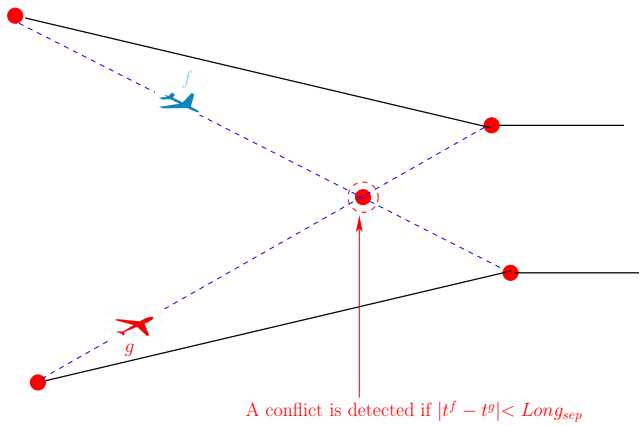

FIGURE 3.8 – Conflict between two aircraft at a crossing node

passing the same node n at times $t^{f_n^1}$ and $t^{f_n^2}$, respectively. Therefore, a conflict is detected between f_n^1 and f_n^2 at node n, if the longitudinal separation norm is violated on this node, *i.e* $|t^{f_n^1} - t^{f_n^2}| < Lon_{sep}$ (see Figure 3.9). The implemented algorithm to compute the number of node conflicts is described in details in Algorithm 1. Nevertheless, this algorithm can underestimate the real number of conflicts; for instance, if we consider

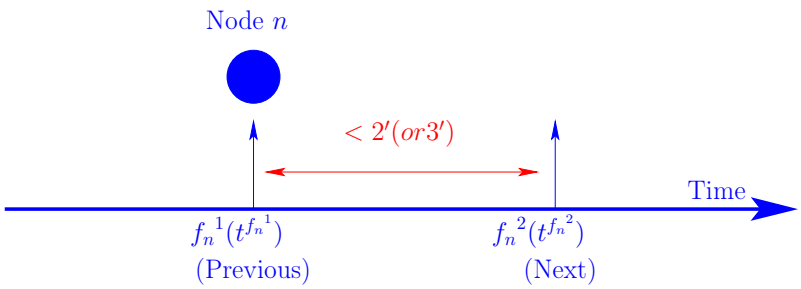

FIGURE 3.9 – Conflict at a node

Algorithm 1: Computing the number of conflicts at WOTN grid nodes

Input: N: is the set of WOTN grid nodes
$\{F_n\}_{n\in N}$: where F_n is a set including all the flights passing a node n
Output: Φ_N: Total number of conflicts on WOTN nodes

$\Phi_N = 0$
for $n \in N$ **do** // for each node n
  $Nb = Number(\{F_n\})$ // count the number of passing flights
  $[f_n{}^1, f_n{}^2, ..., f_n{}^{Nb}] = sort(\{F_n\})$ // sort flights based on their passing times
  for $i = 1 \rightarrow Nb - 1$ **do** // for each pair of consecutive flights
    if $t^{f_n^{i+1}} - t^{f_n^i} < Lon_{sep}$ **then** // if the longitudinal separation is violated
      $\Phi_N = \Phi_N + 1$ // then the number of conflicts is increased
    end
  end
end

three flights f_n^1, f_n^2 and f_n^3, passing through the same node n. Then, let us suppose that the three flights are successive, *i.e* $t^{f_n^1} < t^{f_n^2} < t^{f_n^3}$, and that each two aircraft are in conflict, *i.e* $|t^{f_n^1} - t^{f_n^2}| < Lon_{sep}$, $|t^{f_n^2} - t^{f_n^3}| < Lon_{sep}$ and $|t^{f_n^1} - t^{f_n^3}| < Lon_{sep}$. Therefore, Algorithm 1 computes 2 conflicts (between f_n^1 and f_n^2 and between f_n^2 and f_n^3). However, the conflict between f_n^1 and f_n^3 is not counted. In order to compute exactly the real number of conflicts, we have to check the longitudinal separation between each two pairs of flights, and not only between successive flights. Nevertheless, implementing this process involves more computational time $(Nb * (Nb-1)/2$, where Nb is the number of passing flights through a node). Nevertheless, in our case, Algorithm 1 is sufficient since we aim at resolving all conflicts, and thus, once the algorithm return zero conflicts, then the number of real conflicts is zero as well.

Furthermore, since each link is delimited by two nodes, we can detect conflicts at links by comparing the sequence order of aircraft at the entry and exit nodes of a link. If there are two swapped flights, then an *overtaking* conflict is detected. This conflict happens when the leader aircraft is slower than the following one. Figure 3.10 illustrates an example of a conflict between two flights at a link. In fact, if we consider two successive flights f_l^1 and f_l^2 passing through the same link l, with $t^{f_l^1} < t^{f_l^2}$ (*e.i* f_l^1 enters the link

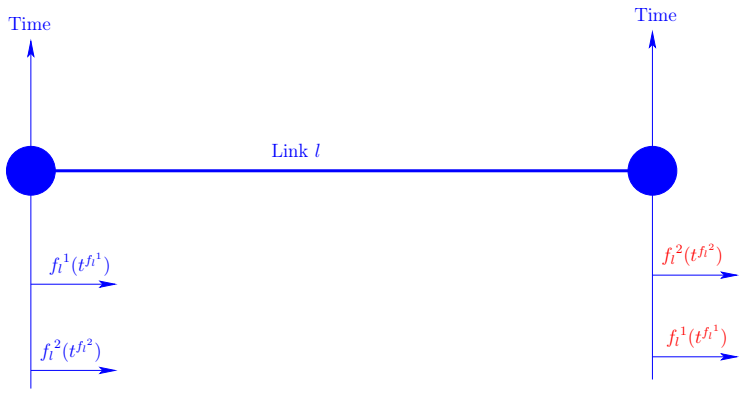

FIGURE 3.10 – Conflict at a link

l before f_l^2), then, a conflict is detected between f_l^1 and f_l^2 at link l when the flight f_l^2 exit the link before the flight f_l^1. The algorithm to compute the total number of conflicts at WOTN links is described in Algorithm 2. The last instruction in Algorithm

Algorithm 2: Computing the number of conflicts at WOTN grid links

Input: L: is the set of WOTN grid links
$\{I_l\}_{l\in L}$: where I_l is a set containing all the flights entering a link l
$\{O_l\}_{l\in L}$: where O_l is a set containing all the flights exiting a link l
Output: Φ_L: Total number of conflicts on WOTN links

1 $\Phi_L = 0$
2 **for** $l \in L$ **do** // for each link l
3 $Nb = Number(\{I_l\})$ // count the number of flights passing through link l
4 $[f_l^1, f_l^2, .., f_l^{Nb}] = sort(\{I_l\})$ // sort flights according to their entry times
5 $[g_l^1, g_l^2, .., g_l^{Nb}] = sort(\{O_l\})$ // sort flights according to their exit times
6 **for** $i = 1 \rightarrow Nb$ **do** // for each corresponding pair of flights from I_l and O_l
7 **if** $f_l^i \neq g_l^i$ **then** // if the corresponding pair of flights are different
8 $\Phi_L = \Phi_L + 1$ // then the number of conflicts is increased
9 **end**
10 **end**
11 $\Phi_L = \Phi_L/2$ // to not count the same conflict twise
12 **end**

2 ($\Phi_L = \Phi_L/2$) is set in order to not compute a conflict between two flights as two conflicts. In fact, if we consider three aircraft f_l^1, f_l^2 and f_l^3 that enter the same link l in the order $[f_l^1, f_l^2, f_l^3]$, and exit this link on the order $[f_l^2, f_l^1, f_l^3]$, then, the algorithm 2 validates the *If* condition at line 7 two times (the first when $f_l^1 \neq f_l^2$ and the second when $f_l^2 \neq f_l^1$). Therefore, if we do not consider the last instruction (at line 11), then the algorithm counts two conflicts, although only one overtaking takes place. Furthermore, similarly to Algorithm 1, Algorithm 2 can miss some conflicts. In fact, if the exit order was rather $[f_l^3, f_l^2, f_l^1]$, which means that f_l^3 overtakes the two flights $f_l^1$and f_l^2 and f_l^2 in

its turns overtakes f_l^1, then, Algorithm 2 computes two conflicts, although there actually are three conflicts. Nevertheless, similar to the number of conflicts at nodes, we do not need to compute the exact number of conflicts since we are searching for a conflict-free solution, and once Algorithm 2 returns zero conflicts, this means that there actually are no conflicts between flights.

Finally, the total number of conflicts, denoted Φ_{tot}, in the WOTN grid is simply computed as follows:

$$\Phi_{tot} = \Phi_N + \Phi_L \tag{3.6}$$

The present study aims at finding a conflict-free configuration between a set of flights, and thus to satisfy the following equation:

$$\Phi_{tot} = 0 \tag{3.7}$$

The rest of this section is devoted to the optimization formulation aiming to search for an optimal conflict-free flight planning for a set of NAT flights.

3.2.6 Optimization formulation

For each flight f, we represent the input data presented in Section 1.4.3 as follows:

— T_{In}^f the desired track entry time,

— $Track_{In}^f \in 1, 2, \ldots, N_y$ the desired entry track which represents the closest track to the departure airport,

— $Track_{Out}^f \in 1, 2, \ldots, N_y$ the desired exit track which represents the closest track to the destination airport,

— V^f the desired flight airspeed,

— $FL_i^f \in 1, 2, \ldots, N_z$ where $i \in 1, 2, ..., N_x$, the flight levels at each waypoint expressed in feet. The distance between each two consecutive flight levels is equal to 1000 feet.

Furthermore, we define the following decision variables:

— $ATrack_{In}^f = Track_{In}^f + / - 1$ the assigned entry track.

— $ATrack_{Out}^f = Track_{Out}^f + / - 1$ the assigned exit track.

— $D_{in}^f \in [0, 20min]$ the time delay at the entry point.

As mentioned in section 3.2.2, when an aircraft enters a predefined track at a predefined flight level, it is required to follow the same track and flight level unless a maneuver is performed. Such maneuvers can only be executed at waypoints of the filter sections. At each such waypoint, a flight has three alternative maneuvers available: either it continues along the same track or it moves to an adjacent one (northern or southern). We model

these maneuvers with the following decision variables:

$$X_i^f = \begin{cases} 1 & \text{if the flight switches to the northern adjacent track at the waypoint i} \\ 0 & \text{if the flight continues along the same track} \\ -1 & \text{if the flight switches to the southern adjacent track at the waypoint i} \end{cases} \tag{3.8}$$

where $i \in \{1, 2, ..., N_x - 1\}$ represent the waypoints where a rerouting from one track to another is possible, i.e. the waypoints of the filter regions.

Furthermore, we also allow aircraft to perform step climbs but only at waypoints. Step climbs are necessary for the aircraft in order to follow its optimal altitude profile in terms of fuel consumption. Therefore, contrary to the re-routing maneuver, this maneuver is allowed at all the WOTN waypoints, namely waypoints of both filter and parallel regions. The initial flight level profiles are recorded from flight plans, which are given data. Given that we restrict flight level changes to waypoints and do not allow them inside a link, and since flight trajectories inside WOTN are different from the trajectories recorded from flight plans, it is almost impossible to perform step climbs at the exact predefined positions. Therefore, we propose to perform the step climbs at the closest waypoint to the specified position in flights plans.
This maneuver is represented by a binary vector $[Z_i^f]_{i\in\{1,2,\dots,N_x-1\}}$ characterizing the flight altitude profile at each waypoint i as follows:

$$Z_i^f = (FL_i^f - FL_{i-1}^f)/10 = \begin{cases} 1 & \text{if the flight climbs to the next level at waypoint i} \\ 0 & \text{otherwise} \end{cases} \tag{3.9}$$

with $(Z_1^f = 0)$. As mentioned in 3.2.3, a relaxation on the desired vertical profile can be considered in order to enlarge the state space. Therefore, the decision variable that models step climb changes is presented as follows:

$$\begin{cases} AZ_i^f = Z_i & \text{if the desired step climb is performed at the planned waypoint i} \\ AZ_i^f = Z_{i-1}^f \Rightarrow AZ_{i-1}^f = Z_i^f & \text{if the desired step climb is switched to the previous waypoint i-1} \\ AZ_i^f = Z_{i+1}^f \Rightarrow AZ_{i+1}^f = Z_i^f & \text{if the desired step climb is switched to the next waypoint i+1} \end{cases} \tag{3.10}$$

In order to model the constraint imposed to step climb changes (already discussed in Section 3.2.3), let us introduce two new vectors, $[Climb_j^f]_{j\in 1,2,..,N_c^f}$ and $[AClimb_j^f]_{j\in 1,2,..,N_c^f}$ (where N_c^f is the number of desired step climbs of flight f), which contain the index of the waypoints where desired and assigned step climbs are performed, respectively. Therefore,

these two vectors can be calculated as follows:

$$N_c^f = \sum_{i \in \{1,2,\ldots,N_x-1\}} Z_i^f \tag{3.11}$$

$$\forall j \in \{1,2,\ldots,N_c^f\}, Climb_j^f = i \quad \text{where} \quad Z_i^f = 1 \tag{3.12}$$

$$\forall j \in \{1,2,\ldots,N_c^f\}, AClimb_j^f = i \quad \text{where} \quad AZ_i^f = 1 \tag{3.13}$$

where $i \in 1,2,..,N_x$.
Therefore, the step climb constraint is verified, if and only if:

$$\forall j \in \{1,2,\ldots,N_c^f\}, |Climb_j^f - AClimb_j^f| \leq 1 \tag{3.14}$$

This means that the difference between the waypoint where the desired step climb is planned and the waypoint where the step climb is effectively assigned has to be at most equal to one.

It is possible to regroup together all these decision variables into a specific vector, Ω^f for each flight f, as follows:

— $\Omega^f = (ATrack_{In}^f, ATrack_{Out}^f, D_{In}^f, [X_i^f]_{i \in \{1,2,\ldots,N_x-1\}}, [AZ_i^f]_{i \in \{1,2,\ldots,N_x-1\}})$.

Thus, the set of decision variables related to a set S of flights is expressed as:

— $\Omega = \{\Omega^f\}_{f \in S}$

The decision variables of each flight must satisfy the following **constraints**:

$$ATrack_{In}^f = Track_{In}^f + / - 1 \tag{3.15}$$

$$ATrack_{Out}^f = Track_{Out}^f + / - 1 \tag{3.16}$$

$$0 \leq {D_{in}}^f \leq 20min. \tag{3.17}$$

$$\sum_{i \in \{1,2,\ldots,N_x-1\}} X_i^f = ATrack_{Out}^f - ATrack_{In}^f \tag{3.18}$$

$$\sum_{i \in \{1,2,\ldots,N_x-1\}} AZ_i^f = \sum_{i \in \{1,2,\ldots,N_x-1\}} Z_i^f = N_c^f \tag{3.19}$$

$$\forall j \in \{1,2,\ldots,{N_c}^f\}, |Climb_j^f - AClimb_j^f| \leq 1 \tag{3.20}$$

Furthermore, as the main objective of the present work is to generate conflict-free flight trajectories, the decision variables must satisfy the constraint in equation 3.6.

To sum up, the main goal of this work is to generate a set of optimal trajectories for a set S of eastbound flights while satisfying several constraints. There are different route optimization criteria, which typically involve minimizing the total cost of deviation from the initial flight plans. In this study, we have chosen the following optimization criteria to deal with our optimization problem:

— C: the total cruising time, summed over all flights

— D: the total assigned delay, summed over all flights

— R: the total deviation delay induced by the deviations from desired tracks among all flights

The cruise time of a flight f, denoted c^f, represents the time needed to fly the sum of distances between the track waypoints, from entering to exiting the WOTN. Thus, total cruise time C is defined as the sum of cruise times over all flights:

$$C = \sum_{f \in S} c^f \tag{3.21}$$

The total assigned delay D represents the sum of assigned delays over all flights, and thus is expressed in terms of *minutes*. It is calculated as follows:

$$D = \sum_{f \in S} D^f_{in} \tag{3.22}$$

The deviation delay for each flight, denoted r^f, represents the required additional time to deviate from the desired track and reach the new assigned one. To compute this parameter, we start by computing the additional distance required to deviate from the desired track to reach the assigned one. This distance is represented in Figure 3.11 with $dist_1$ and $dist_2$ for the additional distance induced by changing the desired entry and exit tracks, respectively. These two distances are computed as follows :

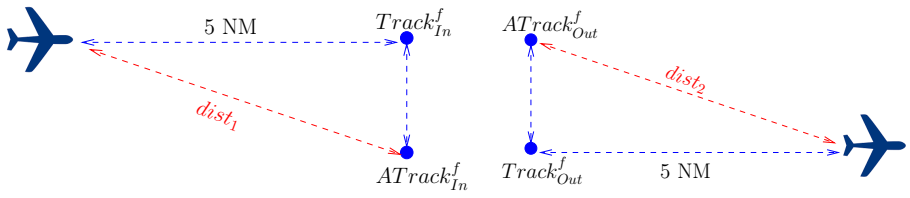

(a) Additional distance when changing the desired entry track

(b) Additional distance when changing the desired exit track

FIGURE 3.11 – Additional distance when changing the desired entry and exit tracks

$$dist_1 = \sqrt{dist(Track^f_{In}, ATrack^f_{In}) + 5^2} \tag{3.23}$$

$$dist_2 = \sqrt{dist(Track^f_{Out}, ATrack^f_{Out}) + 5^2} \tag{3.24}$$

where the function $dist(A, B)$ returns the distance between two points A and B. The deviation delay for each flight f is then computed as follows:

$$r^f = \frac{dist_1 + dist_2}{V^f} \tag{3.25}$$

It is calculated in terms of time in order to be added with the rest of optimization criteria, namely C and D, which are also computed in terms of time. Therefore, the total deviation

delay R is simply deduced by summing up deviation delays over all flights:

$$R = \sum_{f \in S} r^f \tag{3.26}$$

The **objective function**, that we aim to minimize, must take into account all the criteria mentioned above. All these criteria are expressed in terms of time, and thus the objective function can be expressed as their weighted sum:

$$F_{obj} = d * D + c * C + r * R \tag{3.27}$$

where the non-negative weighting coefficients *(d,c,r)* are used to balance the three criteria according to the user preferences, and to consider various trade-offs as well.

The hard constraints of the problem (except boundary constraints on decision variables) are conflict-avoidance constraints. We address these constraints by performing relaxation in the objective function. Therefore, we add the number of induced conflicts to the objective function as the most important criterion to minimize. Ideally, we would like to reduce this number to zero. The objective function becomes then:

$$F_{obj} = \Phi_{tot} + a * (d * D + c * C + r * R) \tag{3.28}$$

where the coefficient a is added in order to give the highest priority to the conflict-free criterion. If all conflicts are resolved, the system continues to minimize the other criteria (cruising time, deviations and delays) while ensuring that the resulting solution remains conflict-free.

Thus, the optimization formulation of our problem is given by:

$$\begin{aligned}
\underset{\Omega=\{\Omega^f\}_{f\in S}}{\text{minimize}} \quad & F_{obj}(\Omega) \\
\text{subject to} \quad & \Phi_{tot}(\Omega) = 0, \\
& ATrack^f_{In} = Track^f_{In} + / - 1, \\
& ATrack^f_{Out} = Track^f_{Out} + / - 1, \\
& 0 \leq D^f_{in} \leq 20min, \\
& \sum_{i \in \{1,2,\ldots,N_x-1\}} X^f_i = ATrack^f_{Out} - ATrack^f_{In}, \\
& \sum_{i \in \{1,2,\ldots,N_x-1\}} AZ^f_i = \sum_{i \in \{1,2,\ldots,N_x-1\}} Z^f_i = N^f_c, \\
& \forall j \in \{1,2,\ldots,N^f_c\}, |Climb^f_j - AClimb^f_j| \leq 1.
\end{aligned} \tag{3.29}$$

3.3 Resolution algorithm

As our objective function defined in 3.29 cannot be explicitly expressed in terms of the proposed decision variables, we are dealing with a highly combinatorial "black-box" problem. We thus resort to stochastic optimization methods to tackle this problem. We

start by pre-processing the flight set using a Sliding Window (SW) method. The latter consists in dividing the problem into a set of sub-problems. Then, each sub-problem is treated separately and sequentially by a Simulated Annealing (SA) algorithm.

3.3.1 Adaptation of SW and SA to our problem

The application of the SW method to our problem starts with sorting the flights according to their NAT entry times. Then, a time window interval of length T_w beginning at the earliest entry time is fixed. In each time window, four types of flight are identified:

— **Planned flights** are those that are scheduled to enter the WOTN after the time window.

— **Completed flights** are those that exited the WOTN before the time window.

— **On-going flights** are those that entered the WOTN before the time window and are still operating in the considered time interval.

— **Active flights** are those that entered the WOTN in the considered time window.

Once the flight types are assigned to all flight, we proceed with the conflict resolution method. Planned and completed flights are not considered for the time window being processed. We apply the SA algorithm to fix the decision variables of the active flights while considering the on-going trajectories as constraints. Hence, the decision variables of on-going flight are not modified. At the next iteration, we shift the time window by T_s (with $T_s < T_w$). This process is repeated until all flights are completed. Figure 3.12 illustrates a schematic example of the SW process.

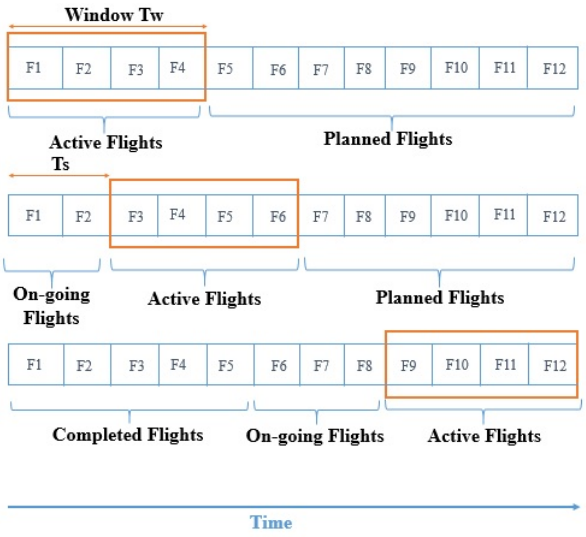

FIGURE 3.12 – Sliding window algorithm

Once a time window is defined with active flights identified and the on-going flight variables fixed, we apply the standard SA algorithm. This algorithm is described in detail in Section 1.3 and Appendix A. The SA algorithm is adapted to solve our problem as following:

— The search space consists of all possible sets of flight trajectories. A solution is determined when the decision variables for each flight in the flight set are fixed.
— The energy function represents the objective function of our optimization problem, as described in 3.29.
— A neighbor solution is obtained by applying a local change to the current solution $\vec{x}_i$ in order to generate a new solution $\vec{x}_j$. It consists in changing one decision variable of an individual flight. The process of getting a neighbor solution is divided into two steps. First, we select a flight to be modified as being the one that generates the largest number of conflicts. Then, we select the decision variable to be modified. In order to satisfy aircraft preferences as much as possible, we consider a priority order when modifying flight decision variables. We attribute the highest probability to the en-route track change maneuver, since it does not affect the trajectory length much. Then, we consider modifying the entry/exit tracks. If a conflict-free solution does not exist, we delay the flight departure time. The last maneuver is to change the flight level (compared to the one requested by the aircraft). This maneuver is to be considered as a last resort as it involves an increase in fuel consumption.
— The acceptance probability of the neighbor solution $\vec{x}_j$ is given by $e^{(f(\vec{x}_i)-f(\vec{x}_j))/T}$, where T is the temperature, $f(\vec{x}_i)$ is the objective value of the current solution, $\vec{x}_i$, and $f(\vec{x}_j)$ is the objective value of the neighbor solution, $\vec{x}_j$.
— The temperature decreases via a geometrical law given by $T_i = \alpha * T_{i-1}$.
— The process stops when the temperature T goes below a predefined final temperature, T_f. T_f is adjusted to be: $T_f = \beta * T_0$ (with $\beta << 1$).

The objective function is evaluated via a simulation process which requires a simulation environment. In such a case, the optimization algorithm controls the vector of decision variables, X, which are used by the simulation process in order to compute the performance (quality) y of such decisions, as shown in Section 1.3.3.

3.3.2 Results with the $WOTN_{OTS}$

In this section, we present the experimental settings and computational results in order to validate our proposed approach aiming to optimize the strategic eastbound flight planning over the NAT by establishing the $WOTN_{OTS}$. For the following simulations, the parameter values used to specify the optimization problem are as follows:

— The initial temperature $T_0 = 0.01$
— The objective function coefficients $a = 0.5$ and $d = c = r = 1$,
— Number of iterations in each temperature schedule $N = 500$,
— The ratio of the temperature decrease $\alpha = 0.95$,
— The stopping criterion $\beta = 0.0001$,
— The sliding window parameters in minutes: $T_w = 120$, $T_s = 30$.

SA and SW parameters are empirically set. Furthermore, we adjust the objective function parameters in order to give a higher priority to reducing the number of conflicts, thus we

set $a = 0.5$. In addition to this, we give equal priorities to the other different criterion, namely total cruise time, total delay and total track shift ($d = c = r = 1$).

To start with, we consider a simplistic situation between three aircraft in conflict. Then, we illustrate the maneuver of resolution held by our algorithm. As illustrated in Figure 3.13, we consider three aircraft $A1$, $A2$ and $A3$ with their entry times 05:31, 05:41 and 05:45, respectively. The vertical flight profile of the three considered aircraft is

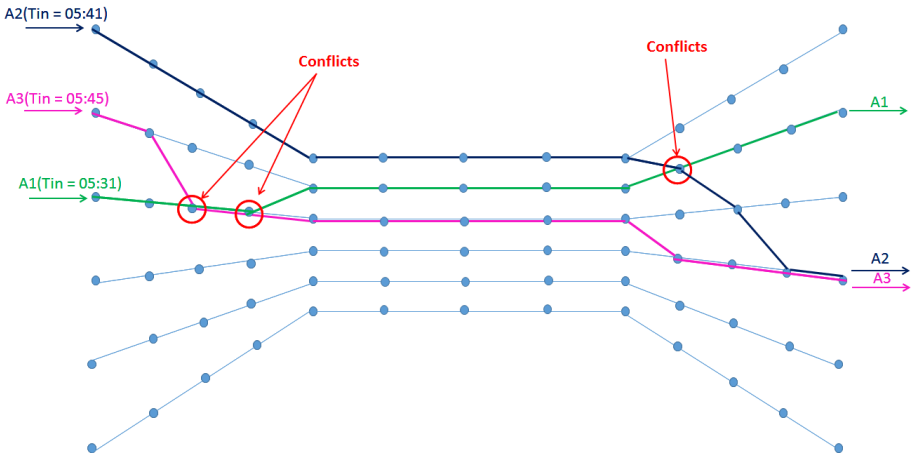

FIGURE 3.13 – Representation of conflicts between three aircraft trajectories

presented in Figure 3.14. It is clear that $A1$, $A2$ and $A3$ fly at the same flight level, namely $FL5$, in the entry filter section of the route structure. Then, $A2$ and $A3$ perform step climb maneuvers in the parallel section such as given by their optimal vertical profiles. In contrast, $A1$ keeps the same flight level during the entire trajectory. These vertical profiles explain the occurrence of a conflict between $A1$ and $A3$ in the entry filter section and between $A1$ and $A2$ in the exit filter section.

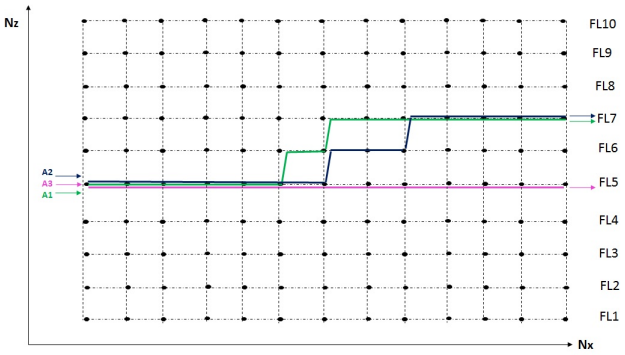

FIGURE 3.14 – Vertical section of the route structure

To resolve these conflicts, the trajectories of the three aircraft inside the route structure are changed as shown in Figure 3.15. The vertical profile as well as the entry and exit desired tracks have not been changed for the three flights. Nevertheless, the aircraft $A1$ is delayed by 5 minutes. In other more complicated situations, when the algorithm does not

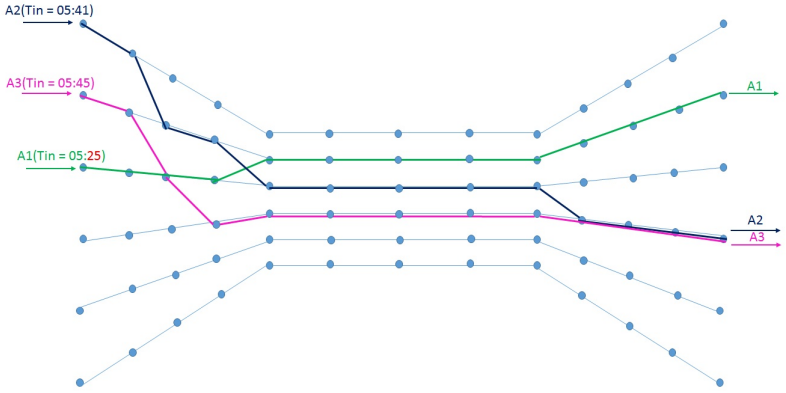

FIGURE 3.15 – Conflict resolution

find a conflict-free configuration, it opts for changing the desired vertical flight profile. In this case, the modification has to keep the new vertical flight profile as close as possible to the desired one. As described in section 3.2.6, the vertical flight profile is represented by an array of 0's and 1's as follows: 0 if the aircraft continues at the same flight level and 1 when the aircraft climbs to the upper flight level (see Figure 3.16-a). Thus, modifying a desired vertical profile only requires to shift one step climb to an adjacent waypoint. For instance, let us consider the example of aircraft $A1$: if it is necessary to change its desired vertical profile only two possibilities exist. These possibilities are presented in Figure 3.16-b and 3.16-c. The choice between the two assigned vertical flight profiles is randomly made.

Furthermore, we perform simulations on two real traffic days over the NAT OTS (3^{rd} and August 4^{th}, 2006). Each flight set contains 331 and 378 flight, respectively. The simulation results for both studied flight sets are presented in table 3.1.

TABLE 3.1 – Conflict resolution results on two real traffic days

Test		03/08/2006	04/08/2006
Number of flights		331	378
Number of conflicts	Before	1055	1548
	After	0	1
Number of flights changing their vertical profile		69	78

As we can see in table 3.1, we conclude that the SA and SW algorithm found almost conflict-free solutions for the two studied flight sets. Considering the second flight set (August 4^{th}), we remark that 1 residual conflict is unsolved. This remaining conflict can be solved by setting the parameter a of the objective function to 0.1. Thus, we give higher priority to the number of conflicts than to the other criteria. Furthermore, we evaluate the number of flights that change their vertical profile. In each flight set, almost 70 flights change their optimal step climbs, thus all the other flights, that is almost 80% of the flight set, keep the vertical profile that ensures the least fuel consumption. In addition, we evaluate the delay assigned to get the conflict-free solution. Results prove that about

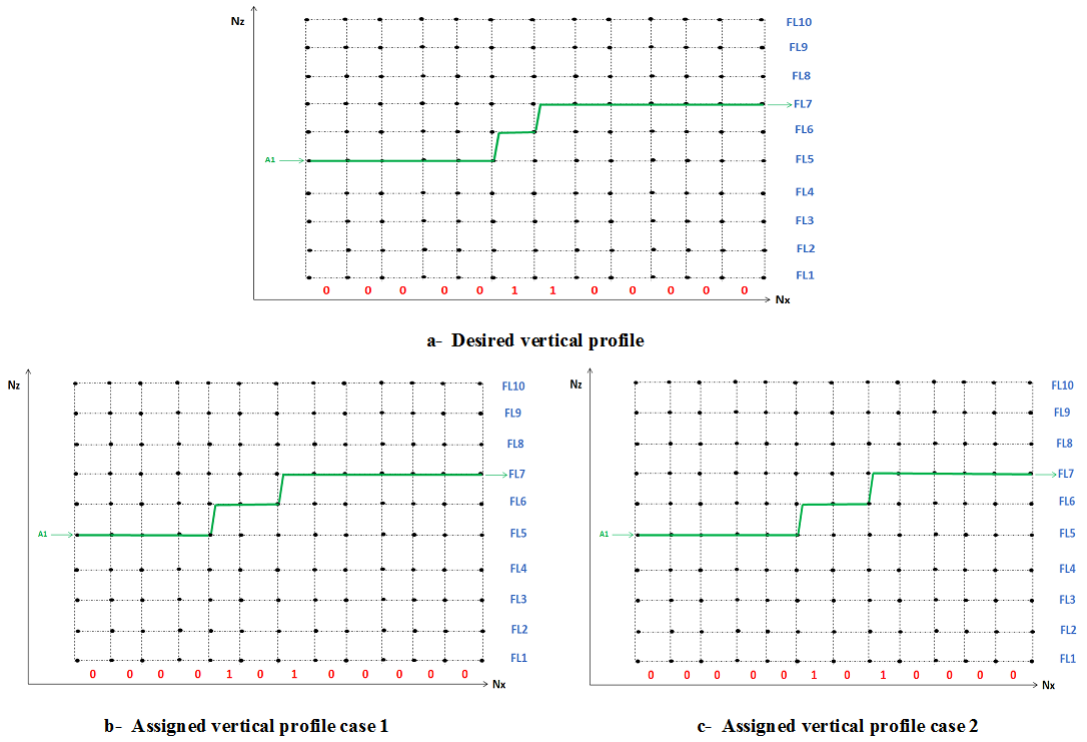

FIGURE 3.16 – Vertical profile change

TABLE 3.2 – Conflict resolution results with different SA configurations

α	N	Number of conflict	Number of flights changing their vertical profile
0,95	500	119	440
	1000	63	375
0,99	500	46	268
	1000	32	200

300 flights in each set are within 10 minutes of the assigned delay and only some flights approach the limit delay which is 20 minutes. These encouraging results allowed us to expand the number of flights and re-experiment the simulations. Thus, we randomly generate a flight set containing 1000 flights. Initially, the considered flight set generates 5501 conflict. After applying SA and SW algorithm, the number of conflicts is down to 119, which represents a significant reduction. However, a conflict-free solution does not exist with the previously mentioned configuration of the SA. For this reason, different SA algorithm configurations are considered. Table 3.2 summarizes the obtained results. We notice that the number of remaining conflicts, as well as the number of flights that change their requested vertical profiles, are strongly affected by the change of both SA parameters α and N. Slowly lowering the temperature, by decreasing the parameter α, influences the result more, though, more CPU time is needed to get an optimal solution. Nevertheless, although the search space is further explored by increasing the parameters α and N, no conflict-free solution is found. The number of conflicts decreases from 5501 to 32. This

is considered, in our case, as a very interesting result. In fact, we are tackling strategic conflict resolution, and therefore, any remaining conflicts could be resolved further in pre-tactical and tactical phases.

In the rest of this section, tests were performed with a set of NAT flights selected from the flight plan on July 15^{th} 2012 as described in section 1.4.3.

3.3.3 Results with the WOTN

In these simulations, we use the following values for the parameter of the optimization algorithm, which are set empirically:

— The initial temperature $T_0 = 0.01$

— The stopping criterion $\beta = 0.0001$,

— The sliding window parameters in minutes: $T_w = 180$, $T_s = 30$.

Several different objective functions were tested. First, we aimed at finding conflict-free trajectories for the considered flights set of July 15^{th} 2012. Thus, the objective function was defined as: $F_{obj}^{(1)} = C_t$ $(a = 0)$. The algorithm easily found a **conflict free** solution. Thus, we intended to evaluate the effect of introducing other criteria to the objective function. Here, we focused on the entry delay, D, and the deviation from the desired track, R. Hence, we performed the simulations with the following objective functions:

— $F_{obj}^{(2)} = C_t + 0.1 * D$

— $F_{obj}^{(3)} = C_t + 0.1 * R$

— $F_{obj}^{(4)} = C_t + 0.1 * (D + R)$

In addition to this, we intended to observe the effect at changing the SA configuration parameters, i.e. the ratio of the temperature decrease, α, and the number of iteration in each temperature schedule, N. The reference flight set that we used in our simulations contains 546 eastbound flights. Initially, this flight set induced 380 conflicts. The most important result is the number of conflicts remaining after algorithm execution. Using a basic wind forecast scenario (referred to as s_0 in section 1.4.3), we were able to obtain a **conflict free** trajectory set with different algorithm configurations. Some results of simulations are shown in Table 3.3.

Based on these simulations, we observe that with the objective function $F_{obj}^{(1)}$, the algorithm performance was poor regarding the number of flights which were assigned their desired tracks and departure times. It is not surprising since these two criteria do not appear in the objective function. The benefits from introducing $F_{obj}^{(2)}$, $F_{obj}^{(3)}$ and $F_{obj}^{(4)}$ are thus clearly seen and the resulting solutions emphasizes the validity of our model.

Another important conclusion that can be made from these results is that the configuration of the SA has a strong effect on the result quality. Increasing the number of iterations, by increasing α and N, for different objective functions increases the number of non-delayed and non-deviated flights. For instance, for the tests with the objective function $F_{obj}^{(2)}$, increasing α from 0.95 to $0,97$ and N from 200 to 500 leads to an increase in the number of non-delayed flights from 67% to 82% and to a decrease of the total entry delay from 17 hours to 9 hours (almost by a half).

TABLE 3.3 – Result of simulations with different criteria implemented in the objective function

Number of flights	Initial number of conflicts	Objective function	α	Number of iterations	% of flights with desired entry tracks	% of flights with desired exit tracks	% of flights without delays	Total delays (hours)
546	380	F1	0.95	200	47.9%	49.8%	5.31%	88.4
		F2	0,95	200	54.3%	51.6%	67.7%	17.28
				500	48.7%	49.8%	75.6%	10.5
			0.97	200	50.18%	53.8%	75.4%	12
				500	50.3%	45.6%	82%	9.1
		F3	0.95	200	93.7%	95.9%	4.3%	89.9
				500	95.4%	97%	4.5%	88.6
			0.97	200	94.6%	97%	5.31%	88
				500	96%	97.5%	4.76%	89
		F4	0.95	200	90.2%	94.5%	62%	20.8
				500	93.4%	95.9%	65.9%	17.8
			0.97	200	92.3%	95.7%	65.2%	18.05
				500	***93.4%***	***97%***	***69.41%***	***14.7***

Comparing the results of tests with $F_{obj}^{(2)}$ and $F_{obj}^{(3)}$ in Table 3.3, it can be concluded that the two criteria (number of non-delayed flights and number of non-deviated flights) are opposite, and the decrease of the one leads to the increase of the other. Hence, the best solution would be a trade-off between these performance criteria. Such a trade-off is achieved with the objective function $F_{obj}^{(4)}$, where the number of deviated and delayed flights are reduced simultaneously. Table 3.3 shows that the best solution (highlighted in **bold**) is found with the configuration $\alpha = 0.97$ and $N = 500$, and with the objective function $F_{obj}^{(4)}$: Compared to the resulting solution found with $F_{obj}^{(1)}$, the number of flights entering/exiting a desired track is increased from 47% to 93% and from 49% to 97% respectively, and the number of non-delayed flights is increased from 5.31% to 69.41%, leading to a significant decrease in the total entry delay from 88.4 hours to 14.7 hours.
These encouraging results motivated us to explore other performance criteria. Thus, we focused on investigating the potential benefits from including the total cruise time into the objective function. More simulations are performed using the following objective functions:

- $F_{obj}^{(4)} = C_t + 0.1 * (D + R)$
- $F_{obj}^{(5)} = C_t + 0.1 * C$
- $F_{obj}^{(6)} = C_t + 0.1 * (C + D + R)$

The obtained results are summarized in Table 3.4.
In these simulations, we set $\alpha = 0.97$ and $N = 500$. With the objective function $F_{obj}^{(5)}$, we minimized cruising time only, and obtained the reduction in the total cruising time

TABLE 3.4 – Comparing results with different objective functions

Objective function	$F_{obj}^{(4)}$	$F_{obj}^{(5)}$	$F_{obj}^{(6)}$
% of flights with desired entry track	93,4%	20%	**89%**
% of flights with desired exit track	97%	8.2%	**92.5%**
% of flights without delay	69.41%	3.85%	**71%**
Total entry delay (hours)	14.7	103	**8.7**
Total cruising time (hours)	3897.379	3829.581	**3855.205**
Average cruising time (hours)	7.13	7	**7.06**

of approximately 70 hours. These time savings come from attributing to the aircraft tracks with preferable winds. However, using $F_{obj}^{(5)}$ has a negative impact on the number of non-delayed and non-deviated flights: the number of non-deviated flights is decreased down to 8%, and the number of non-delayed flights is about 4%. Thus, comparing results from Table 3.4, we conclude that the best trade-off is given by the objective function $F_{obj}^{(6)}$ (highlighted in **bold**), taking into account all the criteria. The cruising time is decreased by almost 40 hours, without dramatic influence on the other criteria of the objective function. We believe this is a very satisfying solution that proves the effectiveness of our algorithm. Based on this solution, further analyses was performed in order to prove the benefits from using wind-optimal tracks.

To do so, we compared the obtained cruising times along the WOTN with the corresponding cruising times along great circle routes. The great-circle distance is the shortest distance between two points on the Earth's surface. In our case, it represents the shortest distance between the entry track waypoint and the exit track waypoint for each flight. Obviously, the great-circle trajectory length is shorter than the corresponding trajectory obtained using the WOTN. However, we were interested in comparing the cruising times when following wind-optimal tracks and great-circle routes. Simulations showed that all flights in the considered flight set decreased their cruising times when using wind-optimal tracks compared to the great-circle routes. Moreover, about 76.5% of flights decreased their cruising times from 30 to 53 minutes. Knowing that flights spend on average about 4 hours in the WOTN, we conclude that 76.5% of flights gained more than 12.5% from their total cruising time in the NAT airspace. Thus, we observed that flights can cross the NAT airspace faster, even following longer trajectories. Clearly, this is due to using trajectories with preferable winds.

3.3.4 Comparison between wind-optimal trajectories and WOTN

In this section, we compare our approach of the NAT traffic organization using the route structure WOTN, to the wind-optimal trajectories described in Appendix B. The explicit results of conflict resolution using wind optimal trajectories can be found in [89, 94]. Here, we test both algorithms on the same data set (546 eastbound flights on July 15*th* 2012). First, we reveal the difference in the cruising times along the trajectories obtained using the two approaches. Next, we evaluate the robustness of these trajectories under changing winds.

3.3.4.1 Cruising time evaluation

Here, we compare the best solution based on the WOTN described in the previous section 3.3.3 (highlighted in **bold** in Table 3.4) with the solution resulting from the conflict resolution with wind-optimal trajectories (Appendix B). Our simulations revealed that almost 23% of flights reduce their cruising times when using the WOTN. The gain in cruising time does not exceed 10 minutes, and only 3.6% of flights gain more than 5 minutes. The fact that the conflict resolution algorithm based on wind-optimal trajectories yielded greater cruising times for some flights comes from the nature of conflict resolution maneuvers: when the trajectory shape is modified, the resulting trajectory is no longer wind-optimal, and in some cases, this leads to important cruising time increases. The rest of flights (about 77%) have greater cruising times when following the WOTN. For about 57% of flights the difference in cruising times is less then 30 minutes, while the remaining 20% of flights extend their travel times by more than 30 minutes. This is not particularly surprising, as wind-optimal trajectories are constructed independently for each single flight based on its characteristics. However, we observed that for about 80% of flights the increase in cruising time is less than 30 minutes, while for 60% of flights this increase is less than 10 minutes. We thus conclude that the proposed WOTN yields efficient routes for the majority of flights.

At the same time, we found out that for about 5.5% of flights, their cruising times are increased by more than one hour when compared to wind optimal trajectories. This issue can be explained by the fact that the location of the wind-optimal tracks is basically around latitude 50°(by construction), and thus flights departing from the north of the USA (around latitude 60°) and heading to the north of Europe (keeping almost the same latitude 60°), as well as flights departing from the south of the USA (around latitude 30°) and heading to the south of Europe (around latitude 40°), receive significant extensions to their trajectories when using the WOTN.

3.3.4.2 Robustness evaluation

In this section, we evaluate the robustness of the two obtained solutions based on wind-optimal trajectories and WOTN under wind uncertainties. To do so, we performed the conflict resolution with the two approaches using the nominal forecast wind, denoted $s0$ (refer to Section 1.4.3), and then we re-evaluated the resulting solutions with different wind scenarios. Tests were performed with the 4 different wind scenario ($s1$, $s2$, $s3$ and $s4$) described in section 1.4.3. The results are summarized in Table 3.5. From these results we

Table 3.5 – Comparing results with different wind scenarios

	Initial nb. of conflicts	Residual conflicts	Residual conflicts with scenarios:			
			s1	s2	s3	s4
Wind-optimal trajectories	307	0	92	106	135	159
WOTN	380	0	16	22	10	5

observe that when the conflict resolution approach based on wind-optimal trajectories is used, a large number of conflicts reappear once the conflict-free trajectory set is evaluated in different wind fields. With the wind scenario $s4$, the number of reappeared conflicts is about 159 which represents almost 50% of the initial number of conflicts. In addition to this, when the conflict resolution approach based on the WOTN is used, the number of reappeared conflicts is significantly lower, i.e. it does not exceed 22. Thus, we conclude that the WOTN is much more robust regarding the wind changes than a set of individual wind-optimal routes, which is particularly important for the strategic planning involving important uncertainties. This is due to the traffic organization in the WOTN which structure the traffic into flow in the central area of the network. This organization is less sensitive regarding the wind uncertainties.

3.4 Conclusions

In this chapter, a new approach for scheduling transatlantic flights at the strategic level of flight planning is presented. The proposed approach relies on a new route structure, the Wind-Optimal Track Network (WOTN), that replaces the actual NAT OTS and benefits from the jet stream direction.

The optimization algorithm implemented in order to improve flight routes and reduce the associated congestion, delays and cruising times is presented. Simulations were performed on real North Atlantic traffic data under the assumption of reduced separation norms, and the obtained optimized trajectories were compared to wind-optimal trajectories that are described in Appendix B.

The performed simulations demonstrated that the algorithm is able to find conflict-free trajectory configuration under the reduced separation norms. Besides, the results revealed strong benefits from flying wind-optimal routes in North Atlantic airspace. By comparing the approach to wind-optimal trajectories, we conclude that flying wind-optimal trajectories leads to better results in term of cruising times than using the WOTN. However, the WOTN was found to be much more robust regarding wind changes.

Thus, our approach highlights the importance of taking advantages from the favorable winds in order to decrease the flight cruising times, on the one hand, and the importance of implementing a route structure in order to increase the robustness under wind uncertainties, on the other hand.

Nevertheless, in real conditions, some special cases may occur, such as an urgent need to return to a departure airport after entering the parallel tracks or exiting the route structure for other reasons. These cases can be considered within our WOTN, if exiting WOTN is requested at filter sections. In this case, the aircraft has to re-route between tracks until it gets to a border track, and thus can exit WOTN. However, if exiting WOTN is requested at parallel section, it can not be considered with the actual route structure configurations. In fact, if an aircraft desires to leave the route structure from a middle track in the parallel section, it is obliged to cross other tracks, which automatically causes conflicts with other flights flying within the crossing tracks. Even though these cases are

not frequent, it is important for the route structure to comply with it. This problem is considered and resolved in the next Chapter.

Chapter 4

Contingency procedures within WOTN

In this chapter, we present an improvement of the proposed WOTN route structure in order to take into account some particularities of NAT flights.

During flight, unexpected circumstances can occur due to interferences, errors or malfunctions. In such conditions, contingency plans need to be carried out by the aircraft in order to guarantee its safe operation. Depending on the remaining flight capabilities of the aircraft system, responses to these contingencies can either be to re-route from its trajectory and continue towards the destination, or to leave its assigned trajectory to reach an intermediate airport or return to its departure airport.

The present chapter is organized as follows. Section 4.1 details the current procedures applicable in case of oceanic flight contingencies. Section 4.2 discusses how these procedures may be handled within our proposed route structure WOTN. Section 4.3 proposes an improvement of the proposed route structure in order to comply with current contingency procedures. The mathematical model is detailed, and numerical results from computational experiments are presented.

4.1 Current oceanic contingency procedures

Depending on the various circumstances surrounding each emergency situation, contingencies can cause a partial or total disruption of the air traffic system. Contingency actions for total disruption, such as that caused by volcanic ash [1], have to encompass information and procedures from the whole ATM system. These cases are out of the scope of the current study, and more details about these circumstances can be found in [51]. Nevertheless, circumstances affecting individual aircraft can also occur, and are the main subject of the present chapter.

Although possible contingencies cannot all be covered, specific procedures are provided for the most frequent circumstances. These circumstances include:

— unexpected meteorological conditions such as severe turbulence, or

1. Volcanic ash are very small solid particles, carrying electrical charges, ejected from a volcano during an eruption. These particles can reach very height altitudes and remain a threat to aviation for several months.

— aircraft performance problems such as pressurization failure, loss of the required navigation and/or communication capabilities, or
— Medical emergencies.

Such situations provoke either inability to maintain assigned flight level and/or assigned trajectory or an imminent need to turn-back to the departure airport or to an alternate airport.

In the case of small deviations due to severe weather, the common applied procedures in the OTS are as follows:

— If the deviation is less than 10 NM, the aircraft must remain on the same assigned track and flight level, and no changes are needed.
— If the deviation is greater than 10 NM, the aircraft is required to perform a level change of 300 feet:
  — If the aircraft is deviating north of the assigned track, then it has to descend 300 feet.
  — However, if the aircraft is deviating south of the assigned track, then it has to climb 300 feet.
— When the aircraft reaches its assigned track (i.e. is within 10NM from the assigned track), it has to regain the last assigned flight level.

In more complex contingency procedures involving a turn-back, oceanic in-flight requirements include the following instructions:

— to re-route from the assigned track by 15 NM, and
— to climb or to descend to a level which differs from those normally used by 500 feet if below $FL410$ and by 1000 if above $FL410$.

Therefore, when the aircraft is following an OTS track and needs to perform a turn-back procedure, the first maneuver to be held is to leave the assigned track by turning at least 45° to the right or to the left. The direction in which the aircraft must turn is determined by the position of the aircraft relative to the OTS. In fact, if the aircraft is near the edge of the OTS, it is recommended for it to turn in such a manner as to avoid OTS tracks. Otherwise, if the aircraft is within the system, other factors can affect the direction of turn, such as the direction to an alternate airport or the traffic flow in the adjacent tracks. In general, it is recommended to turn in such a manner as to avoid the most part of NAT traffic.

Next, once the aircraft deviates from its assigned track and is laterally clear of any conflicting traffic in the adjacent tracks, it is required to either climb or descend 500 feet from the assigned flight level (since OTS tracks are below $FL410$).

Finally, once the aircraft maintains a new track and flight level that differs from those normally used by the traffic flow, it is possible to initiate the turn-back by turning 180°.

4.2 Incoherence of WOTN with contingency procedures

In this section, the contingency procedures, described in the previous section, are applied to WOTN in order to evaluate their coherence within it. First, let us distinguish

two types of contingency procedures, namely lateral and vertical.

Since WOTN vertical levels are the same as OTS and no vertical separation reductions are considered, vertical procedures can be applied easily. Therefore, the aircraft flying within WOTN is able to perform efficiently any request to climb or to descend by either 300 feet or 500 feet.

However, lateral contingency procedures are more challenging to perform. Contingency procedures are established in order to facilitate the exit of the aircraft from any structured tracks in case of emergencies. Considering our route structure model in Figure 4.1, it is clear that, in filter sections, the aircraft can easily exit the route structure by performing re-routings between way-points.

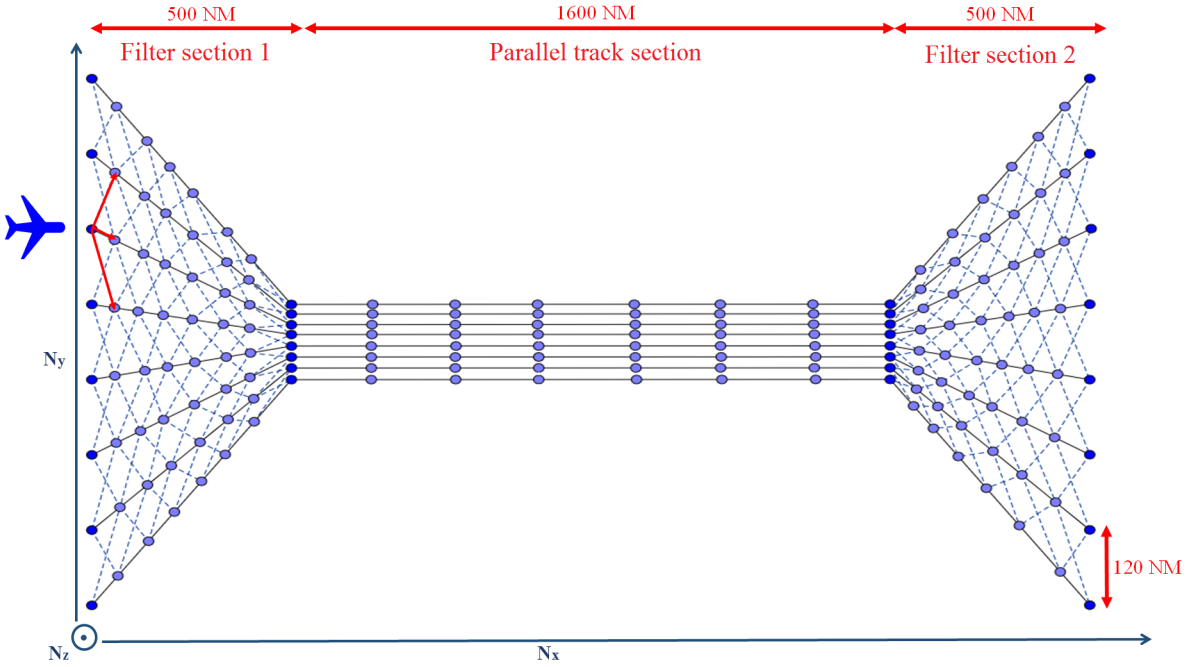

FIGURE 4.1 – Horizontal section of the WOTN grid model

For instance, let us consider an aircraft that urgently needs to turn-back towards an alternate airport when following the WOTN entry filter. In this case, changing the flight level is the first action to perform.

Based on the ATC clearances, the aircraft is required either to climb or to descend by 500 feet, as described in Figure 4.2.

Furthermore, the aircraft is required to follow the projection of WOTN way-points in the assigned flight level, as described in Figure 4.3. The flight has two ways of exiting the WOTN, either to follow the green or the red trajectory in Figure 4.3. This choice depends on the flight destination, on the one hand, and on ATC clearances, on the other hand.

Exiting of the WOTN from the exit filter section is similar to exiting from the entry filter section. However, exiting the parallel section can not be performed in the same manner as the lateral separation is very reduced in comparison. In fact, if we apply the same

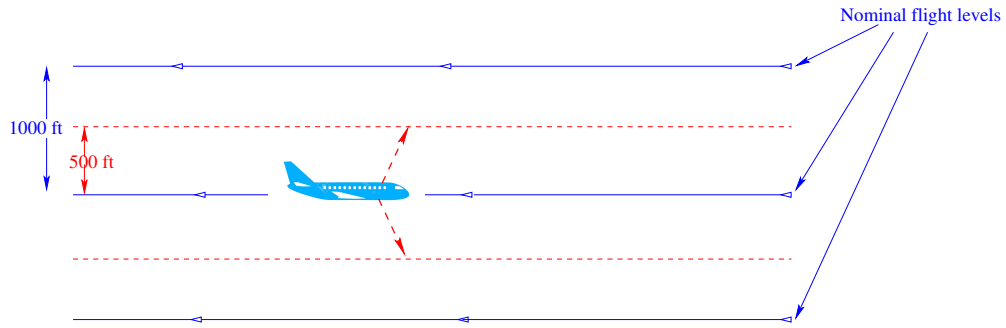

FIGURE 4.2 – Flight level change

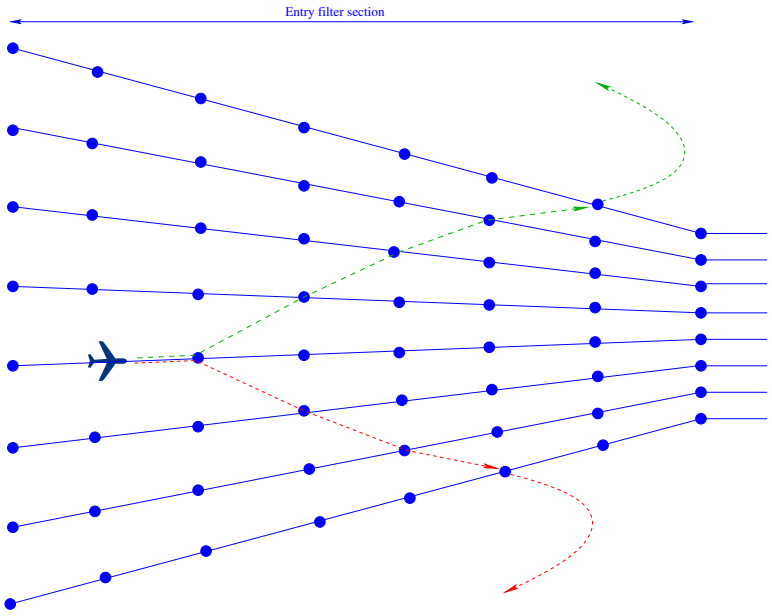

FIGURE 4.3 – WOTN exit procedures in the entry filter section

contingency procedures which are applied to OTS, then middle tracks are constructed between nominal center lines in order to be followed by deviating flights. Since basic WOTN tracks are separated by 12 NM, the newly constructed tracks are only 6 NM from one another. This lateral separation is operationally unacceptable.

Another problem can be detected in WOTN parallel section when oceanic procedures involving flight deviations around severe weather are deployed. In fact, in such conditions, the aircraft is expected to continue within its track if it is deviated less than 10 NM, otherwise, it is expected to change its flight level. In case of WOTN parallel section, an aircraft deviating around severe weather will get very close to the adjacent track, and it is even very likely to cross it. Actually, in this particular issue, we believe that the reduced spacing between WOTN tracks is beneficial since aircraft flying in adjacent parallel tracks experience almost the same weather. Therefore, all aircraft are penalized by the same deviation. Thus, severe weather changes the entire shape of WOTN parallel section, rather than affecting a single flight trajectory. For instance, Figure 4.4 illustrates the WOTN tracks in the presence of strong winds caused by jet streams. WOTN tracks

are in red color. The parallel track section is completely merged within the jet stream and follows its shape.

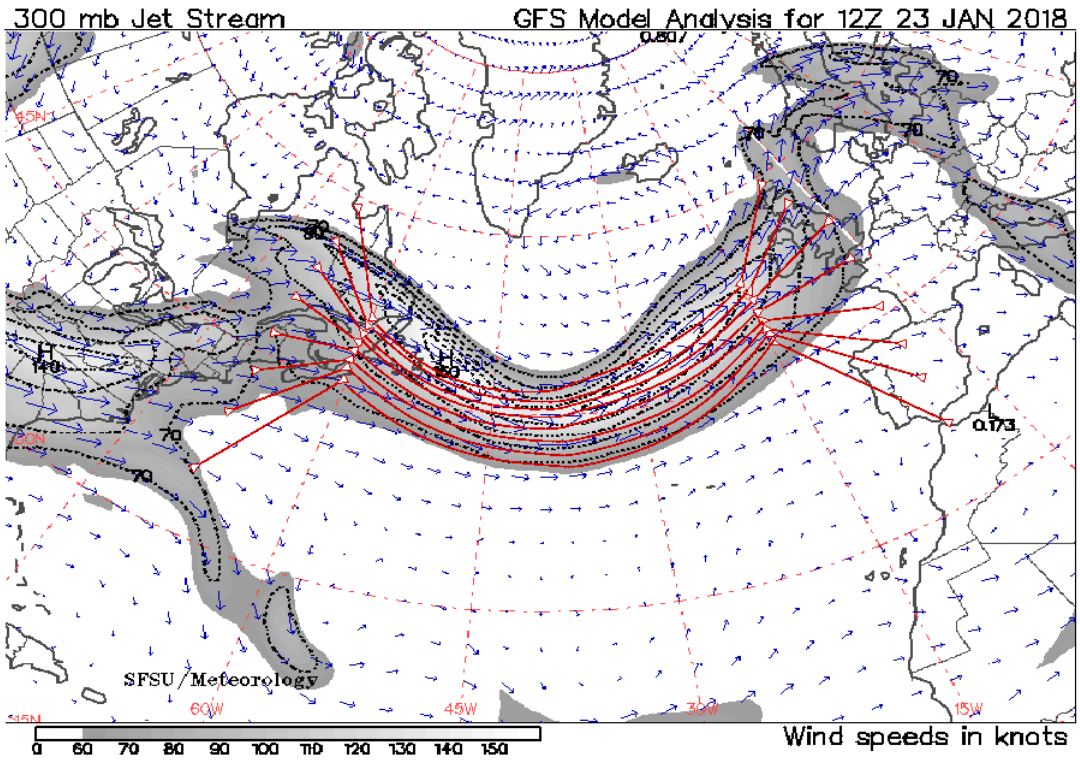

FIGURE 4.4 – WOTN tracks in the jet streams

In the following sections, we introduce two approaches to allow aircraft flying on WOTN parallel tracks to exit the route structure safely and efficiently.

4.3 Mathematical model

In this section, we present our solutions to allow WOTN flights to safely exit the parallel track section. The proposed approaches are an improvement on the WOTN traffic organization in order to take into account some specificities of NAT flights. Therefore, the same WOTN and flight models, presented in Section 3.2, are considered here. Nevertheless, the proposed methods add new constraints to the conflict detection and optimization formulation strategies.

4.3.1 Approach description

In order to establish the feasibility of exiting WOTN parallel tracks, we propose two configurations for flight progress inside parallel track section. The first configuration, referred to as *chevron*, makes WOTN flights fly on a chevron structure (see Figure 4.5). While the second one, referred to as *rhombus*, oblige flights to fly on a rhombus structure (see Figure 4.6). The main objective is to organize the traffic in a manner that, at any given time, aircraft on the middle tracks are ahead of aircraft on the edge tracks.

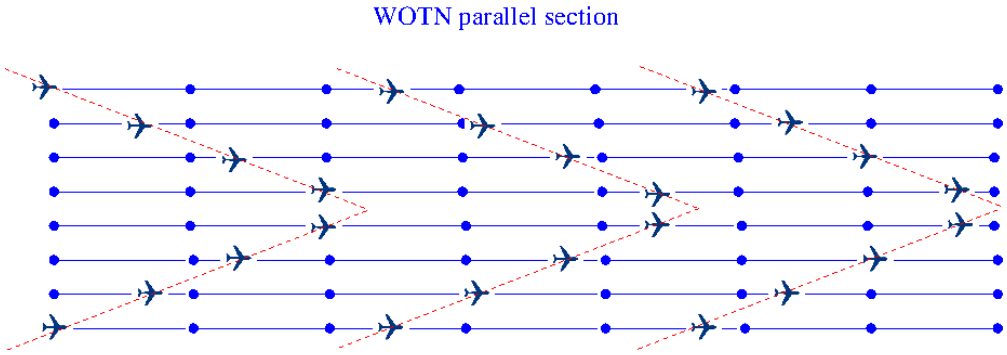

FIGURE 4.5 – WOTN traffic organized on chevron

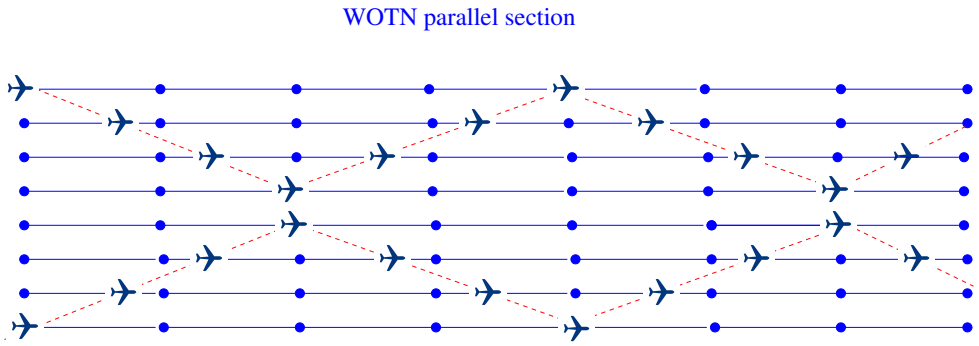

FIGURE 4.6 – WOTN traffic organized on rhombus

By applying this traffic pattern, flights in middle tracks become able to exit WOTN without conflicting with other flights in adjacent tracks. The exit procedure is highlighted in Figure 4.7 and Figure 4.8.

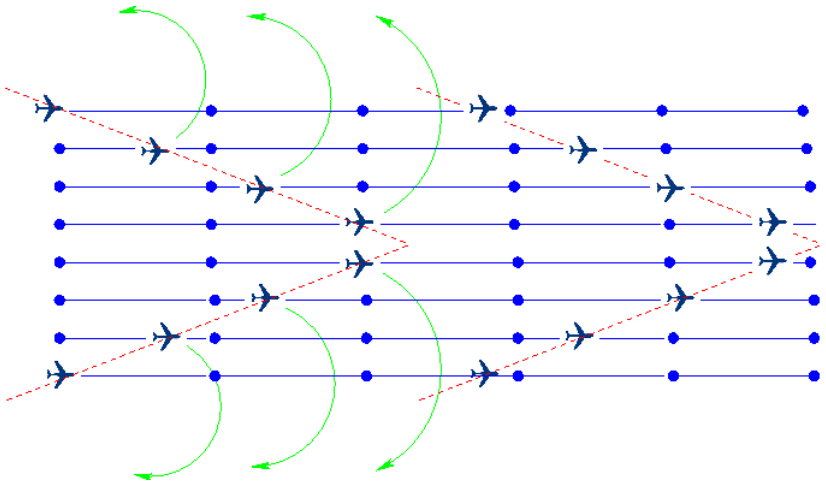

FIGURE 4.7 – WOTN exit procedure in the chevron configuration

Therefore, an aircraft that needs to exit the WOTN parallel tracks has to:

1. First, change its flight level by climbing or descending 500 feet.

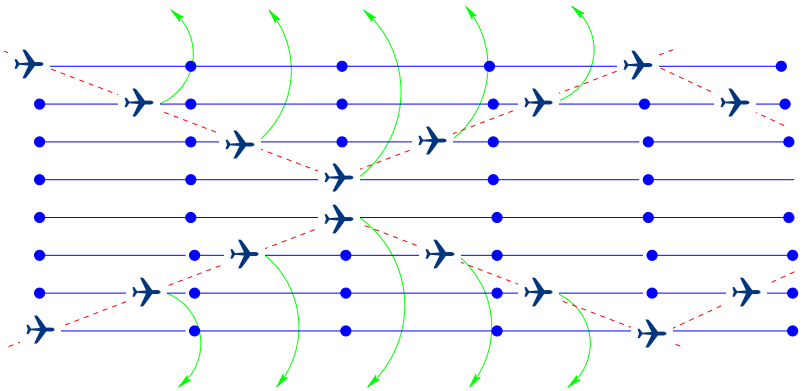

FIGURE 4.8 – WOTN exit procedure in the rhombus configuration

2. Then, turn north if it is following one of the four northern tracks, or south otherwise.
3. Finally, ATC takes charge to guide the aircraft safely to its new destination.

With these ways of organizing traffic, we are assuming that every WOTN flight can experience an emergency. Thus, we are considering the worst case in order to deal with all the possible contingencies. Nevertheless, it is essential to compute exactly the spacing needed between each two successive aircraft in adjacent tracks, and to optimize the flight track allocation in order to ensure an efficient use of WOTN especially in case of high traffic density. In the next section, the conflict detection procedures are described for the two proposed configurations.

4.3.2 Conflict detection model

In addition to the conflict detection strategy described in 3.2.5, new conflicts are detected inside the parallel track section. In fact, we have to ensure that when an aircraft exits the WOTN parallel section, it is not in conflict with other aircraft while crossing adjacent tracks. Therefore, a separation distance d_{Sep} has to be established between the crossing point in adjacent tracks and the other aircraft flying these tracks (see Figure 4.9).

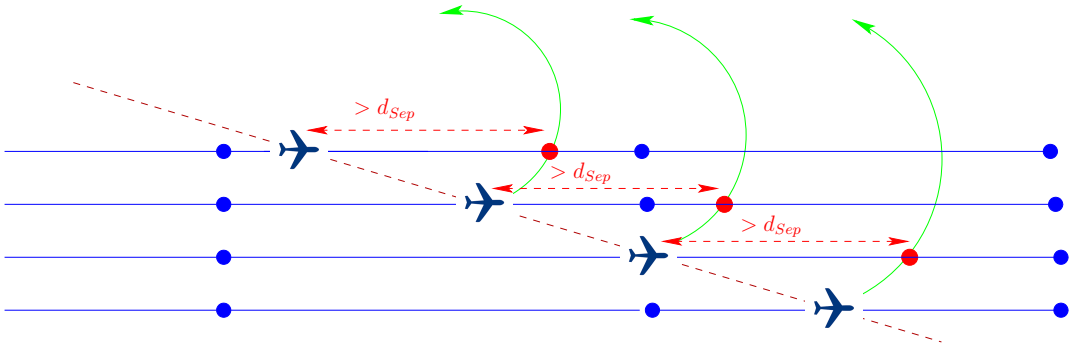

FIGURE 4.9 – Separation norm between aircraft in adjacent tracks

First of all, let us define the new separation norms that must be satisfied between the deviating aircraft and other flights in adjacent tracks. In this work, we keep the same vertical separation defined in the current contingency procedures for OTS flights. Furthermore, since we are no longer following parallel tracks, we no longer must consider the reduced lateral separation norm of 12 NM. Therefore, we assume that establishing the same lateral separation required by free oceanic flight is sufficient to ensure the traffic safety. Therefore, we recall the following separation norms currently applied for separating oceanic flights in case of emergencies:

— Vertical separation, V_{Sep}, which is equal to 500 feet below $FL410$ (all WOTN tracks are below $FL410$).

— Lateral separation, Lat_{Sep}, which is assumed to be 30 NM.

— Longitudinal separation, Lon_{Sep}, which is assumed to be 3 minutes.

In case of emergency, the aircraft is required first to perform a descent or a climb of V_{Sep}. Thus, the vertical separation norm is automatically satisfied. Typically, vertical separation between oceanic flights has to be equal to 1000 feet. In emergency cases, this separation is reduced to 500 feet. Nevertheless, vertical separation alone is not sufficient and a lateral spacing has to be maintained as well between aircraft, even if they are separated by V_{Sep} vertically.

In our case study, lateral and longitudinal separation norms coincide. In fact, a 3 minute spacing represents approximately the required time for the fastest commercial aircraft ($v_{max} = 600kts = 10NM/min$) to overfly 30 NM. Therefore, by maintaining only longitudinal separation we ensure a conflict free traffic.

Let us consider a deviating aircraft f, and two flights f_1 and f_2 flying in the adjacent track, such as described in Figure 4.10. The flight f crosses the adjacent track at moment T_{Cross}. At that moment, T_{Cross}, time T_1 remains for the flight f_1 to arrive at the crossing point, while flight f_2 has already passed through the crossing point at time T_2.

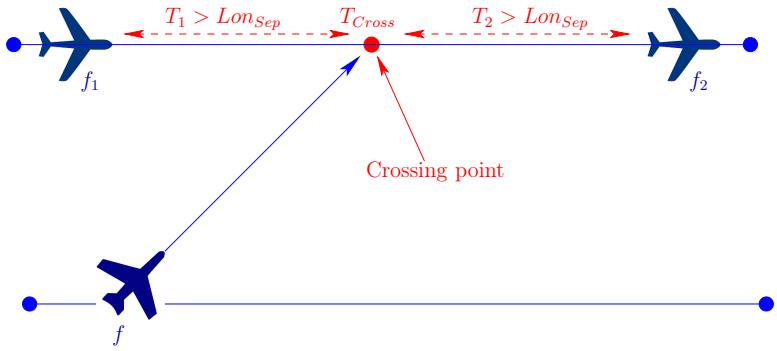

FIGURE 4.10 – Longitudinal separation for deviating aircraft

Therefore a conflict is detected if one of the two following equations is verified:

$$T_1 < Lon_{Sep} \tag{4.1}$$

$$T_2 < Lon_{Sep} \tag{4.2}$$

In order to simplify our model, we focus on computing the time spacing, t_{min}, that has to be kept between aircraft flying in parallel tracks to ensure no conflicts arise in case of a deviation. This time spacing is highlighted in Figure 4.11.

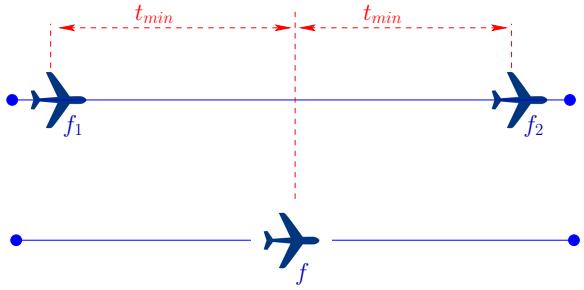

FIGURE 4.11 – Spacing time between aircraft in adjacent tracks

Thus, let us compute the distance traveled by the aircraft from exiting its assigned track to crossing the adjacent one. To do so, we assume that the aircraft performs a 45° turn once it exits its track. This assumption is realistic since, in real operations, the aircraft do perform this 45° turn when exiting OTS tracks.

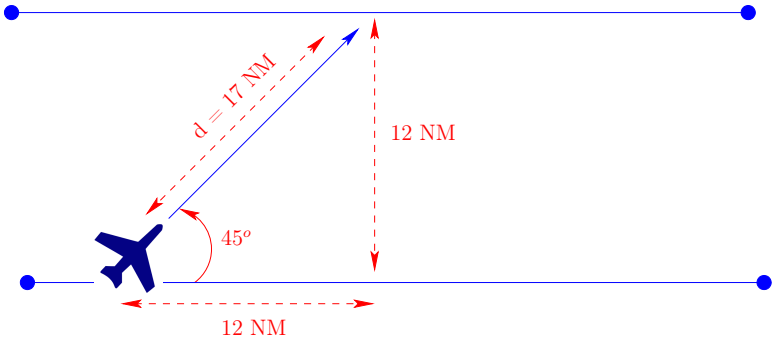

FIGURE 4.12 – Distance covered by the aircraft to cross adjacent track

Therefore, giving that the tracks are separated by 12 NM, the distance d covered by the aircraft to cross the adjacent track is simply computed as follows (see Figure 4.12):

$$d = \sqrt{12^2 + 12^2} = 16.9706 \approx 17NM \tag{4.3}$$

Typically, oceanic flight speeds range between $v_{min} = 450kts = 7.5NM/min$ and $v_{max} = 600kts = 10NM/min$. Let us consider the worst case by assuming that the deviating flight is flying at v_{min}. Then, the time required by the slowest aircraft to cross its adjacent track is equal to almost $t_c = 2.3$ minutes. Thus, we can simply deduce: $t_{min} = t_c + Lon_{Sep} = 5.3$ minutes.

Therefore, in order to avoid conflicts when an aircraft deviates from its track, we end up with the chevron and rhombus flight configurations presented in Figure 4.13 and Figure 4.14, respectively, for the four northern tracks of WOTN. The configuration of flights flying the four southern tracks is determined in a similar manner.

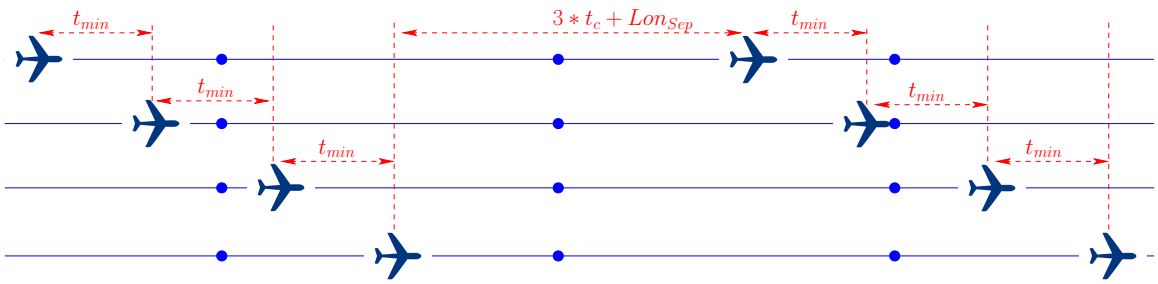

FIGURE 4.13 – Chevron flight configuration in northern WOTN tracks

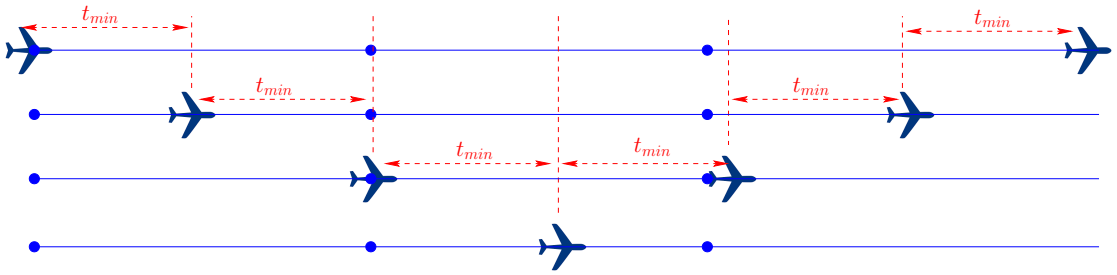

FIGURE 4.14 – Rhombus flight configuration in northern WOTN tracks

Conflicts that are predicted to occur when a contingency procedure is performed, are referred to as $\phi_{Chevron}$ and $\phi_{Rhombus}$ for the flight configurations based on chevron and rhombus, respectively. It can be noticed that each aircraft flying on an inner track is constrained by the flights flying on the edge tracks. For instance, let us consider a flight f, flying along track j:

- $\phi_{Chevron}$ are detected as follows:
  - the passing time of f through each way-point i of track j, denoted t^f_{ij} is determined.
  - t^f_{ij} is compared to the passing times, denoted t^g_{ik}, of each flight g through the corresponding way-point i on each track k that belongs to:
    - the tracks above the track j, if track j belongs to the four northern WOTN tracks, or
    - the tracks below the track j, if track j belongs to the four southern WOTN tracks.
  - a $\phi_{Chevron}$ is detected if and only if one of the following equations is verified (Figure 4.13):

$$0 < t^f_{ij} - t^g_{ik} < t_{min} * |j - k| \tag{4.4}$$

$$0 < t^g_{ik} - t^f_{ij} < 3 \times t_c + Lon_{Sep} + (t_{min} * (3 - |j - k|)) \tag{4.5}$$

- $\phi_{Rhombus}$ are detected as follows:
  - the passing time of f through each way-point i of track j, denoted t^f_{ij} is determined.

— t_{ij}^{f} is compared to all the passing times, denoted t_{ik}^{g}, of each flight g through the corresponding way-point i at each track k that belongs to:
  — the upper tracks, if track j belongs to the four northern WOTN tracks, or
  — the lower tracks, if track j belongs to the four southern WOTN tracks.
— a $\phi_{Rhombus}$ is detected if and only if the following equation is verified (Figure 4.14):

$$|t_{ij}^{f} - t_{ik}^{g}| < t_{min} * |j - k| \tag{4.6}$$

The algorithms implemented to compute the number $\phi_{Chevron}$ and $\phi_{Rhombus}$ are described in Algorithms 3 and 4, respectively.

In each flight configuration, we aim at resolving all the conflicts, namely $\phi_{Chevron}$ and $\phi_{Rhombus}$ for chevron and rhombus configuration, respectively. Therefore, our main goal is to satisfy the following equations:

$$\phi_{Chevron} = 0 \tag{4.7}$$

$$\phi_{Rhombus} = 0 \tag{4.8}$$

To do so, we formulate our problem as an optimization problem that we present and discuss in the next section.

4.3.3 Optimization formulation

The flight configurations that we aim at implementing restrict the solution space of the problem, making it more difficult to solve. For this reason, we introduce a new degree of freedom to separate aircraft in the horizontal space by performing a speed regulation within the WOTN parallel section. The alternate speed assigned to each flight f is modeled as follows.

Alternative flight speed We associate, for each flight f, another decision variable which represents the flight-speed shift v_f. Thus, the assigned flight speed, AV^f, of the flight f is computed as follows:

$$AV^f = V^f + \frac{V^f \times v^f}{100} \tag{4.9}$$

where V^f is the initially-planned flight speed which is a given data of our problem. The assigned speed is only applied in the WOTN parallel track region, elsewhere we restore the initially-planned flight speed.

Allowed change for the alternative flight speed In order to restrict the flight speed change, the flight speed shift is constrained. Thus, we consider a speed interval shift of $[-6\%, +3\%]$, which is a commonly used interval for speed regulation of en-route flights [83].

Algorithm 3: Computing the number of $\phi_{Chevron}$ at WOTN parallel tracks

Input: $T = \{0, 1, .., Nb_T\}$: is the set of WOTN tracks and Nb_T is the number of tracks
$\{w_{ji}\}_{i \in \{0,1,..,Nb_W\}}$: is a set containing the way-points of the parallel section of the track j, and Nb_W is the number of way-points.
$\{F_{w_{ji}}\}$: is a set of all passing flights through the way-point w_{ji}
Output: $\phi_{Chevron}$: Total number of $\phi_{Chevron}$ on WOTN parallel tracks

$\phi_{Chevron} = 0$
for $j = 1 \rightarrow Nb_T - 1$ **do**
    // only middle tracks are considered
    if $j \leq (Nb_T/2)$ **then**
        // in case of southern tracks
        $start = j - 1$
        $end = 0$
    else
        // in case of northern tracks
        $start = j + 1$
        $end = Nb_T$
    end
    for $i = 0 \rightarrow Nb_W$ **do**
        // for each waypoint of the parallel section of track j
        $Nb_F = number(F_{w_{ji}})$
        // compute the number of flights passing through the way-point w_{ji}
        $F_{w_{ji}} = [f^1_{w_{ji}}, f^2_{w_{ji}}, .., f^{Nb_F}_{w_{ji}}]$
        // sort the passing flights in a vector
        for $l = 0 \rightarrow Nb_F$ **do**
            // for each flight in $F_{w_{ji}}$
            for $k = start \rightarrow end$ **do**
                // for all the more southern or northern tracks
                $Nb_G = number(F_{w_{ki}})$
                $G_{w_{ki}} = [g^1_{w_{ki}}, g^2_{w_{ki}}, .., g^{Nb_G}_{w_{ki}}]$
                for $m = 0 \rightarrow Nb_G$ **do**
                    if $t^{f^l_{w_{ji}}} - t^{g^m_{w_{ki}}} > 0$ **then**
                        if $t^{f^l_{w_{ji}}} - t^{g^m_{w_{ki}}} < t_{min} \times |j - k|$ **then**
                            // if the difference between the flight's passing times verify equation 4.4
                            $\phi_{Chevron} + +$
                        end
                    else
                        if $t^{g^m_{w_{ki}}} - t^{f^l_{w_{ji}}} < 3 \times t_c + Lon_{Sep} + (t_{min} \times (3 - |j - k|))$ **then**
                            // if the difference between the flight's passing times verify equation 4.5
                            $\phi_{Chevron} + +$
                        end
                    end
                end
            end
        end
    end
end

Algorithm 4: Computing the number of $\phi_{Rhombus}$ at WOTN parallel tracks

Input: $T = \{0, 1, .., Nb_T\}$: is the set of WOTN tracks and Nb_T is the number of tracks

$\{w_{ji}\}_{i \in \{0,1,..,Nb_W\}}$: is a set containing the way-points of the parallel section of the track j, and Nb_W is the number of way-points.

$\{F_{w_{ji}}\}$: is a set of all passing flights through the way-point w_{ji}

Output: $\phi_{Rhombus}$: Total number of $\phi_{Rhombus}$ on WOTN parallel tracks

$\phi_{Rhombus} = 0$
for $j = 1 \rightarrow Nb_T - 1$ **do**
    // only middle tracks are considered
    if $j \leq (Nb_T/2)$ **then**
        // in case of southern tracks
        $start = j - 1$
        $end = 0$
    else
        // in case of northern tracks
        $start = j + 1$
        $end = Nb_T$
    end
    for $i = 0 \rightarrow Nb_W$ **do**
        // for each waypoint of the parallel section of track j
        $Nb_F = number(F_{w_{ji}})$
        // compute the number of flights passing through the way-point w_{ji}
        $F_{w_{ji}} = [f^1_{w_{ji}}, f^2_{w_{ji}}, .., f^{Nb_F}_{w_{ji}}]$
        // sort the passing flights in a vector
        for $l = 0 \rightarrow Nb_F$ **do**
            // for each flight in $F_{w_{ji}}$
            for $k = start \rightarrow end$ **do**
                // for all the more southern or northern tracks
                $Nb_G = number(F_{w_{ki}})$
                // compute the number of flights passing through the way-point w_{ki}
                $G_{w_{ki}} = [g^1_{w_{ki}}, g^2_{w_{ki}}, .., g^{Nb_G}_{w_{ki}}]$
                // sort the passing flights in a vector
                for $m = 0 \rightarrow Nb_G$ **do**
                    if $|t^{f^l_{w_{ji}}} - t^{g^m_{w_{ki}}}| < t_{min} \times |j - k|$ **then**
                        // if the difference between the flight's passing times verify equation 4.6
                        $\phi_{Rhombus}++$
                    end
                end
            end
        end
    end
end

Decision variables Recall that we have defined the set of the following decision variables related to each flight f:

— $\Omega^f = (ATrack^f_{In}, ATrack^f_{Out}, D^f_{In}, [X^f_i]_{i\in\{1,2,\ldots,N_x-1\}}, [AZ^f_i]_{i\in\{1,2,\ldots,N_x-1\}})$.

Let us set the new decision variable related to the flight speed setting, namely v^f for each flight f. This decision variable has to verify the following constraint:

$$-6 \leq v^f \leq +3. \tag{4.10}$$

Therefore, we redefine the set of decision variables related to each flight f as given:

— $\Omega^f = (ATrack^f_{In}, ATrack^f_{Out}, D^f_{In}, v^f, [X^f_i]_{i\in\{1,2,\ldots,N_x-1\}}, [AZ^f_i]_{i\in\{1,2,\ldots,N_x-1\}})$.

Then, recall that the set of decision variables related to a set S of flights is defined as follows:

— $\Omega = \{\Omega^f\}_{f\in S}$

Objective function Recall that we have defined the objective function as follows:

$$F_{obj} = \Phi_{tot} + a * (d * D + c * C + r * R) \tag{4.11}$$

where Φ_{tot} is the total number of conflicts at WOTN nodes and links, D is the total assigned delay over all flights, C is the total cruising time over all flights and R is the total time induced by a deviation from desired tracks over all flights. In order to limit the number of flights that changes their speed profile and to reduce the flight speed deviation as well, let us introduce another optimization criteria, V, which defines the deviation from the planned airspeed over all flights:

$$V = \sum_{f\in S} |V^f - AV^f| \tag{4.12}$$

This criteria is added to the objective function with a weighting coefficient v:

$$F_{obj} = \Phi_{tot} + a * (d * D + c * C + r * R + v * V) \tag{4.13}$$

Furthermore, in order to establish the chevron or rhombus flight structure, we have to eliminate the corresponding number of conflicts, namely $\phi_{Chevron}$ and $\phi_{Rhombus}$. Therefore, this number of conflicts is added to the objective function. The objective function related to the chevron structure, referred to as F^C_{obj}, is defined as follows:

$$F^C_{obj} = \Phi_{tot} + \phi_{Chevron} + a * (d * D + c * C + r * R + v * V) \tag{4.14}$$

and the objective function related to the rhombus structure, referred to as F^R_{obj}, is defined as follows:

$$F^R_{obj} = \Phi_{tot} + \phi_{Rhombus} + a * (d * D + c * C + r * R + v * V) \tag{4.15}$$

Thus, the optimization formulation of our problem, modeled in the same way as presented in 3.2.6, is given by:

$$
\begin{aligned}
\underset{\Omega=\{\Omega^f\}_{f\in S}}{\text{minimize}} \quad & F^C_{obj} || F^R_{obj} \\
\text{subject to} \quad & \Phi_{tot}(\Omega) = 0, \\
& \phi_{Chevron} = 0 \text{ or } \phi_{Rhombus} = 0, \\
& ATrack^f_{In} = Track^f_{In} + / - 1, \\
& ATrack^f_{Out} = Track^f_{Out} + / - 1, \\
& 0 \leq D^f_{in} \leq 20min, \\
& -6 \leq v^f \leq +3, \\
& \sum_{i\in\{1,2,\ldots,N_x-1\}} X^f_i = ATrack^f_{Out} - ATrack^f_{In}, \\
& \sum_{i\in\{1,2,\ldots,N_x-1\}} AZ^f_i = \sum_{i\in\{1,2,\ldots,N_x-1\}} Z^f_i = N^f_c, \\
& \forall j \in \{1,2,\ldots,N^f_c\}, |Climb^f_j - AClimb^f_j| \leq 1.
\end{aligned}
\tag{4.16}
$$

4.4 Computational results

In order to solve our optimization problem, we rely on the resolution algorithm described in Section 3.3. First, we present results of the chevron configuration method, then we display the results related to rhombus configuration. Finally, a comparison between the two configurations is discussed.
The parameters of simulated annealing and sliding window algorithms are set empirically as follows :

- The initial temperature $T_0 = 0.01$
- The objective function coefficients $a = 0.1$ and $d = c = r = 1$,
- Number of iterations in each temperature schedule $N = 500$,
- The ratio of the temperature decrease $\alpha = 0.97$,
- The stopping criterion $\beta = 0.0001$,
- The sliding window parameters in minutes: $T_w = 180$, $T_s = 60$.

The two proposed configurations add new constraints to the WOTN traffic. Therefore, we start by focusing on the number of flights that can be performed within a single flight level under these flight configurations. Then, we evaluate a real flight set.

4.4.1 Results for one flight level

Our first preliminary study considers several flight sets flying on the same flight level. These flight sets are referred to as FS_1, FS_2, FS_3 and FS_4 and contains respectively 50, 100, 150 and 200 flight flying on $FL350$ at the time period between 00:00 UTC and 08:00 UTC. In this case, we do not allow changing the flight level in the conflict resolution maneuvers, since, our goal is to evaluate the capacity of WOTN tracks at a given flight level when implementing the two proposed flight configurations. Results for the two flight

configurations, chevron and rhombus, are presented in Table 4.1 and Table 4.2, respectively. Here we examine the number of residual conflicts for both chevron and rhombus

TABLE 4.1 – Results for the chevron flight configuration

Flight set	Nb Flights	Number of *point-to-point* conflicts(Φ_{tot})			Number of Chevron conflicts ($\phi_{Chevron}$)		
		before	after	% of resolved conflicts	before	after	% of resolved conflicts
FS_1	50	175	0	100 %	1177	0	100 %
FS_2	100	321	0	100%	2089	0	100%
FS_3	150	570	8	98.5	3476	2	99.9
FS_4	200	981	142	85.5	5220	54	98.9

TABLE 4.2 – Results for the rhombus flight configuration

Flight set	Nb Flights	Number of *point-to-point* conflicts(Φ_{tot})			Number of Rhombus conflicts ($\phi_{Rhombus}$)		
		before	after	% of resolved conflicts	before	after	% of resolved conflicts
FS_1	50	175	0	100 %	1225	0	100 %
FS_2	100	321	0	100%	1886	0	100%
FS_3	150	570	10	98.2%	2447	4	99.8%
FS_4	200	981	74	92.4%	4178	32	99.2%

configurations. For both flight sets FS_1 and FS_2, all conflicts between aircraft trajectories are resolved ($\Phi_{tot} = 0$). Furthermore, the resulting solution is free of chevron and rhombus conflicts when implementing the chevron structure and the rhombus structure, that is $\phi_{Chevron} = \phi_{Rhombus} = 0$. Nevertheless, with the two flight sets FS_3 and FS_4, some conflicts remain after applying our algorithm. The number of remaining conflicts for the flight set FS_3 is relatively small and we assume that these remaining conflicts can be easily handled by controllers in pre-tactical and tactical phases. However, the remaining number of conflicts for flight set FS_4 is relatively big. Indeed, for chevron configuration $\Phi_{tot} = 74$ and $\phi_{Chevron} = 54$, and for rhombus configuration, $\Phi_{tot} = 142$ and $\phi_{Rhombus} = 32$. Thus, we conclude that when implementing chevron or rhombus flight configurations, the limiting capacity of the WOTN tracks is close to 150 flight per flight level between midnight and 08:00 UTC.

Let us now evaluate the performance of the resulting solution in terms of satisfying the initially planned flight parameters. The values of different flight parameters resulting from conflict resolution for the set of flights S_3 are presented in Table 4.3.

The first important result that can be deduced is that both strategies, chevron and rhombus, have almost the same influence on the quality of the resulting solution. Furthermore, the percentage of flights with desired airspeed is 84% for both strategies which is an important result. Indeed, keeping the desired flight airspeed is directly related to keeping the optimal flight profile in terms of fuel consumption.

TABLE 4.3 – WOTN results without traffic organization compared to WOTN results with *chevron* and *rhombus*

criteria	before	Chevron	Rhombus
Number of potential conflicts	0	0	0
% of flights with desired entry track	89%	79.6%	81%
% of flights with desired exit track	92.5 %	92.6%	94.3%
% of flights with desired flight level	100 %	80.5%	82.2%
% of flights without speed change	100%	98%	99%
% of flights without delay	71%	42.6%	48.7%
mean delay (minutes)	3.4	11.7	8.5
Total entry delay (hours)	8.5	45.5	37.6
Total cruising time (hours)	3855.2	3866.76	3866.7

Based on the input NAT flight data on July 2012, we examine the distribution of flights on different flight levels for four of these 30 days, namely, July 1st, 2nd, 15th and 20th. For all the data, aircraft do not change their flight level along the entire NAT flight. Results are displayed in Figure 4.15. It is clearly seen that FL350 accommodates more than 150 flight in all the considered traffic days. On July 2^{nd}, 2012, FL370 accommodates also more than 150 flight. Basically, the flight distribution within flight levels presented in 4.15 describes the optimal flight level for each aircraft. Unfortunately, keeping the optimal flight levels is not possible with our methodology since we have found a capacity limit of almost 150 flight per flight level. A solution is to generate an equal flight distribution within the three flight levels FL330, FL350 and FL370. Concretely, this means that some flights flying on FL350 switch their optimal flight profile to one level up or down (FL370 or FL330). This solution is an acceptable solution since the flight level change is to an adjacent one. Nevertheless, in some cases, we are obliged to change the flight level of many flights. For instance, if we consider the day traffic on July, 20^{th}, 63 flights are required to change their flight level, which represents almost 11% of all eastbound day traffic.

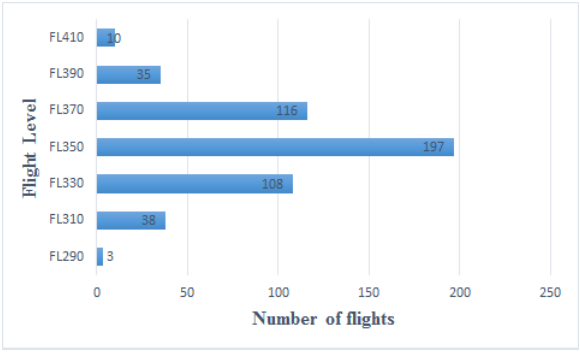

(a) July 1^{st}, 2012

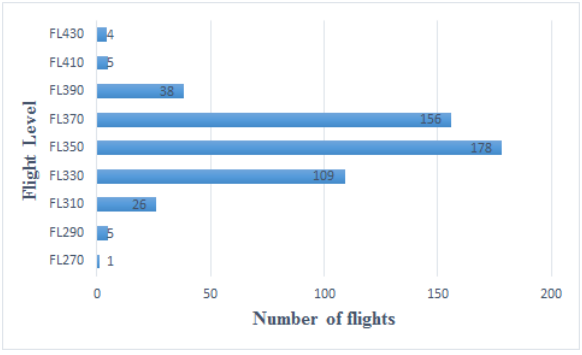

(b) July 2^{nd}, 2012

In the next section, simulations are performed with a day's worth of traffic over the NAT on *July* 15, 2012. Results are considered for two cases: either flight level change is authorized or not.

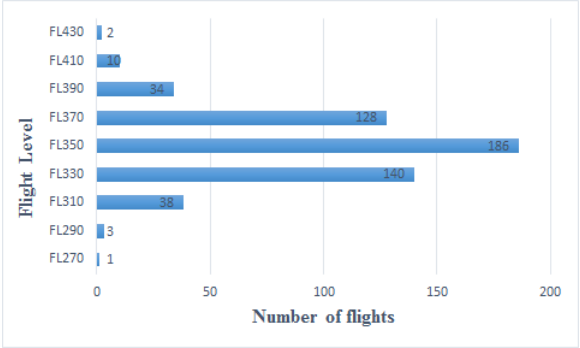

(c) July 15^{th}, 2012

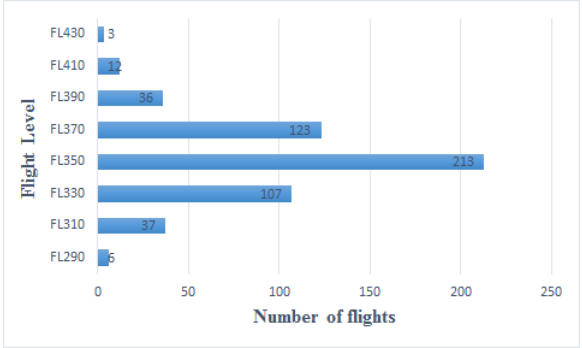

(d) July 20^{th}, 2012

FIGURE 4.15 – Flight distribution within flight levels

4.4.2 Chevron and rhombus configuration results with a day traffic

In this section, simulations are performed with a day of NAT traffic on *July* 15, 2012. The flight set contain 546 eastbound flight. In these simulations, flights are allowed to change their desired flight level in order to resolve conflicts with others. First off all, results on the remaining number of conflicts are presented. Then, a discussion on the quality of the proposed solution is made.

After applying our algorithm, a conflict-free solution is found for both flight configurations, chevron and rhombus (Table 4.4). Even thought both chevron and rhombus

	Before	After Chevron	After Rhombus
Number of *point-to-point* conflicts (Φ_{tot})	1477	0	0
Number of *flight-to-flight* conflicts	380	0	0
Number Chevron conflicts ($\phi_{Chevron}$)	6431	0	-
Number Rhombus conflicts ($\phi_{Rhombus}$)	5629	-	0

TABLE 4.4 – Summary of the conflict resolution results

flight structures add more constraints to aircraft, we found a resulting solution free of both chevron and rhombus conflicts. This result is very important and proves that a chevron or rhombus flight organization can be implemented within real traffic. The additional constraints imposed by the proposed flight configuration, chevron and rhombus, are ensured by adjusting our problem decision variables. Changes in decision variables are allowed to a limited extent. Indeed, our proposed solution has to be as close as possible to the initially planned flight parameters. For this reason, results related to the shift of flight parameters from the desired ones are displayed in Table 4.5.

One can observe that the two proposed flight structures with a day's worth of traffic over the NAT, chevron and rhombus, yield almost to similar results in terms of modified flight plans. However, the rhombus flight structure is found to be slightly better than the chevron one when comparing all the flight parameters. The most important result to be highlighted is that the number of flights that change their desired speed is very low. It is equal to 4 and 7 flights for the chevron and rhombus structures, respectively. Furthermore,

TABLE 4.5 – Results with chevron and rhombus strategies

criteria	Chevron	Rhombus
% of flights with desired entry track	79.6%	81%
% of flights with desired exit track	92.6%	94.3%
% of flights with desired flight level	80.5%	82.2%
% of flights without speed change	98%	99%
% of flights without delay	42.6%	48.7%
mean delay (minutes)	11.7	8.5
Total entry delay (hours)	45.5	37.6
Total cruising time (hours)	3866.76	3866.7

the number of flights keeping their desired flight level is very important as well. It is very interesting for these two parameters, flight level and speed, to be as close as possible to the planned ones since they are directly related to the fuel consumption. Indeed, maintaining desired flight levels and speeds leads to reducing the fuel consumption.

In addition to this, our proposed approach is very costly in terms of attributed delays. In fact, less than half of flights keep their desired entry times, while the others are penalized with delays. This result was not surprising since we add too more new constraints to our system. Furthermore, even though we add additional degrees of freedom to modify the flight level and speed parameters, these allowed shifts are very constrained since these two decision variables influence the fuel consumption. Therefore, a large percentage of flights with assigned delays is expected. Finally, the strong point of our approach is that it does not affect the shapes of flight paths, and thus trajectories still benefit from a favorable wind.

4.5 Conclusions

In this chapter, we propose an approach to deal with oceanic contingencies within WOTN. The proposed approach relies on organizing the passing times of flights within each track in order to facilitate exiting the route structure at any given time. This problem adds new constraints to our system presented in Chapter 3, and new types of conflicts between aircraft are taken into account, namely chevron and rhombus conflicts. For this reason, we include an additional degree of freedom to modify the flight levels and speeds. Our problem is modeled as an optimization problem and solved with a method combining sliding window approach and a simulated annealing algorithm. Computational results prove that our proposed approach can be successfully implemented within our route structure WOTN, already proposed in Chapter 3. Indeed, the special cases that may occur within NAT traffic are taken into consideration by our model and a solution to safely guide aircraft in emergency situations towards an alternate destination is implemented and validated. Nevertheless, the proposed approach is costly in terms of flight delays. In fact, since we add new constraints to our system, additional delays are assigned to the flights in order to get a conflict free set of flights.

Conclusions and perspectives

In the present thesis, our research work focuses on different ways of improving the situation of air traffic over the North Atlantic oceanic airspace (NAT). The proposed approaches are investigated under the ATM modernization framework. We conclude by a summary of the main contributions presented in the current research, followed by perspectives inspired by the study.

Contributions

The current research treats the problem of planning air traffic trajectories over the NAT airspace. This oceanic airspace presents several particularities. First, NAT is exposed to a very strong winds caused by the jet stream, which makes the problem of flight trajectory planning very sensitive to wind uncertainties. Second, flights operating on NAT are required to satisfy very rigid separation norms. This leads to sub-optimal flight routes in terms of cruise time and fuel consumption, in order to avoid conflicting with each other. Recently, an innovative surveillance system, Automated-Dependent Surveillance Broadcast (ADS-B), has been implemented and start to be operated especially in oceanic air spaces. ADS-B makes it possible for flights to exchange information between each other and with ATC controllers. In the light of ADS-B technology, new methods for planning NAT flight trajectories are possible.

The first part of our research introduces an approach to allow NAT flights to operate on Free Flight trajectories and to apply Multi-Agent Systems methods based on the Flocking Model in order to generate conflict free trajectories. The idea of this approach is inspired roughly from two specific behavior of the NAT flights:

— within NAT flights, we are not confronted with the problem of intersecting flights. In fact, eastbound and westbound traffic are treated separately and do not operate on the same flight levels.

— eastbound traffic, the subject of our study, would prefer to fly in the direction of wind and exploit the strong tailwind caused by jet streams, as this offers an optimal fuel consumption.

Therefore, the NAT eastbound traffic is regarded as a set of birds flying in the same direction, behaving like a swarm, and searching for the optimal path to reach their destinations, while maintaining a minimum separation distance between each other. Assuming that all aircraft are equipped with an ADS-B system, the proposed approach adopts the Flocking rules in order to construct a set of conflict-free flight trajectories. The trajectory construction process and the flight parameter allocation was modeled as an optimization

problem that we solve using a simulated annealing algorithm. This approach successfully assigns routes that are very close to the wind-optimal ones. However, these resulting trajectories are not robust to wind-uncertainties.

The second part of our research introduces a new route structure referred to as Wind-Optimal Track Network (WOTN) in order to replace the current route structure for the eastbound NAT traffic, namely Organized Track System (OTS). Three major factors leads as to replace the eastbound OTS. First, OTS tracks are not all wind-optimal and we notice that OTS middle tracks involve more favorable winds than the edge tracks. Second, re-routing from one track to another is very rarely authorized in the OTS, which in turn increases cruise times and traffic congestion at the input and output of the OTS. Finally, OTS tracks, of which there are only 6, are approaching their limit and becoming inefficient regarding the traffic density growth. The proposed route structure WOTN is thought out in order to undertake these issues. In fact, WOTN offers reliable transitions between tracks at the input and output of the NAT. Furthermore, it is constructed such a manner that all tracks benefit from the wind. Finally, it is extended to cover the entire NAT airspace and it includes eight tracks. We propose to implement WOTN under the reduced separation norms that are feasible thanks to ADS-B. By comparing this approach to wind-optimal trajectories, we conclude that flying wind-optimal trajectories leads to better results in term of cruising times than using the WOTN. However, the WOTN was found to be much more robust regarding wind changes.

Finally, the last part of our work proposes an approach for structuring the traffic within WOTN in such a manner as to enable each aircraft to safely exit the WOTN at any given time. This procedure is very important as NAT flights may experience contingencies during their flight, which makes them obliged to exit WOTN tracks and turn back to an alternate airport. We propose two flight structures, namely *Chevron* and *Rhombus*, and we investigate the possibility of implementing such structures with WOTN traffic. Each of these two structures adds new constraints to our problem, and new types of conflicts between aircraft are taken into account. As a result, additional degree of freedom is considered by allowing flight level and speed changes. The resulting solution proves that our proposed approaches can be successfully implemented within WOTN. Nevertheless, it is costly in terms of flight delays. In fact, since we add new constraints to our system, additional delays are assigned to the flights in order to find a conflict-free flight configuration.

Perspectives

The aforementioned tracks of our work represent a preliminary study that can be followed by several research directions in the future work.

Regarding our first track of research, a simplified model for constructing conflict-free flight trajectories was considered. This model is based on the Flocking rules that has to be applied by each aircraft and at each sample time of its trajectory. This approach has been programmed sequentially which involves highly complex computations and very

high computation times. In future work, the algorithm can be parallelized in order to alleviate the problem of computation time and to deal with a larger number of flights. In fact, with a parallel computing process, each aircraft can be run as an independent thread. Then, each thread updates its information in a global shared memory between all the threads. The problem is then solved concurrently for each thread taking into account the shared information. In addition to this, our approach can be combined with a wind networking process in which flights exchange wind information between each other [64]. This reduces the wind uncertainty problem.

Furthermore, the main weak point of our research is the given data used in the simulations which are not recent. This problem is due to the lack of data sources. We will try again to get more recent data and re-evaluate our proposed approach, then compare the resulting trajectories with the currently used ones. Moreover, we intend to search for data history of the NAT traffic in recent years and perform deep learning on the flight preferences. This study can help us with the flight trajectory planning process in order to understand more the flight priorities.

In addition to this, we applied a simplified model to conflict resolution within WOTN. This approach can be extended in order to include further criteria and options to match the real air-traffic situation in NAT. For instance, the aircraft speed and flight level can be combined as an additional decision variable in order to take into account the fuel consumption criteria. Moreover, a single objective function with weighting coefficients has been applied. This explains the fact that optimizing some criteria can be expensive regarding the rest of criteria. Thus, a multi-objective approach can be applied and yields for better results in term of finding the best trade-off between different criteria. In this case, the optimization problem resolution converges to the Pareto optimal solutions.

Finally, even though WOTN is designed and implemented based on the specifities of eastbound NAT flights, a similar approach is currently discussed for structuring continental air traffic. Indeed, a new concept envisioned by NextGen TBO referred to as air-stream flow corridors [111, 121] aims to absorb as many flights as possible in the high density traffic flows in order to alleviate controller workload thanks to the aircraft onboard enhanced capabilities. An air-stream flow corridor is a long and narrow air highway intended for use by aircraft to fly from an entry to an exit with minimal interference with other traffic. Inside a flow corridor, multiple closely spaced parallel lanes are operated. The corridor is separated from other traffic and to enter or exit the corridor, aircraft use air ramps. Therefore, our route structure can be adapted to a continental traffic and redesigned as a network of air-streams in order to handle complicated air traffic situations in continental airspace.

Appendix A

Simulated Annealing (SA) Basics

A.1 Local search (or Monte Carlo) algorithms

These algorithms optimize the cost function by exploring the neighborhood of the current point in the solution space.

In the next definitions we consider (S, f) an instantiation of a combinatorial optimization problem (S: set of feasible solutions, f: objective function to be minimized).

Let $\mathcal{N}$ be an application that defines for each solution $i \in S$ a subset $S_i \subset S$ of solutions "close" (to be defined by the user according to the problem of interest) to the solution i. The subset S_i is called the *neighborhood* of solution i.

In the next definitions, we consider that $\mathcal{N}$ is a neighborhood structure associated with (S, f).

A *generating mechanism* is a mean for selecting a solution j in any neighborhood S_i of a given solution i.

A local search algorithm is an iterative algorithm that begins its search from a feasible point, randomly drawn in the state space. A generation mechanism is then successively applied in order to find a better solution (in terms of the objective function value), by exploring the neighborhood of the current solution. If such a solution is found, it becomes the current solution. The algorithm ends when no improvement can be found, and the current solution is considered as the approximate solution of the optimization problem. One can summarize the algorithm by the following pseudo-code for a minimization problem:

Local search

1. **Draw an initial solution i;**
2. **Generate a solution j from the neighborhood S_i of the current solution i;**
3. **If $f(j) < f(i)$ then j becomes the current solution;**
4. **If $f(j) \geq f(i)$ for all $j \in S_i$ then END;**
5. **Go to step 2;**

A solution $i^* \in S$ is called a *local optimum with respect to $\mathcal{N}$ for (S, f)* if $f(i^*) \leq f(j)$ for all $j \in S_{i^*}$.

The neighborhood structure $\mathcal{N}$ is said to be *exact* if, for every local optimum with respect to $\mathcal{N}$, $i^* \in S$, i^* is also a global optimum of (S, f).

Thus, by definition, local search algorithms converge to local optima unless one has an exact neighborhood structure. This notion of exact neighborhood is theoretical because it generally leads in practice to resort to a complete enumeration of the search space.

Intuitively, if the current solution "falls" in a subdomain over which the objective function is convex, the algorithm remains trapped in this subdomain, unless the neighborhood structure associated with the generation mechanism can reach points outside this subdomain.

In order to avoid being trapped in local minima, it is then necessary to define a process likely to accept current state transitions that momentarily reduce the performance (in terms of objective) of the current solution: this is the main principle of simulated annealing.

A.2 Metropolis Algorithm

The Metropolis algorithm [72] is a basic component of SA. In 1953, three American researchers (Metropolis, Rosenbluth, and Teller [72]) developed an algorithm to simulate the physical annealing process. Their aim was to reproduce faithfully the evolution of the physical structure of a material undergoing annealing. This algorithm is based on Monte Carlo techniques which consist in generating a sequence of states of the solid in the following way.

Starting from an initial state i of energy E_i, a new state j of energy E_j is generated by modifying the position of one particle.

If the energy difference, $E_i - E_j$, is positive (the new state features lower energy), the state j becomes the new current state. If the energy difference is less than or equal to zero, then the probability that the state j becomes the current state is given by:

$$Pr\{\text{Current state} = j\} = e^{\left(\frac{E_i - E_j}{k_b . T}\right)}$$

where T represents the temperature of the solid and k_B is the Boltzmann constant ($k_B = 1.38 \times 10^{-23}$ joule/Kelvin).

The acceptance criterion of the new state is called the *Metropolis criterion.* If the cooling is carried out sufficiently slowly, the solid reaches a state of equilibrium at each given temperature T. In the Metropolis algorithm, this equilibrium is achieved by generating a large number of transitions at each temperature. The thermal equilibrium is characterized by the *Boltzmann statistical distribution.* This distribution gives the probability that the solid is in the state i of energy E_i at the temperature T:

$$Pr\{X = i\} = \frac{1}{Z(T)} e^{-\left(\frac{E_i}{k_b T}\right)}$$

where X is a random variable associated with the current state of the solid and $Z(T)$ is a normalization coefficient, defined as:

$$Z(T) = \sum_{j \in S} e^{-\left(\frac{E_j}{k_b T}\right)}.$$

Appendix B

Wind-optimal trajectories on NAT

In this chapter, we describe a method devoted to organize the traffic in the NAT based on wind-optimal trajectories, which may become operationally acceptable thanks to more precise surveillance, reduction of the separation norms, and more efficient aircraft separation (including airborne separation) [57, 110]. The first step of the proposed method evolves creating new aircraft routes, taking into account aircraft performance metrics and environmental conditions. At the next step, the set of such trajectories is evaluated using required separation norms in order to detect potential conflicts. Finally, the trajectories are slightly modified in order to avoid these conflicts and guarantee conflict-free flight progress together with trajectory optimality.

B.1 Calculating wind-optimal trajectories

The problem of creating cost-optimal, wind-optimal, or climate-optimal routes has been addressed in many different ways in literature for the decades [7, 36, 40, 54, 57, 76, 77, 104, 113]. The results of these simulations reveal significant benefits from flying such routes, in terms of time and fuel savings [76, 104], and emissions and contrails reductions [40, 77]. Here, the approach based on the Pontryagin's Minimum Principle, discussed by Ng et al. in [76], is used. Following this approach, the wind-optimal trajectories are found by determining the optimal heading angle for aircraft during cruise, that minimizes the travel time in the presence of winds. In case of a constant altitude, the minimum-time trajectory is obtained by integrating aircraft equations of motion given below:

$$\dot{\phi} = \frac{V^f sin(\psi) + W_v}{R} \tag{B.1}$$

$$\dot{\lambda} = \frac{V^f cos(\psi) + W_u}{R cos(\phi)} \tag{B.2}$$

Here, ϕ is latitude, λ is longitude, V^f is airspeed, ψ is heading angle, R is the Earth radius. W_u is the east-component of the wind velocity, and W_v is the north-component of the wind velocity. The dynamic equation for the optimal aircraft heading is:

$$\dot{\psi} = \frac{-F(\psi, \phi, \lambda, W_u, W_v, V^f)}{R cos(\phi)} \tag{B.3}$$

where $F(\psi, \phi, \lambda, W_u, W_v, V^f)$ is aircraft heading dynamics in response to winds (see [76] for more details). The resulting trajectory is represented as a sequence of 4-dimensional geographical points (ϕ, λ, h, t), where ϕ is latitude, λ is longitude, h is altitude and t is time (recorded with 1 minute interval).

In order to guarantee safe flight progress, it is important assure that the calculated wind-optimal trajectories remain conflict-free. For this purpose, a conflict resolution algorithm was developed [92], which permits to evaluate the number of potential conflicts for an arbitrary set of trajectories and to reduce this number by slight trajectory modification.

B.2 Conflict detection for wind-optimal trajectories

In this work, all transatlantic flights are assumed to cruise at predefined flight levels, which guarantees vertical separation. However, horizontal and temporal separation remains the issue in the case of wind-optimal trajectories. It was decided, that the rational separation norms for the free flights in the NAT could be 30 NM for horizontal separation, and 3 minutes for temporal separation. Then, a point-to-point conflict detection method based on the 4-dimensional grid is adopted, which was first developed by Chaimatanan et al. [19]. For each 4D-trajectory point (ϕ, λ, h, t), placed in the appropriate cell depending on its coordinates, the separation between this point and all the points in the same and neighbor cells is verified, and if violated, then a point-to-point conflict is detected (see [92] for more details), and the total number of point-to-point conflicts, C_t, is increased. Figure B.1 demonstrates the potential conflicts detected for a set of wind-optimal trajectories for 546 eastbound transatlantic flights on July 15^{th} 2012, where the conflict points are marked in red. One can easily see that wind-optimal trajectories are concentrated along a narrow flow which corresponds to the jet stream current. For this reason, the traffic within this flow is highly congested. Thus, strategic conflict resolution becomes important in this case.

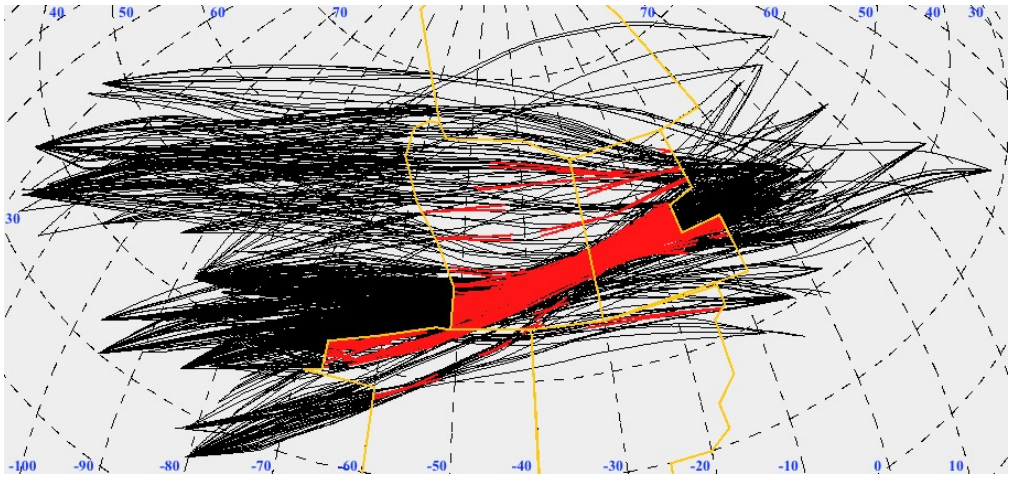

FIGURE B.1 – Potential conflicts detected for wind-optimal trajectories on July 15^{th} 2012

Conflict resolution for wind-optimal trajectories The conflict resolution problem is addressed as an optimization problem. The input data for this problem are:

— $W(\phi, \lambda, h, t)$- wind fields (4D-grids of W_u and W_v wind coordinates);

— N eastbound wind-optimal trajectories, $f = 1, \ldots, N$,

  — flown at a constant airspeed V^f,

  — and given as a sequence of 4D-route points $q_i^f = (\phi_i^f, \lambda_i^f, h, t_i^f)$

In order to resolve conflicts, two trajectory modification maneuvers are allowed: delaying a flight at the departure and shifting a trajectory geometrically. To create a new trajectory for a delayed flight, f, a given fixed delay, d^f, is added to the estimated time, t, at each 4D-point (ϕ, λ, h, t). d^f takes integer values from 0 to 20 minutes. Static wind fields are used for the flight time calculation. However, as demonstrated in [106], delaying flights is not enough for conflict resolution, thus, trajectory shape modification is applied. To modify the geometrical shape of a trajectory, a bijective transformation between an arbitrary curve on a sphere and a curve on the xy-plane are exploited, as demonstrated in Figure B.2 (see [92], [94] for more details). The bijective function curvature can be con-

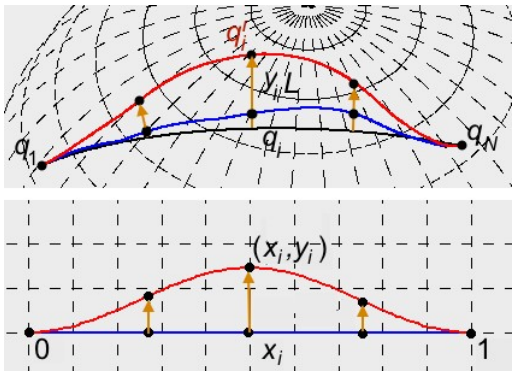

FIGURE B.2 – Trajectory shape modification approach

trolled independently for each flight, f, using a single variable, $b^f \in [-1, 1]$. Thus, the vector of decision variables of the optimization problem is given by: $z = (d^1, b^1, ..., d^N, b^N)$, where :

— $d^f \in 0, 1, ..., N^d_{max}$ is the departure time delay of flight f,

— $b^f \in [-1, 1]$ is the rate of trajectory deviation from the initial one for flight f.

The physical constraints of the problem are the separation norms between the 4D trajectory points, which has been relaxed in the objective function. As a result, the only constraints of this formulation are the boundary constraints on the decision variables, and the objective function is designed to minimize the total number of point-to-point conflicts, $C_t(z)$, induced by the set of modified trajectories corresponding to the variables z. In addition to this, in order to keep the resulting solution as close to the wind-optimal trajectories as possible [94], trajectory modification maneuvers are penalized, and as a result two more terms are included into the objective function:

— $\Delta T_c(z)$ - total cruising time increase calculated over N flights; and

— $\Delta T_d(z)$ - total departure delays assigned to N flights,

with associated weighting coefficients, α and β. Therefore, the following optimization problem is found:

$$\begin{aligned} \min_{z} & C_t(z) + \alpha \Delta T_c(z) + \beta \Delta T_d(z), \\ & s.t. d^f \in 0, 1, ..., N^d_{max}, \\ & b^f \in [-1, 1], f = 1, ..., N. \end{aligned} \tag{B.4}$$

The objective function cannot be explicitly represented in terms of decision variables (d_f, b_f), and has to be evaluated with a simulation process. This problem is therefore a difficult high-dimensional mixed-integer black box (derivative-free) optimization problem. Thus, to resolve authors choose to apply a standard Simulated Annealing (SA). More details on the application of the SA to the conflict resolution af wind-optimal trajectories can be found in[92, 94]. Furthermore, the explicit results of conflict resolution using wind optimal trajectories can be found in [89, 94].

Bibliography

[2] The Federal Aviation Administration. “Enhanced Surveillance Capabilities in FAA Controlled Oceanic Airspace: Operational Need and Added Benefits”. In: RTCA, 2017.

[3] Adrian K Agogino and Kagan Tumer. “A multiagent approach to managing air traffic flow”. In: *Autonomous Agents and Multi-Agent Systems* (2012), pp. 1–25.

[4] AIRBUS. *Growing Horizons 2017/2036*. Global Market Forecast, 2017.

[5] Sameer Alam et al. “An ensemble approach for conflict detection in free flight by data mining”. In: *Transportation research part C: emerging technologies* (2009).

[6] David Alejo et al. “The velocity assignment problem for conflict resolution with multiple aerial vehicles sharing airspace”. In: *Journal of Intelligent and Robotic Systems* (2013), pp. 1–16.

[7] Einar Ingvi Andresson. “Lateral Optimization of Aircraft Tracks in Reykjavik Air Traffic Control Area”. PhD thesis. School of Science and Engineering, Reykjavik University, 2012. URL: http://hdl.handle.net/1946/12682.

[9] Nicolas Barnier and Cyril Allignol. “Combining flight level allocation with ground holding to optimize 4D-deconfliction”. In: *ATM Seminar 2011, 9th USA/Europe Air Traffic Management Research and Development Seminar*. 2011.

[10] Antonio Bicchi and Lucia Pallottino. “On optimal cooperative conflict resolution for air traffic management systems”. In: *IEEE Transactions on Intelligent Transportation Systems* (2000), pp. 221–231.

[11] Karl Bilimoria et al. “Comparison of centralized and decentralized conflict resolution strategies for multiple-aircraft problems”. In: *18th Applied Aerodynamics Conference*. 2000, p. 4268.

[12] Henk A. P. Blom and G. J. Bakker. “Safety Evaluation of Advanced Self-Separation Under Very High En Route Traffic Demand”. In: American Institute of Aeronautics and Astronautics, 2015.

[13] Béatrice Bonnemaison, Francis Casaux, and Thierry Miquel. “Operational assessment of co-operative ASAS applications”. In: *USA/Europe ATM RD Seminar*. 1998.

[14] J Boškovic, J Jackson, and Raman Mehra. “Sensor and tracker requirements development for sense and avoid systems for unmanned aerial vehicles”. In: *Proceedings of the Guidance, Navigation, and Control Conference*. Vol. 1. 2013.

[15] Romaric Breil et al. “Multi-agent Systems to Help Managing Air Traffic Structure”. In: *Journal of Aerospace Operations* Preprint (2017), pp. 1–30.

[19] S. Chaimatanan, D. Delahaye, and M. Mongeau. "A Hybrid Metaheuristic Optimization Algorithm for Strategic Planning of 4D Aircraft Trajectories at the Continental Scale". In: *IEEE Computational Intelligence Magazine*. Vol. 9. 4. 2014, pp. 46–61. DOI: 10.1109/MCI.2014.2350951.

[20] Supatcha Chaimatanan, Daniel Delahaye, and Marcel Mongeau. "A methodology for strategic planning of aircraft trajectories using simulated annealing". In: *ISIATM 2012, 1st International Conference on Interdisciplinary Science for Air traffic Management*. 2012.

[21] Supatcha Chaimatanan, Daniel Delahaye, and Marcel Mongeau. "Strategic deconfliction of aircraft trajectories". In: *ISIATM 2013, 2nd International Conference on Interdisciplinary Science for Innovative Air Traffic Management*. 2013.

[22] Ryan C Chartrand et al. "Operational Improvements from the In-Trail Procedure in the North Atlantic Organized Track System". In: *Proceedings of the 8th AIAA Aviation Technology, Integration and Operations (ATIO) Conference*. 2008, pp. 14–19.

[23] Manolis A Christodoulou and Sifis G Kodaxakis. "Automatic commercial aircraft-collision avoidance in free flight: the three-dimensional problem". In: *IEEE Transactions on Intelligent Transportation Systems* 7.2 (2006), pp. 242–249.

[24] Mario SV Valenti Clari et al. "Cost-benefit study of free flight with airborne separation assurance". In: *Air Traffic Control Quarterly* 9.4 (2001), pp. 287–309.

[25] Valour Consultancy Craig Foster Senior Consultant. "Aircraft Surveillance Versus Tracking". In: VALOUR CONSULTANCY, 2016.

[26] S. Devasia et al. "Decoupled Conflict-Resolution Procedures for Decentralized Air Traffic Control". In: *IEEE Transactions on Intelligent Transportation Systems* (2011).

[27] C. Dey. *GRIB (Edition 1)*. The WMO format for the storage of weather product information, the exchange of weather product messages in gridded binary form as used by NCEP central operations, U.S. Department of Commerce, National Oceanic, and Atmospheric Administration, National Weather Service, National Centers for Environmental Prediction, office Note 388, 1998.

[28] Gilles Dowek, Cesar Munoz, and Alfons Geser. *Tactical conflict detection and resolution in a 3-D airspace*. Tech. rep. INSTITUTE FOR COMPUTER APPLICATIONS IN SCIENCE and ENGINEERING HAMPTON VA, 2001.

[29] Bryson A. E. and Y. C. Ho. *Applied Optimal Control Taylor and Francis Levittown PA*. Vol. 2. 1975, pp. 42–89.

[30] European and North Atlantic Office of ICAO. *NAT OPS BULLETIN*. Dec. 2017. URL: https://www.icao.int/EURNAT/EUR%20and%20NAT%20Documents/NAT%20Documents/NAT%20OPS%20Bulletins/NAT%20OPS%20Bulletin%202017_003.pdf.

[31] European and North Atlantic Office of ICAO. *North Atlantic operations and airspace manual-NAT Doc 007*. International Civil Aviation Organization (ICAO), Jan. 2018.

[32] RTCA (Firm) and Radio Technical Commission for Aeronautics. Task Force 3. *Final Report of RTCA Task Force 3 Free Flight Implementation*. RTCA, Incorporated, 1995.

[33] Flight Safety Foundation. "Benefits Analysis of Space-Based ADS-B". In: Flight Safety Foundation, 2016.

[34] Emilio Frazzoli et al. "Resolution of conflicts involving many aircraft via semidefinite programming". In: *Journal of Guidance, Control, and Dynamics* (2001).

[35] Christine M Gerhardt-Falk et al. *Simulation of the North Atlantic Air Traffic and Separation Scenarios*. Tech. rep. FEDERAL AVIATION ADMINISTRATION TECHNICAL CENTER ATLANTIC CITY NJ, 2000.

[36] B. Girardet et al. "Wind-optimal path planning: Application to aircraft trajectories". In: *2014 13th International Conference on Control Automation Robotics Vision (ICARCV)*. 2014, pp. 1403–1408. DOI: 10.1109/ICARCV.2014.7064521.

[37] T. Gneiting and A.E. Raftery. "Weather forecasting with ensemble methods". In: *Atmospheric Science* (2005).

[38] S. Grabbe, B. Sridhar, and A. Mukherjee. "Central East Pacific flight scheduling". In: *AIAA Guidance, Navigation, and Control Conference and Exhibition*. 2007.

[39] Shon Grabbe, Banavar Sridhar, and Nadia Cheng. "Central east pacific flight routing". In: *Air Traffic Control Quarterly*. Vol. 15. 3. 2007, pp. 239–264.

[40] Volker Grewe et al. "Feasibility of climate-optimized air traffic routing for trans-Atlantic flights". In: *Environmental Research Letters*. Vol. 12. 3. 2017, p. 034003. URL: http://stacks.iop.org/1748-9326/12/i=3/a=034003.

[41] Isabelle Grimaud, Eric Hoffman, and Karim Zeghal. "Limited delegation of separation assurance to the flight crew". In: *Air and Space Europe* (2001), pp. 285 –287.

[42] Karen Harper et al. "Air traffic controller agent model for free flight". In: American Institute of Aeronautics and Astronautics, 1999.

[43] Jacco M Hoekstra, Ronald NHW van Gent, and Rob CJ Ruigrok. "Designing for safety: the 'free flight'air traffic management concept". In: *Reliability Engineering and System Safety* 75.2 (2002), pp. 215–232.

[44] JM Hoekstra, RCJ Ruigrok, and RNHW Van Gent. "Free flight in a crowded airspace?" In: *Progress in Astronautics and Aeronautics* 193 (2001), pp. 533–546.

[45] I. Hwang and C. E. Seah. "Intent-Based Probabilistic Conflict Detection for the Next Generation Air Transportation System". In: *Proceedings of the IEEE* (2008).

[46] Inseok Hwang and Chze Eng Seah. “Intent-based probabilistic conflict detection for the next generation air transportation system”. In: *Proceedings of the IEEE* (2008).

[51] International Civil Aviation Organisation (ICAO). *Procedures for air navigation services : Air Traffic Management*. Doc 4444, 2016.

[53] Emma A Irvine et al. “Characterizing North Atlantic weather patterns for climate-optimal aircraft routing”. In: *Meteorological Applications* 20.1 (2013), pp. 80–93.

[54] Emma A Irvine et al. “Characterizing North Atlantic weather patterns for climate-optimal aircraft routing”. In: *Meteorological Applications*. Vol. 20. 1. Wiley Online Library, 2013, pp. 80–93.

[55] Kenneth M Jones. “Pair-Wise Trajectory Management-Oceanic (PTM-O).[Concept of Operations—Version 3.9]”. In: (2014).

[56] R. J. Kerczewski, I. Greenfeld, and B. W. Welch. “Communications, navigation and surveillance for improved oceanic air traffic operations”. In: *2005 IEEE Aerospace Conference*. 2005, pp. 1799–1805. DOI: 10.1109/AERO.2005.1559472.

[57] D. B. Kirk, W. S. Heagy, and M. J. Yablonski. “Problem resolution support for free flight operations”. In: *IEEE Transactions on Intelligent Transportation Systems*. Vol. 2. 2. 2001, pp. 72–80. DOI: 10.1109/6979.928718.

[58] Daniel B Kirk, Winfield S Heagy, and Michael J Yablonski. “Problem resolution support for free flight operations”. In: *IEEE Transactions on Intelligent Transportation Systems* (2001), pp. 72–80.

[59] S. Kirkpatrick, D. Gelatt C, and M.P. Vecchi. *Optimization By Simulated Annealing*. IBM Research Report RC 9355. Acts of PTRC Summer Annual Meeting, 1982.

[60] R. Koelle and A. Tarter. “Towards a distributed situation management capability for SESAR and NextGen”. In: *2012 Integrated Communications, Navigation and Surveillance Conference*. 2012, O6–1–O6–12.

[61] Jimmy Krozel. “Free flight research issues and literature search”. In: *Under NASA contract NAS2-98005* (2000).

[62] James K Kuchar and Lee C Yang. “A review of conflict detection and resolution modeling methods”. In: *IEEE Transactions on intelligent transportation systems* 1.4 (2000), pp. 179–189.

[63] Timilehin Labeodan et al. “On the application of multi-agent systems in buildings for improved building operations, performance and smart grid interaction – A survey”. In: *Renewable and Sustainable Energy Reviews* 50.Supplement C (2015), pp. 1405 –1414.

[64] Karim Legrand, Daniel Delahaye, and Christophe Rabut. "Wind and Temperature Networking Applied to Aircraft Trajectory Prediction". In: *ICRAT 2016? 7th edition of the International Conference on Research in Air Transportation*. Philadelphia, United States, June 2016. URL: https://hal-enac.archives-ouvertes.fr/hal-01343595.

[65] Weiyi Liu and Inseok Hwang. "Probabilistic trajectory prediction and conflict detection for air traffic control". In: *Journal of Guidance, Control and Dynamics* (2011).

[66] Magnus Ljungberg and Andrew Lucas. *The OASIS Air Traffic Management System*. 1992.

[67] P Louyot. "ASEP-ITM simulations from traffic data". In: *DSNA, ASSTAR WP8, Tech. Rep* (2007).

[68] Lan Ma et al. "Improved flight conflict detection algorithm based on Gauss-Hermite particle filter". In: *Wuhan University Journal of Natural Sciences* 22.3 (2017), pp. 269–276.

[69] Zhi-Hong Mao, David Dugail, and Eric Feron. "Space partition for conflict resolution of intersecting flows of mobile agents". In: *IEEE Transactions on Intelligent Transportation Systems* (2007).

[70] Zhi-Hong Mao, Eric Feron, and Karl Bilimoria. "Stability and performance of intersecting aircraft flows under decentralized conflict avoidance rules". In: *IEEE Transactions on Intelligent Transportation Systems* 2.2 (2001), pp. 101–109.

[71] Yoshinori Matsuno et al. "Stochastic optimal control for aircraft conflict resolution under wind uncertainty". In: *Aerospace Science and Technology* (2015).

[72] N. Metropolis et al. "Equation of state calculation by fast computing machines". In: *Journal of Chemical Physics* 21.6 (1953), pp. 1087–1092.

[73] S. C. Mohleji and J. Hoffman. "Performance analysis of North Pacific Operations using an automated air traffic control system simulation". In: *IEEE Transactions on Control Systems Technology* 1.3 (1993), pp. 179–185. ISSN: 1063-6536. DOI: 10.1109/87.251885.

[74] Martin Molina, Sergio Carrasco, and Jorge Martin. "Agent-Based Modeling and Simulation for the Design of the Future European Air Traffic Management System: The Experience of CASSIOPEIA". In: *PAAMS 2014 International Workshops, Salamanca, Spain*. Springer International Publishing, 2014.

[75] H. K. Ng, B. Sridhar, and S. Grabbe. "A practical approach for optimizing aircraft trajectories in winds". In: *2012 IEEE/AIAA 31st Digital Avionics Systems Conference (DASC)*. 2012, pp. 3D6–1–3D6–14. DOI: 10.1109/DASC.2012.6382319.

[76] H. K. Ng et al. "Cross-polar aircraft trajectory optimization and the potential climate impact". In: *2011 IEEE/AIAA 30th Digital Avionics Systems Conference*. 2011, pp. 3D4–1–3D4–15. DOI: 10.1109/DASC.2011.6096060.

[77] H. K. Ng et al. “Three-dimensional trajectory design for reducing climate impact of Trans-Atlantic flights”. In: *14th AIAA Aviation Technology, Integration, and Operations Conference, AIAA paper, vol. AIAA*. 2014. DOI: 10.2514/6.2014-2289. URL: https://doi.org/10.2514/6.2014-2289.

[78] Hok K Ng et al. “Cross-polar aircraft trajectory optimization and the potential climate impact”. In: *Digital Avionics Systems Conference (DASC), 2011 IEEE/AIAA 30th*. IEEE. 2011, pp. 3D4–1.

[79] Lucia Pallottino, Antonio Bicchi, and Stefania Pancanti. “Safety of a decentralized scheme for free-flight ATMS using mixed integer linear programming”. In: *American Control Conference, 2002. Proceedings of the 2002*. IEEE. 2002, pp. 742–747.

[80] Lucia Pallottino, Eric M Feron, and Antonio Bicchi. “Conflict resolution problems for air traffic management systems solved with mixed integer programming”. In: *IEEE transactions on intelligent transportation systems* (2002), pp. 3–11.

[81] T. N. Palmer. “The economic value of ensemble forecasts as a tool for risk assessment: From days to decades”. In: *Quarterly Journal of the Royal Meteorological Society* (2002).

[82] Stefan Pettersson and Bengt Lennartson. “Controller design of hybrid systems”. In: *Hybrid and Real-Time Systems*. Springer. 1997, pp. 240–254.

[83] A Philippe et al. “Could erasmus speed adjustments be identifiable by air traffic controllers?” In: (Jan. 2007), pp. 594–604.

[84] M. Prandini et al. “A Probabilistic Approach to Aircraft Conflict Detection”. In: *Trans. Intell. Transport. Sys.* (2000).

[85] A. R. Pritchett et al. “Examining air transportation safety issues through agent-based simulation incorporating human performance models”. In: *Proceedings. The 21st Digital Avionics Systems Conference*. Vol. 2. 2002, 7A5–1–7A5–13 vol.2.

[86] H.F. Rashvand et al. “Distributed security for multi-agent systems-Review and applications”. In: 4 (2011), pp. 188 –201.

[87] Craig W. Reynolds. “Flocks, Herds and Schools: A Distributed Behavioral Model”. In: New York, NY, USA: ACM, 1987.

[88] D. Rivas, R. Vazquez, and A. Franco. “Stochastic prediction of cruising fuel load considering ensemble wind forecast”. In: *Advanced Aircraft Efficiency in a Global Air Transport System Conference (AEGATS)* (2016).

[89] O. Rodionova, B. Sridhar, and H. K. Ng. “Conflict resolution for wind-optimal aircraft trajectories in North Atlantic oceanic airspace with wind uncertainties”. In: *IEEE/AIAA 35th Digital Avionics Systems Conference (DASC)* (2016).

[90] O. Rodionova et al. “North Atlantic Aircraft Trajectory Optimization”. In: *IEEE Transactions on Intelligent Transportation Systems* 15.5 (2014), pp. 2202–2212. ISSN: 1524-9050. DOI: 10.1109/TITS.2014.2312315.

[91] Olga Rodionova. "Aircraft trajectory optimization in North Atlantic oceanic airspace". Theses. Université Paul Sabatier - Toulouse III, June 2015. URL: https://tel.archives-ouvertes.fr/tel-01214990.

[92] Olga Rodionova. "Aircraft trajectory optimization in North Atlantic oceanic airspace". Theses. Université Paul Sabatier - Toulouse III, June 2015. URL: https://tel.archives-ouvertes.fr/tel-01214990.

[93] Olga Rodionova et al. "DECONFLICTING WIND-OPTIMAL AIRCRAFT TRAJECTORIES IN NORTH ATLANTIC OCEANIC AIRSPACE". In: *AEGATS '16, Advanced Aircraft Efficiency in a Global Air Transport System*. 2016.

[94] Olga Rodionova et al. "Deconflicting wind-optimal aircraft trajectories in North Atlantic oceanic airspace". In: *AEGATS 16, Advanced Aircraft Efficiency in a Global Air Transport System*. AAF. Paris, France, Apr. 2016. URL: https://hal-enac.archives-ouvertes.fr/hal-01304633.

[95] Olga Rodionova et al. "Optimization of aicraft trajectories in North Atlantic oceanic airspace". In: *ICRAT 2012, 5th International Conference on Research in Air Transportation*. Berkeley, United States, May 2012, pp xxxx. URL: https://hal-enac.archives-ouvertes.fr/hal-00938895.

[96] Jeffrey S. Rosenschein and Gilad Zlotkin. *Rules of Encounter: Designing Conventions for Automated Negotiation Among Computers*. MIT Press, 1994.

[97] Laith R Sahawneh et al. "Minimum required sensing range for UAS sense and avoid systems". In: *AIAA Infotech@ Aerospace* (2016), p. 1982.

[98] G. Scutari et al. "Decomposition by Partial Linearization: Parallel Optimization of Multi-Agent Systems". In: *IEEE Transactions on Signal Processing* 62.3 (2014).

[99] D. Sislak, P. Volf, and M. Pechoucek. "Agent-Based Cooperative Decentralized Airplane-Collision Avoidance". In: *IEEE Transactions on Intelligent Transportation Systems* (2011), pp. 36–46.

[102] J.M. Sloughter, T. Gneiting, and A.E. Raftery. "Probabilistic wind speed forecasting using ensembles and Bayesian model averaging". In: *Journal of the American Statistical Association* (2010).

[103] Banavar Sridhar et al. "Benefits Analysis of Wind-Optimal Operations For Trans-Atlantic Flights". In: (2014).

[104] Banavar Sridhar et al. "Benefits analysis of wind-optimal operations for trans-atlantic flights". In: *14th AIAA Aviation Technology, Integration, and Operations Conference, AIAA paper, vol. AIAA*. Vol. 2583. 2014, pp. 1–12.

[105] Banavar Sridhar et al. "Strategic Planning of Efficient Oceanic Flights". In: *ATM seminar 2015, 11th USA/EUROPE Air Traffic Management R&D Seminar*. 2015.

[106] Banavar Sridhar et al. “Strategic Planning of Efficient Oceanic Flights”. In: *ATM seminar 2015, 11th USA/EUROPE Air Traffic Management R&D Seminar*. FAA & Eurocontrol. Lisboa, Portugal, June 2015. URL: https://hal-enac.archives-ouvertes.fr/hal-01168653.

[108] Claire Tomlin, George J Pappas, and Shankar Sastry. “Conflict resolution for air traffic management: A study in multiagent hybrid systems”. In: *IEEE Transactions on automatic control* (1998).

[109] *Use of Automatic Dependent Surveillance–Broadcast (ADS–B) Out in Support of Reduced Vertical Separation Minimum (RVSM) Operations*. Vol. 82. 150. Federal Aviation Administration (FAA), Department of Transportation (DOT), Aug. 2017.

[110] K. J. Viets and C. G. Ball. “Validating a future operational concept for en route air traffic control”. In: *IEEE Transactions on Intelligent Transportation Systems*. Vol. 2. 2. 2001, pp. 63–71. DOI: 10.1109/6979.928717.

[111] M. A. Wahid et al. “A framework for flight guidance along air streams”. In: *Proceedings of 2014 IEEE Chinese Guidance, Navigation and Control Conference*. 2014, pp. 2198–2203. DOI: 10.1109/CGNCC.2014.7007514.

[112] Gerhard Weiss. *Multiagent Systems*. The MIT Press, 2013.

[113] Navinda Kithmal Wickramasinghe, Akinori Harada, and Yoshikazu Miyazawa. “Flight trajectory optimization for an efficient air transportation system”. In: *ICAS2012, Brisbane*. 2012.

[116] A. Williams and I. Greenfeld. “Benefits assessment of reduced separations in North Atlantic Organized Track System”. In: *6th AIAA Aviation Technology, Integration and Operations Conference (ATIO)*. 2006, p. 7816.

[117] A. Williams et al. “Beneficial Applications of Airborne Separation Assurance Systems (ASAS) in the Southern Pacific Airspace”. In: *AIAA 5th ATIO and16th Lighter-Than-Air Sys Tech. and Balloon Systems Conferences, Aviation Technology, Integration, and Operations (ATIO) Conferences, American Institute of Aeronautics and Astronautics*. 2005. DOI: 10.2514/6.2005-7337.

[118] Almira Williams et al. “Application of Airborne Systems for Improving North Atlantic Organized Track System Operations”. In: *AIAA 5th Aviation, Technology, Integration, and Operations Conference (ATIO), Arlington, VA*. 2005, pp. 26–28.

[119] Steven Wollkind, John Valasek, and Thomas R. Ioerger. “Automated conflict resolution for air traffic management using cooperative multiagent negotiation”. In: *AIAA Guidance, Navigation, and Control Conference*. 2004, pp. 2004–4992.

[120] Jing Xie and Chen-Ching Liu. “Multi-agent systems and their applications”. In: *Journal of International Council on Electrical Engineering* 7.1 (2017), pp. 188–197.

[121] A. Yousefi, J. Lard, and J. Timmerman. "Nextgen flow corridors initial design, procedures, and display functionalities". In: *29th Digital Avionics Systems Conference*. 2010, pp. 4.D.1–1–4.D.1–19. DOI: 10.1109/DASC.2010.5655340.

[122] Gilad Zlotkin and Jeffrey S. Rosenschein. "Negotiation and Task Sharing Among Autonomous Agents in Cooperative Domains". In: *Proceedings of the 11th International Joint Conference on Artificial Intelligence - Volume 2*. IJCAI. Morgan Kaufmann Publishers Inc., 1989, pp. 912–917.

Netography

[1] Advanced Aircrew Academy. URL: https://www.aircrewacademy.com/follow-the-agonic-line/425-nat-rlatsm-briefing-2 (visited on 05/30/2018).

[8] AvRisk. URL: https://avrisk.net/avrisk/fans-1a-what-is-it-and-why-is-it-important/ (visited on 06/02/2018).

[16] Flight Service Bureau. URL: http://flightservicebureau.org/nat/ (visited on 05/30/2018).

[17] Nav Canada. URL: http://www.navcanada.ca/en/products-and-services/pages/on-board-operational-initiatives-ads-b.aspx (visited on 05/30/2018).

[18] Nav Canada. URL: https://pdfs.semanticscholar.org/presentation/4c57/33e4f05da2a3506f42803af3e164dd5d71e8.pdf (visited on 06/01/2018).

[47] IATA. URL: http://airlines.iata.org/news/iata-reveals-2018-financial-forecast (visited on 05/30/2018).

[48] IATA. URL: http://www.iata.org/pressroom/pr/Pages/2016-10-18-02.aspx (visited on 05/30/2018).

[49] ICAO. URL: https://www.icao.int/EURNAT/ (visited on 05/30/2018).

[50] ICAO. URL: https://www.icao.int/EURNAT/EURandNATDocuments/NATEconomicsandForecast/NATFIRTrafficForecast-2017-04-26.pdf (visited on 05/30/2018).

[52] Iridium. URL: http://investor.iridium.com/static-files/b80afce7-be78-4124-aa34-6f0ab4c7d0b7 (visited on 05/30/2018).

[100] Skybrary. URL: https://www.skybrary.aero/index.php/North_Atlantic_Operations_-_Airspace#Separation (visited on 05/30/2018).

[101] Skybrary. URL: https://www.skybrary.aero/index.php/North_Atlantic_Operations_-_Organised_Track_System (visited on 05/30/2018).

[107] Storm Surfing. URL: http://www.stormsurfing.com/cgi/display_alt.cgi?a=natla_250 (visited on 06/02/2018).

[114] Wikimedia. URL: https://commons.wikimedia.org/wiki/File:NAT-Tracks-24FEB17.png (visited on 05/30/2018).

[115] Roger Wilco. URL: http://www.roger-wilco.net/crossing-the-pond-in-new-and-better-ways (visited on 05/30/2018).